NOTE TO USERS

Page(s) missing in number only; text follows. Page(s) were microfilmed as received.

128

This reproduction is the best copy available.

UMI®

UNIVERSITY OF ALBERTA

SYNTHESIS AND REACTIVITY OF $Co(OH_2)_6^{3+}$, AND REDOX REACTIONS OF A COBALT(II)-OXIME

By

GRANT WANJALA WANGILA ©

A thesis submitted to the Faculty of Graduate Studies and Research in partial fulfillment of the requirements for the degree of Doctor of Philosophy

DEPARTMENT OF CHEMISTRY
EDMONTON, ALBERTA
Fall, 2001

National Library
of Canada

Acquisitions and
Bibliographic Services

395 Wellington Street
Ottawa ON K1A 0N4
Canada

Bibliothèque nationale
du Canada

Acquisitions et
services bibliographiques

395, rue Wellington
Ottawa ON K1A 0N4
Canada

Your file Votre référence

Our file Notre référence

The author has granted a non-exclusive licence allowing the National Library of Canada to reproduce, loan, distribute or sell copies of this thesis in microform, paper or electronic formats.

The author retains ownership of the copyright in this thesis. Neither the thesis nor substantial extracts from it may be printed or otherwise reproduced without the author's permission.

L'auteur a accordé une licence non exclusive permettant à la Bibliothèque nationale du Canada de reproduire, prêter, distribuer ou vendre des copies de cette thèse sous la forme de microfiche/film, de reproduction sur papier ou sur format électronique.

L'auteur conserve la propriété du droit d'auteur qui protège cette thèse. Ni la thèse ni des extraits substantiels de celle-ci ne doivent être imprimés ou autrement reproduits sans son autorisation.

0-612-69017-2

Canada

UNIVERSITY OF ALBERTA

LIBRARY RELEASE FORM

NAME OF AUTHOR: GRANT WANJALA WANGILA

TITLE OF THESIS: SYNTHESIS AND REACTIVITY OF $Co(OH_2)_6^{3+}$, AND REDOX REACTIONS OF A COBALT(II)-OXIME

DEGREE: DOCTOR OF PHILOSOPHY

YEAR THIS DEGREE GRANTED: 2001

Permission is hereby granted to the University of Alberta Library to reproduce single copies of this thesis and to lend or sell such copies for private, scholarly or scientific research purposes only.

The author reserves all other publication and other rights in association with the copyright in the thesis, and except as herein before provided, neither the thesis nor any substantial portion thereof may be printed or otherwise reproduced in any material form whatever without the author's prior written permission.

MICHENER PARK 604H
EDMONTON, ALBERTA
CANADA
T6H 5A1

August 22nd, 2001

UNIVERSITY OF ALBERTA

FACULTY OF GRADUATE STUDIES AND RESEARCH

The undersigned certify that they have read, and recommended to the Faculty of Graduate Studies and Research for acceptance, a thesis entitled "**Synthesis and Reactivity of $Co(OH_2)_6^{3+}$, and Redox Reactions of a Cobalt(II)-oxime**" submitted by Grant Wanjala Wangila in partial fulfillment of the requirements for the degree of Doctor of Philosophy.

R B Jordan

Professor Robert B. Jordan

Josef Takats

Professor Josef Takats

Steven Bergens

Professor Steve H. Bergens

Professor Charles A. Lucy

Professor Gerald Stemke

Professor Alexander McAuley

(External Examiner)

August 08th, 2001

Dedicated to

My wife Susan Kuya Wanjala

&

Sons

Nessbin Simiyu Wanjala

Rodrick Wafula Wanjala

Antony Fedha Wanjala

and

Humphrey Musime Wanjala

who brought Harmony in our family at the end of this work

Abstract

In this study, the crystalline salt $[Co(NH_3)_6][Co(CO_3)_3]$ has been synthesized and characterized stoichiometrically and structurally. It is shown that the salt is a convenient source for solutions of $Co(OH_2)_6^{3+}$.

The reaction of $Co(OH_2)_6^{3+}$ with water has been studied in 1.0 M $HClO_4/LiClO_4$ at 25 °C. The reaction is biphasic, showing an initial increase and then decrease in absorbance at 325 and 605 nm. The rate of increase depends on $[Co(OH_2)_6^{3+}]^2$ and $[H^+]^{-2}$ and is assigned to oligomer formation, while the decrease has an $[H^+]^{-1}$ dependence and is assigned to oxidation of water.

The reaction of $Co(OH_2)_6^{3+}$ with H_2O_2, and $Co(dmgBF_2)_2(H_2O)_2$ in 1.0 M $HClO_4/LiClO_4$ was found to be first-order in both reactants and the $[H^+]$ dependence of the second-order rate constant is given by $k_{2obs} = b/[H^+]$, b at 25 °C is $26.4 \pm 0.5\ s^{-1}$, and $9.23 \pm 0.14 \times 10^2\ s^{-1}$ for H_2O_2 and $Co(dmgBF_2)_2(H_2O)_2$, respectively. For the latter reaction, the $[H^+]$ dependence at lower temperatures shows some saturation effect that allowed an estimate of the hydrolysis constant for $Co(OH_2)_6^{3+}$ as $K_a = 9.5 \times 10^{-3}$ M at 10 and 15 °C. Marcus theory and the known self-exchange rate constant for $Co(OH_2)_5OH^{2+/+}$ were used to estimate an electron self-exchange rate constant of $k_{22} = 1.7 \times 10^{-4}\ M^{-1}\ s^{-1}$ for $Co(dmgBF_2)_2(H_2O)_2^{+/0}$.

The kinetics of the reduction of $Fe(bipy)_3^{3+}$ by $Co(dmgBF_2)_2(H_2O)_2$ in 0.041 M $HNO_3/NaNO_3$ was found to be first-order in both the oxidizing and reducing agents and the second-order rate constant is given by $k_{obs} = k_1 + k_2K[Cl^-]$, with $k_1 = 1.59 \times 10^6\ M^{-1}\ s^{-1}$ and $k_2K = 1.83 \times 10^8\ M^{-2}s^{-1}$, at 25 °C. The term that is first-order in $[Cl^-]$ is attributed to the formation of an ion-pair between $Fe(bipy)_3^{3+}$ and Cl^-. For k_1, the activation

parameters ΔH^* and ΔS^* are 2.22 ± 0.02 kcal mol^{-1} and −22.7 ± 0.8 cal mol^{-1} K^{-1}, respectively. The self-exchange rate constant of $k_{22} \approx 8.7 \times 10^{-3}$ M^{-1} s^{-1} for $Co(dmgBF_2)_2(H_2O)_2^{+/0}$ was estimated using Marcus theory and the known self-exchange rate constant for $Fe(bipy)_3^{3+/2+}$.

Acknowledgments

It is a pleasure to acknowledge the tremendous effort and cooperation of my supervisor Professor Robert B. Jordan of the University of Alberta for his guidance and advice at all stages in my study. His advice, discussions and fruitful suggestions have made the entire work possible. It cannot go unmentioned the amount of time he spent on the computer programming, modeling and helping me analyze my data, and also his readiness to discuss any topic or fix instruments in the laboratory at a knock on his door.

Many thanks goes to Dr. Margaret Sisley without her assistance it could have taken me a long time to master most procedures in the preparative methods and instrumentation in the Research Laboratory, and the Kenyan fraternity in the department and colleagues Patrick M. Kamau and Japhet K. Irangu, for their encouragement and frequent helpful discussions in both academic and social spheres.

My wife Susan Kuya and sons Nessbin, Rodrick and Antony who came to Edmonton at just the right time when I most needed them for love, moral support and encouragement. Their consistent urging and prodding spurred this work into reality. I cannot forget my old parents in Kenya who continued asking; when will you ever finish learning? How will you educate your children? Will you ever get a job? Are you going to eat books in your retirement? They were very hard questions to answer but I kept on assuring them that it's only God who knows the destiny of my existence on this earth.

Finally I'm indebted to Jomo Kenyatta University of Agriculture and Technology (in Kenya) which granted me Study Leave. I'm also indebted to University of Alberta for offering me a teaching assistantship, without which I may not have completed my studies.

Table of Contents

Chapter 1. **Introduction** 1

Aquacobalt(III) 1

Cobaloximes 15

References 21

Chapter 2. **Synthesis and Characterization of Hexaamminecobalt(III) *tris*(carbonato)cobaltate(III) and $Co(OH_2)_6^{3+}$** 24

Introduction 24

Experimental 26

Characterization of $[Co(NH_3)_6][Co(CO_3)_3]$ 29

X-ray crystallography 33

Production of $Co(OH_2)_6^{3+}$ from $[Co(NH_3)_6][Co(CO_3)_3]$ 33

Results 36

Discussion 41

References 45

Chapter 3. **Decomposition of Hexaaquacobalt(III) in Perchloric Acid** 48

Introduction 48

Experimental 57

Results 58

Discussion 76

References 80

Chapter 4. Reaction of Hydrogen Peroxide with Hexaaquacobalt(III) Perchlorate **81**
Introduction 81
Experimental 84
First-order Analysis 86
Results 90
Discussion 95
References 98
Chapter 5. Kinetic Studies of Hexaaquacobalt(III) Perchlorate with Cobaloxime, [Co(dmgBF$_2$)$_2$(H$_2$O)$_2$] **100**
Introduction 100
Experimental 103
Results 109
Reaction Mechanism 116
Discussion 118
References 125
Chapter 6. Kinetic Studies of *tris*(2,2'-bipyridine)Iron(III) Perchlorate with Cobaloxime, [Co(dmgBF$_2$)$_2$(H$_2$O)$_2$] **129**
Introduction 129
Experimental 135
Second-order Analysis 137
Results 139
Discussion 149

References 157

Chapter 7. Conclusion 161

References 166

Appendix. Tables of Experimental Data 168

List of Tables

Table **Page**

1.1 Kinetic Parameters for the Reactions of $Co(OH_2)_6^{3+}$ with Various Ligands. 16

2.1 Determination of the Molar Mass of the $[Co(NH_3)_6][Co(CO_3)_3]$. 31

2.2 Determination of the Equivalent Weight of the $[Co(NH_3)_6][Co(CO_3)_3]$. 32

2.3 Determination of the Yield and Extinction Coefficient of $Co(OH_2)_6^{3+}$. 35

2.4 Comparative Values of Angles and Distances of Various Metal Carbonato Complexes. 39

2.5 Representative Results for the Preparation of Aqueous Cobalt(III) from Crystalline $[Co(NH_3)_6][Co(CO_3)_3]$. 42

4.1 Kinetic Data for the Reaction of H_2O_2 with $Co(OH_2)_6^{3+}$ in 1.0 M $LiClO_4/HClO_4$ at 25 °C. 91

5.1 Kinetic Parameters for the Reaction of $Co(OH_2)_6^{3+}$ with $Co(dmgBF_2)_2(H_2O)_2$. 115

5.2 Self-Exchange Rate Constants Calculated by the Marcus Relationship. 123

6.1 Dependence of k_{obs} on the Reactant Concentrations for the Reaction of $Fe(bipy)_3^{3+}$ with $Co(dmgBF_2)_2(H_2O)_2$ in 3.0×10^{-3} M $HNO_3/3.8 \times 10^{-2}$ M $NaNO_3$ at 15 °C. 140

6.2 Dependence of k_{obs} on the HNO_3 Concentration for the Reaction of $Fe(bipy)_3^{3+}$ with $Co(dmgBF_2)_2(H_2O)_2$ in 3.0×10^{-3} M $HNO_3/3.8 \times 10^{-2}$ M $NaNO_3$ at 15 °C. 141

6.3 Dependence of k_{obs} on Temperature for the Reaction of $Fe(bipy)_3^{3+}$ with $Co(dmgBF_2)_2(H_2O)_2$ in $\mu = 4.1 \times 10^{-2}$ M $NaNO_3/NaCl$. 143

6.4 Experimental and Extrapolated Kinetic Parameters for the Reaction of $Fe(bipy)_3^{3+}$ with $Co(dmgBF_2)_2(H_2O)_2$ in 3.0×10^{-3} M HNO_3 /3.8×10^{-2} M $NaNO_3$. 147

6.5 Rate and Activation Parameters for the Reduction of $Fe(bipy)_3^{3+}$ and $Fe(phen)_3^{3+}$ by Various Reductants. 150

6.6 Self-Exchange Rate Constants for Cobaltoxime Systems Calculated by the Marcus Relationship. 153

6.7 Self-Exchange Rate Constants for Various Co(III)/(II) Complexes at 25 °C. 155

List of Appendix Tables

Appendix **Page**

2.1 Selected Interatomic Distances (Å)Within $[Co(CO_3)_3]^{3-}$. 168

2.2 Selected Interatomic Angles (deg) Within $[Co(CO_3)_3]^{3-}$. 169

5.1 Dependence of k_{1obs} on the Concentration of $Co(OH_2)_6^{3+}$ and Temperature in 8.25×10^{-5} M $Co(dmgBF_2)_2(H_2O)_2$ and 0.60 M $HClO_4$/0.40 M $LiClO_4$. 170

5.2 Dependence of the Rate Constant on Reactant Concentrations and Temperature for the Reaction of $Co(OH_2)_6^{3+}$ with $Co(dmgBF_2)_2(H_2O)_2$ in $\mu = 1.0$ M $LiClO_4/HClO_4$. 172

6.1 Least-squares Analysis of the Temperature and Concentration of NaCl Dependence of the Rate Constants for the Reaction of $Co(dmgBF_2)_2(H_2O)_2$ and $Fe(bipy)_3^{3+}$ in 3.0×10^{-3} M HNO_3 and 3.8×10^{-2} M (NaCl/$NaNO_3$). 175

List of Figures

Figures **Page**

1.1 Structures of $dmgH_2$, $Co(dmgH)_2$ and $Co(dmgBF_2)_2$. 17

2.1 Perspective view of the asymmetric unit of $[Co(NH_3)_6][Co(CO_3)_3]$ showing the atom labeling scheme. Two crystallographically-independent units of each of $[Co(NH_3)_6]^{3+}$ and $[Co(CO_3)_3]^{3-}$ are present. Non-hydrogen atoms are represented by Gaussian ellipsoids at the 20 % probability level. Hydrogen atoms are shown with arbitrarily small thermal parameters. 37

2.2 Comparative angles and distances of $Co(CO_3)_3{}^{3-}$ anion. 38

3.1 The spectrum of 2.8×10^{-2} M $Co(OH_2)_6{}^{3+}$ in 1.00 M $HClO_4$ at 25 °C. Time separation for the spectra is 10 minutes. 59

3.2 The spectrum of 2.09×10^{-2} M $Co(OH_2)_6{}^{3+}$ in 0.45 M $HClO_4$/0.55 M $LiClO_4$ at 25 °C. Time separation for the spectra is 5 minutes. 60

3.3 Variation of the absorbance at 325 nm with time for solutions of 3.30×10^{-3} M (O), 2.20×10^{-3} M ( ), and 1.20×10^{-3} M (●) $Co(OH_2)_6{}^{3+}$ in 0.080 M $HClO_4$/0.92 M $LiClO_4$ at 25 °C. 62

3.4 Variation of the absorbance at 605 nm with time for solutions of 3.30×10^{-3} M (O), 2.20×10^{-3} M ( ), and 1.20×10^{-3} M (●) $Co(OH_2)_6{}^{3+}$ in 0.080 M $HClO_4$/0.92 M $LiClO_4$ at 25 °C. 63

3.5 Variation of the absorbance at 325 nm with time for solutions of 1.82×10^{-2} M $Co(OH_2)_6{}^{3+}$ in 0.11 M (O), 0.20 M ( ), and 0.45 M (●) H^+

in 1.0 M $HClO_4/LiClO_4$ at 25 °C. 64

3.6 Variation of the absorbance at 325 nm with time for solutions of 3.30 $\times 10^{-3}$ M (O), 2.20 $\times 10^{-3}$ M (□), and 1.20 $\times 10^{-3}$ M (●) $Co(OH_2)_6^{3+}$ in 0.080 M $HClO_4$/0.92 M $LiClO_4$ at 25 °C. 65

3.7 Variation of the absorbance at 605 nm with time for solutions of 3.30 $\times 10^{-3}$ M (O), 2.20 $\times 10^{-3}$ M (□), and 1.20 $\times 10^{-3}$ M (●) $Co(OH_2)_6^{3+}$ in 0.080 M $HClO_4$/0.92 M $LiClO_4$ at 25 °C. 66

3.8 Variation of the absorbance at 325 nm with time for solutions of 1.82 $\times 10^{-2}$ M $Co(OH_2)_6^{3+}$ in 0.11 M (O), 0.20 M (□), and 0.45 M (●) H^+ in 1.0 M $HClO_4/LiClO_4$ at 25 °C. 67

3.9 Variation of the observed and calculated absorbance at 325 nm with time for solutions of 3.30 $\times 10^{-3}$ M (O), 2.70 $\times 10^{-3}$ M (□) and 2.20 $\times 10^{-3}$ M (●) $Co(OH_2)_6^{3+}$ in 0.080 M $HClO_4$/0.92 M $LiClO_4$ at 25 °C. 71

3.10 Variation of the observed and calculated (fitted using an average ε_3 value of 426 M^{-1} s^{-1}) absorbance at 325 nm with time for solutions of 3.30 $\times 10^{-3}$ M (O), 2.70 $\times 10^{-3}$ M (□) and 2.20 $\times 10^{-3}$ M (●) $Co(OH_2)_6^{3+}$ in 0.080 M $HClO_4$/0.92 M $LiClO_4$ at 25 °C. 72

3.11 Variation of the observed and calculated absorbance at 325 nm with time for solutions of 18.2 $\times 10^{-3}$ M Co(III) in 0.11 M H^+ (O), 18.2 $\times 10^{-3}$ M Co(III) in 0.20 M H^+ (□) and 26.0 $\times 10^{-3}$ M Co(III) in 0.45 M H^+ (●) in 1.0 M $HClO_4/LiClO_4$ at 25 °C. 74

4.1 Dependence of k_{1obs} on $[H_2O_2]$ with 2.6 $\times 10^{-4}$ M $Co(OH_2)_6^{3+}$ and 5.0 $\times 10^{-2}$ M $HClO_4$ in 1.0 M $LiClO_4/HClO_4$ at 25 °C. 93

4.2 Dependence of k_{2obs} on $[H^+]^{-1}$ with 2.30- 2.70 × 10^{-4} M $Co(OH_2)_6^{3+}$ and 6.00-173 × 10^{-4} M H_2O_2 in 1.0 M $LiClO_4/HClO_4$ at 25 °C. 94

5.1 Dependence of k_{1obs} on $[Co(OH_2)_6^{3+}]$ with 8.25 × 10^{-5} M $Co(dmgBF_2)_2(H_2O)_2$ in 0.60 M $HClO_4$/0.40 M $LiClO_4$ at 10.0 (●), 15.0 (■) and 20.0 °C (□). 111

5.2 Dependence of k_{2obs} on $[H^+]^{-1}$ with 4.29-24.86 × 10^{-4} M $Co(OH_2)_6^{3+}$ and 5.50-9.00 × 10^{-5} M $Co(dmgBF_2)_2(H_2O)_2$ for $[H^+] > 0.2$ M in 1.0 M $LiClO_4$/ $HClO_4$ at 10.0 (●), 15.0 (■), 20.0 (□) and 25.0 °C (O). 112

5.3 Dependence of k_{2obs} on $[H^+]^{-1}$ with 4.29-24.86 × 10^{-4} M $Co(OH_2)_6^{3+}$ and 5.50-9.00 × 10^{-5} M $Co(dmgBF_2)_2(H_2O)_2$ for $[H^+] > 0.021$ M in 1.0 M $LiClO_4$/ $HClO_4$ at 15.0 (□) and 10.0 °C (O). 113

6.1 Dependence of k_{obs} on $[Cl^-]$ with 3.85-6.45 × 10^{-5} M $Fe(bipy)_3^{3+}$, 7.83-10.40 × 10^{-5} M $Co(dmgBF_2)_2(H_2O)_2$ in $\mu = 4.1 \times 10^{-2}$ M $HNO_3/NaNO_3$ at 10.0 (O), 15.0 (□) and 20.0 °C (●). 142

CHAPTER 1. Introduction

The Chemistry of Aquacobalt(III) and Cobaloximes

This study is concerned with the chemistry of aquacobalt(III) and cobaloximes. The details and background of the techniques used are described in the introductions to the relevant Chapters. The present section provides some overall chemical and structural background.

Aquacobalt(III)

The aqua ion, $Co(OH_2)_6^{3+}$, is the simplest complex of cobalt(III). In aqueous solutions containing no complexing agents, Co(III) is a very powerful one-electron oxidizing agent[1,2] as shown in equation (1.1).

$$Co(OH_2)_6{}^{3+} + e^- \longrightarrow Co(OH_2)_6{}^{2+} \qquad E^o = 1.86\ \mathrm{V} \qquad (1.1)$$

In the presence of complexing agents such as NH_3, which form stable complexes with Co(III), the oxidizing power of trivalent cobalt is greatly reduced.[3]

$$Co(NH_3)_6{}^{3+} + e^- \longrightarrow Co(NH_3)_6{}^{2+} \qquad E^o = 0.1\ \mathrm{V} \qquad (1.2)$$

Methods of Preparation of $Co(OH_2)_6^{3+}$. Three methods of preparation of aqueous solutions of cobalt(III) perchlorate have been reported in the literature. Such solutions have been prepared by treatment of $Co_2(SO_4)_3 \bullet 18H_2O$ in perchloric acid with $Ba(ClO_4)_2$ at 0 °C.[4,5] The $Co_2(SO_4)_3 \bullet 18H_2O$ salt was produced by electrolysis of saturated solutions of cobalt(II) sulfate in 5 M sulfuric acid at 5 -10 °C with a current density of 0.05 amp. cm^{-2} for about 4 hours.[6] The salt is unstable and must be stored in the refrigerator over concentrated sulfuric acid desiccant.

A second method,[7,8] involves the reaction of perchloric acid with green solutions formed by the addition of hydrogen peroxide to solutions of cobalt(II) perchlorate in saturated aqueous $NaHCO_3$ or $KHCO_3$.[9] The aqueous cobalt(III) is produced by addition of concentrated acid to destroy the carbonate in the green solution. Weiser[7] reported that the yield of $Co(OH_2)_6^{3+}$ approached 100 % of the theoretical in this method.

Direct electrolytic oxidation of cobalt(II) perchlorate in perchloric acid has been used by many researchers.[4,5,7,8,10] The optimum conditions for production of $\sim 5 \times 10^{-2}$ M $Co(OH_2)_6^{3+}$ occur at low current density (~ 0.002 amp cm^{-2}) and high acidity (~ 3 M) at 0 °C. This gives a maximum yield after 7 hours of 70 % based on the initial cobalt(II) concentration. Davies and Warnqvist[10] found that the use of higher current densities, in an attempt to accelerate the rate of electrolysis, leads to solutions containing cobalt(III) species with properties that are appreciably different from those prepared under the optimum conditions. Similarly, lower acid concentrations in the mixture to be electrolyzed yield solutions with spectral and kinetic properties that differ from those prepared after dilution of solutions obtained under the recommended conditions.

Solutions of $Co(OH_2)_6^{3+}$ traditionally have been characterized by their electronic spectra. Hargreaves and Sutcliffe[5] reported that solutions of $Co(OH_2)_6^{3+}$ in ≥ 3.0 M H^+ prepared by electrolysis of cobalt(II) perchlorate have extinction coefficients of 41 ± 1 and 35 ± 1 M^{-1} cm^{-1} at the absorption maxima of 401 and 605 nm, respectively. Baxendale and Wells[4] reported slightly lower values of 39 and 32.6 $M^{-1}cm^{-1}$ at the same wavelengths for solutions at ≥ 1.02 M H^+ prepared either from $Co_2(SO_4)_3{\bullet}18H_2O$ or by electrolysis. Weiser[7] prepared $Co(OH_2)_6^{3+}$ either from cobalt(III) carbonate solutions or by electrolysis and reported values of 40.5 and 34.8 $M^{-1}cm^{-1}$ at 401 and 605 nm, respectively, for $[H^+] \geq 0.4$ M H^+ at 25 °C or ≥ 0.1 M at 0 °C. Baxendale and Wells[4] also reported a value of 2.97×10^3 $M^{-1}cm^{-1}$ at 250 nm, in agreement with 3.05×10^3 $M^{-1}cm^{-1}$ found by Weiser.[7] It seems probable that all these groups were working with the same species, and that the differences are due to instrumentation or the age of the solutions.

The general goal of these methods is to prepare solutions that, at least initially, contain $Co(OH_2)_6^{3+}$ as the only form of cobalt(III). The acidity, total cobalt(III) and total ionic composition of the solution should be known or easily determinable. The most convenient method would seem to be acidification of the green cobalt(III)-carbonate solutions. Weiser[7] and others[8,10] have found that it does produce $Co(OH_2)_6^{3+}$ in good yield. The main problem is that it is difficult to control the final acidity because of the large amounts of bicarbonate that must be neutralized. The final solutions also contain large amounts of Na^+ (~ 0.90 M), although this can be minimized by using $KHCO_3$ which precipitates as $KClO_4$ on neutralization with $HClO_4$. The use of $Co_2(SO_4)_3{\bullet}18H_2O$ has the advantage of starting with a solid, but the latter is unstable unless stored under rather inconvenient conditions. The direct electrolysis[4,5,7,8,10] yields solutions of known acidity and readily determinable cobalt(III) concentration, but it is rather tedious and produces solutions with a higher acidity (~ 3 M) and a high ratio of $[H^+]:[Co(III)]$ (≥ 600). The latter means that it is difficult to prepare solutions of modest acidity (0.05 – 0.20 M) and spectrophotometrically detectable concentrations of cobalt(III).

From the above summary it is clear that studies of aqueous cobalt(III) would be greatly aided by a convenient, rapid method of preparation, preferably starting from a well-characterized solid.

Electronic Structure of $Co(OH_2)_6^{3+}$. Johnson and Sharpe[11] found that $CsCo(SO_4)_2 \bullet 12H_2O$ was essentially diamagnetic with a magnetic susceptibility of 202×10^{-6} cgs units at 20 °C. This salt contains the $Co(OH_2)_6^{3+}$ ion with a Co-O distance of 1.873(5) Å based on a single-crystal X-ray diffraction study.[12] The fact that a ^{59}Co NMR can be obtained for $Co(OH_2)_6^{3+}$ in aqueous perchloric acid shows that the dissolved ion also is diamagnetic. A detailed NMR study by Navon[13] failed to reveal any sign of exchange with a high spin, paramagnetic form of $Co(OH_2)_6^{3+}$.

Johnson and Sharpe[11] also measured the reflectance spectrum of $CsCo(SO_4)_2 \bullet 12H_2O$ and found absorbance maxima at 1.65×10^4 cm^{-1} (606 nm) and 2.47×10^4 cm^{-1} (405 nm). A simple crystal field theory interpretation predicts that an octahedral, low-spin, d^6 system will have a $^1A_{1g}$ ground state, and that the observed *d-d* transitions are to the $^1T_{1g}$ and $^1T_{2g}$ states, respectively. The crystal field analysis of Johnson and Sharpe[11] gave values for $10Dq$, and Racah parameters B and C of 2.08×10^4, 5.13×10^2 and 4.25×10^3 cm^{-1}, respectively. A more recent crystal field interpretation by Johnson and Nelson[14] has given $10Dq$, and Racah parameters B and C

as 1.675×10^4, 6.60×10^2 and 3.65×10^3 cm^{-1}, respectively. These authors also estimated that the low-spin to high-spin change for $Co(OH_2)_6^{3+}$ has $\Delta G^o \approx 9.0$ kcal mol^{-1}, consistent with Navon's failure to detect the high-spin form. It is interesting to note that $Co(OH_2)_6^{3+}$ breaks the general trend of decreasing $10Dq$ for the analogous species of Ti^{3+} through Fe^{3+}. Both $Mn(OH_2)_6^{3+}$ and $Fe(OH_2)_6^{3+}$ are high spin with $10Dq$ values of 1.58×10^4 and 1.40×10^4 cm^{-1}, respectively, but $Co(OH_2)_6^{3+}$ has a larger $10Dq$ than either of these and is low-spin. Using the intermediate neglect of differential overlap model, Zerner et al.[15] predicted the transition energies as 1.67×10^4 cm^{-1} (599 nm) and 2.49×10^4 cm^{-1}(402 nm), in good agreement with the observation from aqueous solutions or reflectance spectroscopy mentioned above.

Species Present in Aquacobalt(III) Perchlorate Solutions. Bawn and White[16] studied the kinetics of the oxidation of water by cobalt(III) sulfate and perchlorate solutions in ~ 0.1 to 0.8 M perchloric acid. They found that the order of the rate with respect to the cobalt(III) concentration is two at higher (10^{-2} M) concentrations and tends to unity at lower concentrations. To conform to these kinetics, they suggested that two types of rate-determining reactions occurred, one involving a monomeric cobalt(III) species and another involving a dimeric species.

Hargreaves and Sutcliffe[5] studied the spectrum of aqueous cobalt(III) for concentrations of 10^{-3} to 10^{-2} M and [H^+] from 1.0 to 6.0 M. They concluded from the constancy of the spectra that no polynuclear cobalt(III) species are formed under these conditions.

Weiser[7] studied the absorption spectrum of aqueous cobalt(III) in the range 220-900 nm at various concentrations of cobalt(III) ($2.0 \times 10^{-5} - 4.0 \times 10^{-3}$ M) and found that the spectrum was independent of the $HClO_4$ concentration for $[H^+] > 0.4$ M at 25 °C or > 0.1 M at 0 °C . At low acid concentration of ($\leq 2.4 \times 10^{-3}$ M H^+), Weiser[7] observed another species forming with no well defined absorption maxima below 400 nm for [Co(III)] in the range of 0.45×10^{-3} to 3.5×10^{-3} M. The species has a reasonably constant extinction coefficient of ~ 150 $M^{-1}cm^{-1}$ (based on total cobalt(III)) at 402 nm. Weiser proposed that this species is a dimer of composition $[(H_2O)_5Co\text{-}O\text{-}Co(OH_2)_5]^{4+}$, which is formed essentially irreversibly from the monomeric species.

As part of a kinetic study of the oxidation of water by cobalt(III), Baxendale and Wells[4] obtained spectra between 350 to 700 nm for 0.69 to 229×10^{-4} M cobalt(III) containing 0.10, 0.50 and 1.82 M $HClO_4$ in $\mu = 1.82$ M $HClO_4/NaClO_4$. The main changes in the absorbance were a general increase in absorbance below 500 nm, so that the maximum at 401 nm and minimum at 480 nm, which are present at stronger acidities, became a more intense shoulder at 400 nm in 0.10 M $HClO_4$. The extinction coefficient of the cobalt(III) ($\geq 8.84 \times 10^{-3}$ M) increased to 78.1 $M^{-1}cm^{-1}$ at 401 nm and to 47.6 $M^{-1}cm^{-1}$ at 605 nm.

Baxendale and Wells[4] studied the rate of oxidation of water by aqueous cobalt(III) and found that the rate depended on $[Co(III)]^{3/2}$ and $[H^+]^{-2}$. They suggested that $Co(OH_2)_6^{3+}$ undergoes a rapid hydrolysis followed by slow formation of the dimer, $[(H_2O)_5Co\text{-}O\text{-}Co(OH_2)_5]^{4+}$. They also suggested that the dimer is the dominant form for $\geq 10^{-3}$ M cobalt(III), even at 1.0 M H^+.

The spectra of 2.3-8.0 × 10^{-3} M cobalt(III) solutions in 0.06-0.29 M H^+ at $\mu = 1.0$ M $NaClO_4$ were reexamined by Sutcliffe and Weber.[17] They observed that the extinction coefficient at 330 nm increases with increasing $Co(OH_2)_6^{3+}$ concentration and with decreasing acid concentration and attributed the increase in absorbance at 330 nm to hydrolysis and dimerization. They also suggested that it is possible that the dimer may hydrolyze further or form higher polynuclear species.

Hydrolysis of $Co(OH_2)_6^{3+}$. Sutcliffe and Weber[18] studied the hydrolysis of $Co(OH_2)_6^{3+}$ (equation 1.3)

$$Co(OH_2)_6^{3+} \overset{K_a}{\rightleftarrows} Co(OH_2)_5OH^{2+} + H^+ \tag{1.3}$$

by measuring the absorbance at various total [Co(III)] (1.0-5.0 × 10^{-4} M) and [H^+] (0.02-0.10 M) at 285 nm in 1.0 M $NaClO_4$. From this data, they determined the observed extinction coefficient (ε) for a series of acid concentrations. If ε_1 and ε_2 are the molar extinction coefficients of $Co(OH_2)_6^{3+}$ and $Co(OH_2)_5OH^{2+}$, respectively, then it can be shown that

$$\varepsilon[H^+] = \varepsilon_1[H^+] + \varepsilon_2 K_a - \varepsilon K_a \tag{1.4}$$

The most consistent experimental data at 18.45 °C were used to solve equation (1.4) and the best values of ε_1 and ε_2 were found to be 140 and 350 M^{-1} cm^{-1}, respectively. Then these values were used to calculate the K_a for three other temperatures (12.5, 23.6 and 28.2 °C), from which $K_a = 0.017$ M at 25 °C by interpolation. The standard enthalpy and entropy changes were determined to be 10.3 kcal mol^{-1} and 26.3 cal mol^{-1} K^{-1}, respectively. It should be noted that the extinction coefficient of 140 M^{-1} cm^{-1} at 285 nm is much lower than Weiser's[7] value of 184 M^{-1} cm^{-1} at 284 nm. The difference in these values might be attributed to the age, acid concentration and the temperature of the stock solutions of cobalt(III).

Subsequently, the acid dependence of the rates of complexation and ligand oxidation were used to estimate K_a. Sutin et al.[19] studied the reaction with chloride ion ($[H^+]$ 0.40 –3.0 M, $\mu = 3.0$ M, 25 °C), while Hill and McAuley studied malic acid[20] ($[H^+]$ 0.14-0.25 M) and thiomalic acid[21] ($[H^+]$ 0.108-0.33 M), both at $\mu = 0.25$ M and 7.0 °C. These studies reported K_a values of 0.22 ± 0.05, 0.10 ± 0.05 and 0.05 ± 0.01 M, respectively. All of these values are substantially higher than that reported by Sutcliffe and Weber.[18] It was then pointed out by Wells and Mays[22] that these results may have been over-interpreted and the apparent $[H^+]$ dependence that gave rise to the K_a values was either not justified by the data, or was due to ionization of the carboxylic acids. Wells and coworkers found that the reactions of aquacobalt(III) with quinol,[23] hydrazoic acid[22] and bromide[24] all were inconsistent with $K_a \geq 0.1$, but consistent with $K_a \leq 0.1$, as found by Sutcliffe and Weber.[18]

In later studies on the oxidation of Br^- [24] and Cl^-,[25] McAuley and coworkers used the K_a of Sutcliffe and Weber.[18] The new study with Cl^- confirmed the suggestion of Wells and Mays,[22] and McAuley et al[25] proposed that the earlier work may have been in error because of complications from the subsequent redox reactions at lower acidities.

Most recently Martinez co-workers[26] studied the reaction of $Co(OH_2)_6^{3+}$ with $H_3PO_4/H_2PO_4^-$ to yield the 1:1 complex $Co(H_2PO_4)(OH_2)_5^{2+}$. As part of this study, K_a values were determined from the electronic spectra of solutions of [Co(III)] (5 to 6 × 10^{-3} M) at acid concentrations of 0.05-0.4 M at 25 °C. They found values of K_a of 0.012 ± 0.002, 0.009 ± 0.006, 0.015 ± 0.005 at respective ionic strengths of 1.0, 2.0, and 3.0 M $LiClO_4$. Details of the data analysis are not given and < 25 % of the hydrolyzed species will be present at the lowest [H^+], but the K_a in 1 M $LiClO_4$ is similar to that reported by Sutcliffe and Weber[18] in 1 M $NaClO_4$.

Ligand Substitution of $Co(OH_2)_6^{3+}$. There are two distinct changes in absorbance observed in the wavelength range of 250-330 nm in the substitution reactions of $Co(OH_2)_6^{3+}$ with chloride ion,[19,25] bromide ion,[24] malic acid,[20] and thiomalic acid.[21] An initial increase in absorbance was assigned to the formation of an intermediate complex and a slower decrease in absorbance was assigned to the reduction of cobalt(III) by the ligand.

In the absence of cobalt(II) catalysis the mechanism in Scheme 1.1 was suggested,[19-21,24,25] with the ligand represented by X^-.

Scheme 1.1

$$Co(OH_2)_6{}^{3+} + X^- \underset{k_{-1}}{\overset{k_1}{\rightleftharpoons}} Co(OH_2)_5X^{2+} + H_2O \qquad K_1$$

$$Co(OH_2)_6{}^{3+} \rightleftharpoons Co(OH_2)_5OH^{2+} + H^+ \qquad K_a$$

$$\mathrm{Co(OH_2)_5OH^{2+} + X^- \underset{k_{-2}}{\overset{k_2}{\rightleftarrows}} Co(OH_2)_4(OH)X^+ + H_2O} \qquad K_2$$

$$\mathrm{Co(OH_2)_5X^{2+} \rightleftarrows Co(OH_2)_4(OH)X^+ \;+\; H^+} \qquad K_3$$

$$\mathrm{Co(OH_2)_5X^{2+} \xrightarrow{k_3} Products}$$

$$\mathrm{Co(OH_2)_4(OH)X^+ \xrightarrow{k_4} Products}$$

If the concentration of the substitution products are designated as $[\mathrm{CoX}]_\mathrm{T}$ = $[\mathrm{Co(OH_2)_5X^{2+}}]$ + $[\mathrm{Co(OH_2)_4(OH)X^+}]$ and the reactant as $[\mathrm{Co(III)}]_\mathrm{T}$ = $[\mathrm{Co(OH_2)_6^{3+}}]$ + $[\mathrm{Co(OH_2)_5OH^{2+}}]$, and it is assumed that K_a and K_3 are rapidly maintained equilibria, then the rate of formation of $[\mathrm{CoX}]_\mathrm{T}$ is given by equation (1.5)

$$\frac{\partial[\mathrm{CoX}]_\mathrm{T}}{\partial t} = \left(\frac{k_1[\mathrm{H^+}] + k_2K_a}{K_a + [\mathrm{H^+}]}\right)[\mathrm{X^-}][\mathrm{Co(III)}]_\mathrm{T} - \left(\frac{k_{-1}[\mathrm{H^+}] + k_{-2}K_3}{K_3 + [\mathrm{H^+}]}\right)[\mathrm{CoX}]_\mathrm{T}$$

(1.5)

Since $k_{-1} = k_1/K_1$, $k_{-2} = k_2/K_2$ and $K_1/K_a = K_2/K_3$, it is possible to substitute for the reverse rate constants and for K_3 in the numerator of the second term to obtain

$$\frac{\partial[\mathrm{CoX}]_\mathrm{T}}{\partial t} = \left(\frac{k_1[\mathrm{H^+}] + k_2K_a}{K_a + [\mathrm{H^+}]}\right)[\mathrm{X^-}][\mathrm{Co(III)}]_\mathrm{T} - \left(\frac{k_1[\mathrm{H^+}] + k_2K_a}{K_1(K_3 + [\mathrm{H^+}])}\right)[\mathrm{CoX}]_\mathrm{T} \qquad (1.6)$$

Since the total initial cobalt(III) ([Co(III)]$_0$) equals $[\mathrm{Co(III)}]_T + [\mathrm{CoX}]_T$, it is possible to substitute for $[\mathrm{Co(III)}]_T$ in terms $[\mathrm{CoX}]_T$ and $[\mathrm{Co(III)}]_0$ to obtain an integrateble first-order differential equation, from which, under pseudo-first-order conditions ($[\mathrm{H}^+]$, $[\mathrm{X}^-]_0$ >> $[\mathrm{Co(III)}]_0$), the observed rate constant is

$$k_{obs} = \left(k_1[\mathrm{H}^+] + k_2K_a\right)\left(\frac{[\mathrm{X}^-]}{K_a + [\mathrm{H}^+]} + \frac{1}{K_1\left(K_3 + [\mathrm{H}^+]\right)}\right) \tag{1.7}$$

Hill and McAuley[20,21] found that this equation was consistent with their observation, and that at constant $[\mathrm{H}^+]$ the experimental k_{obs} is given by equation (1.8)

$$k_{obs} = k_a + k_b[\mathrm{X}^-] \tag{1.8}$$

Comparison of equation (1.7) and (1.8) shows that, for a particular $[\mathrm{H}^+]$ the ratio k_a/k_b is given by equation (1.9), if $[\mathrm{H}^+] >> K_3$

$$\frac{k_a}{k_b} = \frac{K_a}{K_1[\mathrm{H}^+]} + \frac{1}{K_1} \tag{1.9}$$

Plots of k_a/k_b versus $[\mathrm{H}^+]^{-1}$ were used to determine K_1 and K_a, and the $[\mathrm{H}^+]^{-1}$ dependence of k_a gave k_1 and k_2K_a.

Wells and Mays[22] pointed out the problems with this analysis, as already mentioned in the discussion of K_a determinations. Wells and Mays[22] suggested that k_a is really independent of $[\mathrm{H}^+]$, and, if $[\mathrm{H}^+] >> K_a$, then the k_2K_a term must be negligible.

However, they went on to propose that the $[H^+]^{-1}$ dependence of k_b for malic[20] and thiomalic[21] acids is due to reactions of the conjugate bases of these ligands with $Co(OH_2)_6^{3+}$. But this simply adds another $[H^+]$ independent term to the first factor in brackets in the expression for k_{obs}. In other words they failed to recognize the kinetically indistinguishable pathways of $Co(OH_2)_5(OH)^{2+}$ + HX and $Co(OH_2)_6^{3+} + X^-$.

In a subsequent study of the reaction with the Cl^-, McAuley et al.[25] acknowledge that the earlier observations may have been complicated by the subsequent redox reactions, especially at lower acidities. This study gave values of k_a/k_b that were independent of $[H^+]$, as expected if $[H^+] >> K_a$. However, there are still problems in that the plots of the published k_a and k_b versus $[H^+]^{-1}$ yield small negative intercepts at 2.5 and 8 °C. It must be concluded that any k_1 values derived from these data have a large uncertainty. Furthermore, the k_2K_a value at 13 °C is ~ 25 % smaller than predicted from the values at 2.5 and 8.0 °C. However, a value at 13 °C that is consistent with the temperature dependence is not really inconsistent with the $[H^+]$ dependence data. If only the two lower temperatures are used, one obtains k_2K_a of 10.4 and 31 at 13 and 25 °C, respectively, with $\Delta H^* = 14.9$ kcal mol^{-1} and $\Delta S^* = -1.9$ cal mol^{-1} K^{-1}.

Recently, the reaction of $Co(OH_2)_6^{3+}$ with $H_3PO_4/H_2PO_4^-$ to yield the 1:1 complex $Co(OH_2)_5(PO_4H_2)^{2+}$ was studied by Martinez and co-workers.[26] The results are consistent with a modified version of Scheme 1.1, in which additional terms were included for the reaction of $Co(OH_2)_5(OH)^{2+} + H_3PO_4$ ($k_3\ K_a$) and $Co(OH_2)_5(OH)^{2+} + H_2PO_4^-$ ($k_4K_aK_c$), where K_c is the acid dissociation constant of H_3PO_4. This leads to equation 1.10 for the pseudo-first-order rate constant under conditions of $[H_3PO_4] >> [Co(III)]$,

$$k_{obs} = \left(k_1[\mathrm{H}^+]^2 + \left(k_2K_a + k_3K_c\right)[\mathrm{H}^+] + k_4K_aK_c\right) \times \left\{\frac{[\mathrm{H_3PO_4}]_\mathrm{T}}{\left(K_a + [\mathrm{H}^+]\right)\left(K_c + [\mathrm{H}^+]\right)} + \frac{1}{K_1\left([\mathrm{H}^+]^2 + \left(K_a'' + K_c'\right)[\mathrm{H}^+] + K_a'K_c'\right)}\right\} \quad (1.10)$$

where the kinetic pathways are $Co(OH_2)_6^{3+} + H_3PO_4$ (k_1), $Co(OH_2)_5(OH)^{2+} + H_3PO_4$ (k_2), $Co(OH_2)_6^{3+} + H_2PO_4^-$ (k_3) and $Co(OH_2)_5(OH)^{2+} + H_2PO_4^-$ (k_4), K_c and K_c' are acid dissociation constants for H_3PO_4 and $Co(OH_2)_5(PO_4H_3)^{3+}$, respectively, and K_a' and K_a'' are the hydrolysis constants for $Co(OH_2)_5(PO_4H_2)^{2+}$ and $Co(OH_2)_5(PO_4H_3)^{3+}$, respectively.

The analysis of Martinez co-workers[26] indicated that the k_1 pathway does not make a significant contribution. However, the ionic strength dependence of the values they determined from the data is unusual. The values of (k_2K_a + k_3K_c) decrease by a factor of 16 and then increases by a factor of 2.5 as the ionic strength changes from 1.0 to 2.0 to 3.0 M. For the same ionic strength change, $k_4K_aK_c$ increases monotonically by a factor of 5.

These observations naturally lead to a more detailed examination of the rather limited amount of published data. It appears that the kinetic results were done at $[H^+] \geq 0.5$ M, so that the values of K_a and K_c give the condition that $[H^+] >> K_a, K_c$. It seems probable that $K_a' \approx K_a'' \approx K_a$, so that $[H^+] >> K_a', K_a''$. Finally, the results of preliminary analysis indicate that $K_c' > [H^+], K_a''$. With these conditions and omitting the k_1 pathway, as suggested by Martinez co-worker[26] the expression for k_{obs} simplifies to equation (1.11)

$$k_{obs} = \left(\left(k_2 K_a + k_3 K_c\right)[\mathrm{H}^+] + k_4 K_a K_c\right)\left\{\frac{[\mathrm{H_3PO_4}]_\mathrm{T}}{[\mathrm{H}^+]^2} + \frac{1}{K_1 K_c'[\mathrm{H}^+]}\right\} \tag{1.11}$$

In Figure 1 of the paper by Martinez co-workers,[26] k_{obs} is plotted versus $[\mathrm{H_3PO_4}]_\mathrm{T}$ for a series of $[\mathrm{H}^+]$ (0.50 – 3.0 M) at 3.0 M ionic strength. The plots are linear, as predicted by the above equation. The slopes of these lines at each $[\mathrm{H}^+]$ times $[\mathrm{H}^+]^2$ show a linear dependence on $[\mathrm{H}^+]$ and the above equation predicts that the slope of this line is $(k_2K_a + k_3K_c) = 2.8 \times 10^{-2}$ and the intercept is $k_4K_aK_c = 8.0 \times 10^{-3}$. The above equation also predicts that $[\mathrm{H}^+]$ times the slope to intercept ratio should be a constant equal to K_1K_c'. This is found to be true and is the rationale for the assumption that $K_c' >> [\mathrm{H}^+]$; the data give $K_1K_c' = 1.09 \pm 0.06$.

In Figure 2 of the same paper, values of the first factor in equation (1.11) are plotted versus $[\mathrm{H}^+]$ at 1.0 M ionic strength. The plot has a slope of $(k_2K_a + k_3K_c) = 4.6 \times 10^{-2}$ and an intercept of $k_4K_aK_c \sim 8.0 \times 10^{-3}$. These values of $k_4K_aK_c \sim 8.0 \times 10^{-3}$ do not show the wide variation with ionic strength suggested by Martinez and co-workers.[26] The value of $(k_2K_a + k_3K_c)$ at 1.0 M agrees with the 4.3×10^{-2} given by Martinez and co-workers,[26] but at 3.0 M these authors give 6.5×10^{-2}, which is substantially different from the 2.8×10^{-2} obtained here. The latter value indicates a moderate ionic strength dependence of $(k_2K_a + k_3K_c)$. Unfortunately there are no published data at 2.0 M ionic strength to permit a similar reanalysis. Since different results were ostensibly obtained from the same data, one can only suppose that there was some error in the original analysis.

In addition to these studies in which there is direct evidence for ligand substitution, several redox reactions have been assigned an inner-sphere mechanism in which ligand substitution is rate controlling. This assignment is made on the basis of their similarity in rate to known substitution reactions. Davies and Watkins[27] have summarized the results and the mechanisms of the redox reactions.

All this information is summarized in Table 1.1. This Table gives the results for substitution on $Co(OH_2)_6^{3+}$ (k_{OH2}) and $Co(OH_2)_5(OH)^{2+}$ ($k_{OH}K_a$), where the K_a has been retained in the latter because of uncertainty about its value. If the substitution mechanism is I_D, then one expects k_{OH2} and $k_{OH}K_a$ to be relatively independent of the ligand, and possibly to be somewhat larger for anions because of ion-pair effects. In general, the kinetics is dominated by the $k_{OH}K_a$ pathways and these values do seem to be rather insensitive to the nature of the entering ligand. In many cases k_{OH2} was too small, relative to the $k_{OH}K_a$ term, to be identified, but it does seem that k_{OH2} tends to be in the range of 1 to 10. In the phosphoric acid system, this analysis indicates that the $Co(OH_2)_6^{3+} + H_2PO_4^-$ pathway dominates over the $Co(OH_2)_5(OH)^{2+} + H_3PO_4$ pathway.

Cobaloximes

Bis(dimethylglyoximato)cobalt(II) is commonly called cobaloxime. It is formed by the complexation of cobalt(II) by anions of dimethylglyoxime (2,3-butanedione dioxime, $dmgH_2$, Figure 1.1). In forming the cobaloxime complex, the two chelating $dmgH^-$ ligands are joined by hydrogen bonds to form a rather stable macrocycle ($Co(dmgH)_2$ in Figure 1.1). The hydrogen bonds can be replaced by $-BF_2$ groups to give

Table 1.1. Kinetic Parameters for the Reactions of $Co(OH_2)_6^{3+}$ with Various Ligands.

Ligand, X	k_{OH2} $M^{-1}s^{-1}$	$k_{OH}K_a$ s^{-1}	K_a M^{-1}	Reference
Chloride ion	≤ 3	26	0.22	19[a]
	-	31	< 0.1	25[b]
Malic acid	5.4	7.0	0.10	20[c]
Thiomalic acid	8.2	16	0.05	21[c]
$SC(NH_2)_2$	7	52		28[d]
H_3PO_4	-	(≤ 0.043)	0.012	26[e]
$H_2PO_4^-$	(≤ 6.1)	29	0.012	26[e]
H_2O_2		23		27[a]
HNO_2		17.2		27[a]
Br^-		30.4		27[a]
SCN^-		79.6		27[a]

[a] Data at 25 °C, ionic strength 3.0 M. [b] Extrapolated at 25 °C, ionic strength 0.50 M. [c] Data at 7 °C, ionic strength 0.25 M $NaClO_4$. [d] Extrapolated at 25 °C, ionic strength 0.82-1.50 M. [e] Data at 25 °C, ionic strength 1.0 M

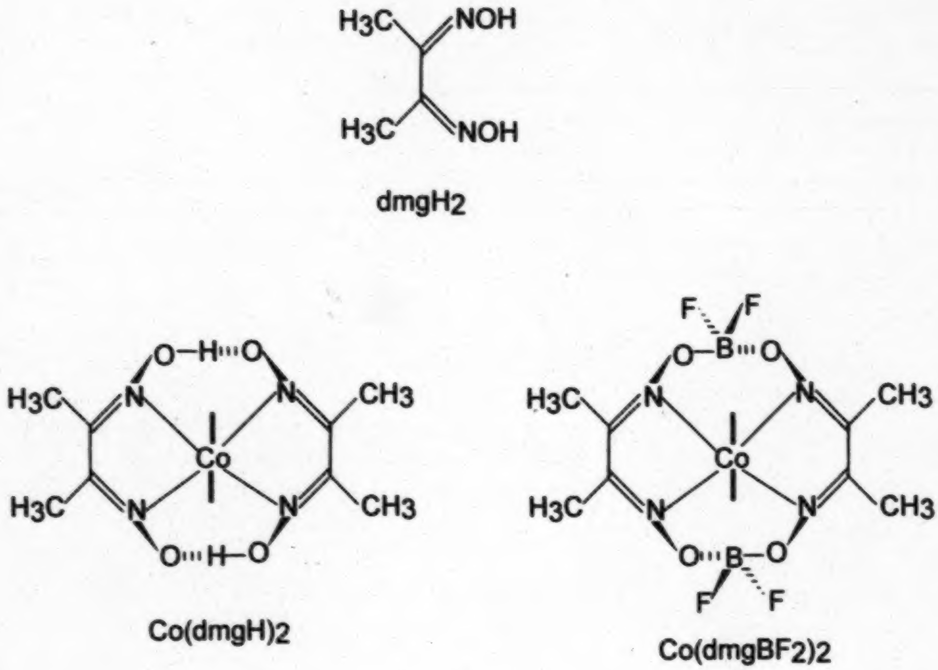
H3C
NOH
H3C
NOH
dmgH2
O
H
O
H3C
N
N
CH3
Co
H3C
N
N
CH3
O
H
O
Co(dmgH)2
F
F
O
B
O
H3C
N
N
CH3
Co
H3C
N
N
CH3
O
B
O
F
F
Co(dmgBF2)2

Figure 1.1. The structures of $dmgH_2$, $Co(dmgH)_2$ and $Co(dmgBF_2)_2$.

an even more stable macrocycle (Co(dmgBF$_2$)$_2$ in Figure 1.1). The axial positions below and above the chelate ring may be occupied by various ligands e.g. water, methanol, etc.

In spite of extensive earlier investigations, complexes of cobaloximes continue to be actively studied. They hold continued interest not only because of their relationship to the intriguing chemistry of vitamin B$_{12}$,[29] but also because they provide a rich chemistry in themselves. For example, they form a wide range of derivatives with different axial ligands and with the methyl groups replaced by other substituents, they can have cobalt in the I, II and III oxidation states and they form stable alkyl complexes.[30,31]

Cobaloximes in Oxidation State (III). These complexes are prepared in basic media (NaOH) by mixing a slight excess of the appropriate glyoxime with a cobalt(II) salt in the presence of an oxidizing agent such as O_2 or H_2O_2.[32] The Co(III) in these complexes has a low-spin d^6 electronic configuration and the complexes are diamagnetic. Cobaloximes(III) are generally kinetically rather inert toward substitution in both acidic and basic aqueous solution. X-ray crystallographic studies of solids[33] and NMR studies in solution[33] reveal that the cobalt atom is 6-coordinate with a square-planar arrangement of the (dmgH)$_2$ and with two axial positions occupied by Lewis bases to form trans-XLCo(dmgH)$_2$ complexes, where X and L may be the same or different Lewis bases. It should be noted that one of the axial ligands could be an alkyl group so that there is a wide range of organometallic derivatives. Although XLCo(dmgBF$_2$)$_2$ complexes are electronically and structurally analogues to the XLCo(dmgH)$_2$ complexes, they do not form organometallic species.

Cobaloximes in Oxidation State (II). The cobalt(II) in cobaloximes has a d^7, low-spin configuration in a tetragonally distorted octahedral arrangement of the ligands. The cobaloxime complexes are prepared in basic media (NaOH) by mixing an appropriate glyoxime with a cobalt(II) salt under anaerobic conditions.[34] These complexes are generally sensitive to oxidation by oxygen, and the sensitivity depends on the nature of the glyoxime ligand. Electron withdrawing groups in the equatorial ligand plane tend to stabilize the Co(II) oxidation state. For example, a solution of $Co(dmgH)_2$ is oxidized in few seconds on exposure to air, while $Co(dmgBF_2)_2$, with the strong electron withdrawing $-BF_2$ substituents, can be handled in air without undergoing any oxidation. The structures of $Co(dmgBF_2)_2$ and $Co(dmgH)_2$ have been characterized by Espenson and co-workers[35] and by Fallon and Gatehouse,[36] respectively.

Cobaloximes and Coenzyme B_{12}. Schrauzer and Deutsch[37] first found that cobaloximes mimic many reactions of coenzyme B_{12} and therefore serve as models for the coenzyme. Both cobaloximes and coenzyme B_{12} can have cobalt in oxidation states (I), (II), and (III). In the coenzyme, these are called B_{12s}, B_{12r}, and B_{12} (where r stands for reduced and s for super-reduced).

One remarkable feature of cobaloximes and coenzyme B_{12} is their ability to form rather stable σ-bonded organometallic alkyl derivatives. The Co-C bond in B_{12} was the first metal-carbon bond to be recognized in biology. The Co-C bond energies for $(py)(PhCH_2)Co(dmgH)_2$ and coenzyme B_{12} (Co-Adenosyl) were found to be ~ 22 and ~ 30 kcal mol^{-1}, respectively.[38,39]

It is now believed that the unique Co-C bonds in these systems may result from two features.[39] First, both the $(dmgH)_2$ in cobaloximes and the corrin ring in B_{12} have some π-conjugation to stabilize a σ-alkyl derivative. Too much π-conjugation does not appear to be favorable. Neither fully saturated ligands, such as 1,4,8,11-tetraazacyclotetradecane ([14]aneN_4), nor the more extensively delocalized porphyrin system, allow cobalt to form stable alkyl complexes. Second, for alkyl derivatives to undergo β-elimination a vacant coordination site cis to the alkyl group is required, as shown in equation (1.12),

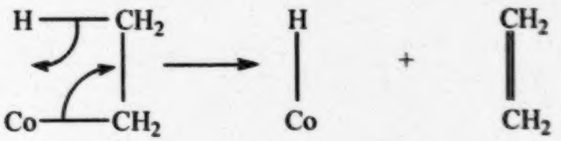

(1.12)

A chelating equatorial ligand inhibits this process by preventing the formation of the vacant site that is needed for β-elimination to take place.

Scope of Present Work

The preceding outline provides a brief overview of the chemistry of cobaloximes. There is great deal of information available on stable cobaloxime(III) complexes. However, the cobaloximes(II) are much less well characterized, and the goal of the present study was to at least partially redress this deficiency. Outer-sphere redox reactions have been studied in order to provide an estimate of the self-exchange rate for cobaloxime(III)/(II) system through the application of Marcus theory. The reactions of $Co(dmgBF_2)_2(H_2O)_2$ with $Fe(bipy)_3^{3+}$ and $Co(OH_2)_6^{3+}$ were studied. It is hoped that this information will be relevant to the properties of the corresponding coenzyme B_{12} species.

An examination of the preparative methods of aqueous cobalt(III) perchlorate in the literature prompted a search for a more convenient method that would allow access to a wider range of Co(III) and H^+ concentrations. Also, contradictory information in the literature on the hydrolysis constant (K_a), the species present in aqueous solution and the complexation mechanism of $Co(OH_2)_6^{3+}$, stimulated our interest to study this system. The cobalt(III) formed from our new preparative method was reacted with $Co(dmgBF_2)_2(H_2O)_2$, water and H_2O_2 (since it was a product of cobalt(III) decomposition in water) and the kinetics of these reactions were studied in detail.

References

(1) Biedermann, G.; Orecchio, S.; Romano, V.; Zingales, R. *Acta Chim. Scand.* **1986**, *A40*, 161.

(2) Warnqvist, B. *Inorg. Chem.* **1970**, *9*, 682.

(3) Cotton, F. A.; Wilkinson, G. *Advanced Inorganic Chemistry*; John Wiley and Sons; New York, New York, 4th Ed. **1980**; pg. 768.

(4) Baxendale, J. H.; Wells, C. F. *Trans. Faraday Soc.* **1957**, *53*, 800.

(5) Hargreaves, G.; Sutcliffe, L. H. *Trans. Faraday Soc.* **1955**, *51*, 786.

(6) Swan, S. Jr.; Xanthakos, T. S. *J. Amer. Chem. Soc.* **1931**, *53*, 400.

(7) Weiser, D. W. *Ph. D. Thesis*, University of Chicago, **1956**.

(8) Habib, H. S.; Hunt, J. P. *J. Amer. Chem. Soc.* **1966**, *88*, 1668.

(9) Hofmann-Bang, N; Wulf, I. *Acta Chem. Scand.* **1955**, *9*, 1230.

(10) Davies, G.; Warnqvist, B. *Coord. Chem. Rev.* **1970**, *5*, 349.

(11) Johnson, D. A.; Sharpe, A. G. *J. Chem. Soc. A,* **1966**, 798.

(12) Beattie, J. K.; Best, S. P.; Skelton, B. W.; White, A. H. *J. Chem. Soc. Dalton* Trans. **1981**, 2105.

(13) Navon, G. *J. Phys. Chem.* **1981**, *85*, 3547.

(14) Johnson, D. A.; Nelson, P. G. *Inorg. Chem.* **1999,** *38*, 4949.

(15) Aderson, W. P.; Edwards, W. D.; Zerner, M. C. *Inorg. Chem.* **1986**, *25*, 2728.

(16) Bawn, C. E. H.; White, A. G. *J. Chem. Soc.* **1951**, 331.

(17) Sutcliffe, L. H.; Weber, J. R. *J. Inorg. Nucl. Chem.* **1960**, *12*, 281.

(18) Sutcliffe, L. H.; Weber, J. R. *Trans. Faraday Soc.* **1956**, *52*, 1225.

(19) Conocchioli, T. J.; Nancollas, G. H.; Sutin, N. *J. Chem. Soc. A,* **1968**, 665.

(20) Hill, J.; McAuley, A. *J. Chem. Soc. A,* **1968**, 1169.

(21) Hill, J.; McAuley, A. *J. Chem. Soc. A,* **1968**, 2405.

(22) Wells, C. F.; Mays, D. *J. Chem. Soc. A,* **1969**, 2175.

(23) Wells, C. F.; Kuritsyn, L. V. *J. Chem. Soc. A,* **1969**, 2930.

(24) Wells, C. F.; Mays, D. *J. Chem. Soc. A,* **1968**, 2740.

(25) McAuley, A.; Malik, M. N.; Hill, J. *J. Chem. Soc. A,* **1970**, 2461.

(26) Ferrer, M.; Llorca, J.; Martinez, M. *J. Chem. Soc. Dalton Trans.* **1992**, 229.

(27) Davies, G.; Watkins, K. O. *J. Phys. Chem.* **1970**, *74*, 3388.

(28) McAuley, A.; Gomwalk, U. D. *J. Chem. Soc. A,* **1969**, 977.

(29) Ochiai, E. *Bioinorganic Chemistry: An Introduction;* Allyn and Bacon; Boston, Massachusetts, **1977**; pg. 311.

(30) Dodd, D.; Johnson, M. D. *J. Organomet. Chem.* **1973**, *52*, 1.

(31) Wong, C. L.; Switzer, J. A; Balakrishnan, K. P.; Endicott, J. F. *J. Amer. Chem. Soc.* **1980**, *102*, 5511.

(32) Ablov. A. V.; Samus, N. M. *Russ. J. Inorg. Chem.* **1960**, *5*, 410.

(33) Bresciani-Pahor, N.; Forcolin, M.; Marzilli, L. G.; Randaccio, L.; Summers, M. F.; Toscano, P. J. *Coord. Chem. Rev.* **1985**, *63*, 1.

(34) Schrauzer, G. N. *Inorg. Synth.* **1968**, *11*, 61.

(35) Bakac, A.; Brynildson, M. E.; Espenson, J. H. *Inorg. Chem.* **1986**, *25*, 4108.

(36) Fallon, G. D.; Gatehouse, B. M. *Cryst. Struct. Comm.* **1978**, *7*, 263.

(37) Schrauzer, G. N.; Deutsch, E. *J. Amer. Chem. Soc.* **1969**, *91*, 3341.

(38) Hay, B. P.; Finke, R. G. *J. Amer. Chem. Soc.* **1986**, *108*, 4820.

(39) Halpern, J. *Science*, **1985**, *227*, 869.

CHAPTER 2. Synthesis and Characterization of Hexaamminecobalt(III) *tris*(carbonato)cobaltate(III) and Hexaaquacobalt(III), [$Co(OH_2)_6^{3+}$]

Introduction

It has long been known that the oxidation of cobalt(II) by hydrogen peroxide in the presence of alkalai metal bicarbonate or carbonate results in an intensely green solution. The colored species is commonly believed to be the $Co(CO_3)_3^{3-}$ ion. Mori et al.[1] and Bauer and Drinkard[2] isolated K^+ and Na^+ salts of the $Co(CO_3)_3^{3-}$ ion, respectively. There is an ambiguity about the ligands on the cobalt(III) in these solids; they can be formulated as $M_3[Co(CO_3)_3]\bullet 3H_2O$ or $M_3[Co(CO_3H)_3(OH)_3]$, where M is K^+ or Na^+. The potassium salt is soluble in water and difficult to separate from bicarbonate impurities. The sodium salt is rather insoluble in water unless excess bicarbonate is present. This may imply that the sodium salt really does not contain the *tris*(carbonato) complex. Their aqueous solutions are somewhat unstable in the absence of excess bicarbonate, forming hydrous cobalt(III) oxide. The two salts, when dry, can be stored on a shelf and have been used as intermediates for synthesis of various cobalt(III) complexes,[1-3] but do not seem to have been used as sources for $Co(OH_2)_6^{3+}$.

The very stable and insoluble $Co(NH_3)_6^{3+}$ salt of $Co(CO_3)_3^{3-}$ ion was first described by McCutcheon and Schuele[4] who prepared it by a somewhat circuitous route starting from $Co(NH_3)_4CO_3^+$. The composition was confirmed by elemental analysis of Co and N. Gillard et al.[5] reported the $Co(en)_3^{3+}$ salt of $Co(CO_3)_3^{3-}$ ion, which was synthesized by simply mixing saturated solutions of $K_3[Co(CO_3)_3]\cdot3H_2O$ and $Co(en)_3Cl_3$ at 0 °C to obtain a crystalline product. They compared the infrared spectrum of the salt to that of free carbonate (1380 cm^{-1}), unidentate carbonate (1450 and 1370 cm^{-1}) and bidentate carbonate (1592 and 1255 cm^{-1}).[6] Gillard et al.[5] suggested that the observed infrared bands at 1585 and 1280 cm^{-1} in $[Co(en)_3][Co(CO_3)_3]$ are consistent with chelated carbonates. In this Chapter, the X-ray structure of $[Co(NH_3)_6][Co(CO_3)_3]$ shows that all the carbonates are chelated.

In addition to the above, Gillard et al.[5] observed infrared bands for $K_3[Co(CO_3)_3]\cdot3H_2O$ at 1495, 1335 cm^{-1} and a weak one at 1600 cm^{-1}, while $Na_3[Co(CO_3)_3]\cdot3H_2O$ has bands at 1470 and 1345 cm^{-1}. They suggested that these species may contain unidentate bicarbonate.

There are three methods of preparing solutions of aqueous cobalt(III) perchlorate in the literature. Such solutions have been prepared by treatment of $Co_2(SO_4)_3\cdot18H_2O$ in perchloric acid with $Ba(ClO_4)_2$ at 0 °C,[7,8] the reaction of perchloric acid with green solutions formed by the addition of hydrogen peroxide to saturated solutions of cobalt(II) perchlorate and $NaHCO_3$ or $KHCO_3$ [9,10] and the direct electrolytic oxidation of cobalt(II) perchlorate in perchloric acid.[8-14] The preparative details, merits and demerits of these methods were discussed in Chapter 1. It should be noted that the studies of aqueous cobalt(III) would be greatly aided by a convenient, rapid method of preparation, preferably starting from a well characterized solid.

In the present work, it is shown that the $Co(NH_3)_6^{3+}$ salt of $Co(CO_3)_3^{3-}$ can be prepared in crystalline form and serves as a reliable source of the aqueous cobalt(III) ion.

It is reported here that solutions of aqueous cobalt(III) in a range of initial concentrations and acidities can be conveniently prepared by the reaction of equation (2.1).

$$[Co(NH_3)_6][Co(CO_3)_3]\,(s) + 6HX\,(aq) \longrightarrow [Co(NH_3)_6]X_3\,(s) + Co(OH_2)_6^{3+}\,(aq) + 3CO_2\,(g) + 3X^- \qquad (2.1)$$

The utility of this reaction relies on the very low solubility of $Co(NH_3)_6X_3$ ($X = ClO_4^-$, NO_3^- and $CF_3SO_3^-$). The solid is easily separated from the solution by centrifugation. The final acidity is easily controlled by starting with the appropriate excess amount of the acid HX, and the cobalt(III) is controlled by the mass of $[Co(NH_3)_6][Co(CO_3)_3]$ used.

The chemistry of aqueous cobalt(III) has been the subject of a number of studies,[8-13] but the kinetic stability, redox reactivity and nature of the hydrolyzed and possibly dimeric state of aqueous cobalt(III) remain unsettled questions. There is no doubt this results, at least in part, from the tedious synthesis of aqueous cobalt(III) by electrolysis[8-14] in strongly acidic solutions.

Experimental

Preparation of Hexaamminecobalt(III) Chloride.[15] Two hundred and forty grams of cobalt(II) chloride hexa-hydrate (GFS) and 160 g of ammonium chloride (Fisher Scientific) were added to 200 mL of water. The mixture was stirred until most of the salts were dissolved. Then 4.0 g of activated charcoal (Norit) and 500 mL of concentrated aqueous ammonia (Malinckrodt) were added. The mixture was cooled to

10 °C in ice and 98.0 mL of 30 % hydrogen peroxide (ACP) were added slowly from a burette, while keeping the solution cold and stirring continuously. The resultant yellow brown solution was heated to 60 °C on a steam bath for 30 minutes; the product began to precipitate toward the completion of the heating. The reaction mixture was cooled to 0 °C in ice, and the mixture of activated charcoal and product was collected and dried by vacuum filtration. The mixture was added to a solution of 25.0 mL of concentrated hydrochloric acid (Anachemia) in 1.5 L of hot water and heated until all the salt had dissolved. The charcoal residue was removed by vacuum filtration of the hot solution, and the filtrate was placed in an ice bath and 400 mL of ice-cold concentrated hydrochloric acid was added with stirring. After the mixture had cooled to about 0 °C, the solid precipitate was collected by vacuum filtration and the pure product was washed with 100 mL of ice-cold 60 % ethanol (Caledon) and 100 mL of 95 % ethanol. The yield was 259 g, 96 % of the expected yield based on the initial amount of Co(II) chloride hexa-hydrate. The electronic spectrum of $Co(NH_3)_6Cl_3$ was characterized by its absorption maxima at 472 nm with $\varepsilon = 56.7\ M^{-1}\ cm^{-1}$ in water, which is consistent with that reported by Sargeson and co-workers.[16]

Preparation of $[Co(NH_3)_6][Co(CO_3)_3]$. A solution of $Co(CO_3)_3^{3-}$ was prepared[17] by dissolving 2.9 g (0.010 mole) of cobalt(II) nitrate ($Co(NO_3)_2{\bullet}6H_20$, Fisher Scientific) in 250 mL of water and then adding 75.0 g (0.89 mole) of sodium bicarbonate (ACP). The mixture was stirred for 10 minutes and then 2.0 mL of 30 % hydrogen peroxide (ACP) in 250 mL of water was added gradually over 1 hour while stirring. On dilution with water to 1 liter, the un-dissolved $NaHCO_3$ went into solution and the resultant green solution was stirred overnight.

A 3.10 g (1.15 × 10^{-2} moles) sample of hexaamminecobalt(III) chloride was dissolved in 200 mL of water. To obtain the maximum yield of the dark green crystals, the 200 mL of hexaamminecobalt(III) chloride solution was added to the 1 liter solution of $Co(CO_3)_3^{3-}$ and the solution was stirred for 20 to 30 minutes, covered to reduce loss of solution through evaporation and kept in ice in the refrigerator overnight. The overall reaction is shown in equation (2.2).

$$Co(CO_3)_3^{3-}(aq) + Co(NH_3)_6^{3+}(aq) \longrightarrow [Co(NH_3)_6][Co(CO_3)_3](s) \qquad (2.2)$$

The product was collected by vacuum filtration, washed with copious amounts of water to remove any precipitated hexaamminecobalt(III) chloride and dried on the vacuum line. The yield was 1.166 g, 29.15 % based on the initial cobalt(II) nitrate.

The dark green needle-like crystals are extremely insoluble in water, ethanol, acetone and acetonitrile. Elemental analysis for C, H and N was performed by Microanalytical Laboratory at University of Alberta Chemistry Department. Analysis calculated for $[Co(NH_3)_6][Co(CO_3)_3]$: H, 4.5 %; N, 21.0 % and C, 9.0 %. Found H, 4.5 %; N, 20.5 % and C, 9.2 %.

It should be noted that the green solution remaining after separating the crystals, when treated with excess $Co(NH_3)_6^{3+}$ forms a light green powder which does not give reproducible equivalent weights from different preparations.

Characterization of $[Co(NH_3)_6][Co(CO_3)_3]$

Determination of the Molecular Formula of $[Co(NH_3)_6][Co(CO_3)_3]$. Various amounts of the green crystals were reacted with excess HCl at ~ 0 °C as shown in equation (2.3).

$$[Co(NH_3)_6][Co(CO_3)_3](s) + 6HCl(aq) + 3H_2O(l) \longrightarrow Co(NH_3)_6^{3+}(aq) + 3CO_2(g) + Co(OH_2)_6^{2+}(aq) + 3Cl_2(g) \tag{2.3}$$

The solution was boiled briefly to expel the produced chlorine and carbon dioxide, cooled to room temperature, diluted to 25.0 mL in a volumetric flask and the absorbance was determined in a 1.00 cm path-length cell on the Cary 219 spectrophotometer. The spectrum confirmed the presence of $[Co(NH_3)_6]^{3+}$ from the band maximum at 472 nm. With the assumption that the $[Co(NH_3)_6^{3+}]$ equals $[Co(OH_2)_6^{2+}]$ in the resultant solution, and from their respective extinction coefficients of 56.7 and 3.24 $M^{-1}cm^{-1}$ at 472 nm,[16] the absorbance can be used to calculate $[Co(NH_3)_6^{3+}]$ from equation (2.3).

$$\left[Co(NH_3)_6^{3+}\right] = \frac{Abs_{472nm}}{\left(\varepsilon_{Co(NH_3)_6^{3+}}\right) + \left(\varepsilon_{Co(OH_2)_6^{2+}}\right)} = \frac{Abs_{472nm}}{(56.7 + 3.24)\,M^{-1}cm^{-1}} \tag{2.4}$$

With the assumption that there is 1 mole of $Co(NH_3)_6^{3+}$ per mole of green crystals, then the molar mass is given by equation (2.4).

$$\text{Molar mass} = \frac{\text{mass of green crystals}}{[\text{Co(NH}_3)_6{}^{3+}] \times 0.025\text{L}} \qquad (2.5)$$

The results of several determinations are given in Table 2.1 and give an average molar mass of 400.3 ± 1.4 g/mol, consistent with the predicted value of 400.09 g/mol for $[Co(NH_3)_6][Co(CO_3)_3]$.

Determination the Equivalent Weight. Weighed amounts of dark green crystals were dissolved in water containing known amounts of HCl at ice temperature. The solution was stirred until no carbon dioxide evolved, and then boiled briefly to remove the gases (chlorine and carbon dioxide). The solution was cooled to room temperature and diluted to 25.0 mL in a volumetric flask. Four aliquots of 5.0 mL each were transferred to 25.0 mL Erlenmeyer flasks and 3-drops of bromothymol blue were added, and the solutions were titrated with 0.100 M NaOH. The total amount of $[H^+]$ used to decompose the solid was determined by subtracting the moles of excess (unreacted) acid from the moles of the acid originally added. The equivalent weight was calculated from equation (2.5) and the results are summarized in Table 2.2.

$$\text{equivalent weight} = \frac{\text{mass of green crystals}}{\text{reacted moles of HCl}} \qquad (2.6)$$

The average equivalent weight is 66.63 ± 1.10. This agrees with the predicted value of 400.09/6 = 66.7, if the compound reacts as shown in equation (2.3)

Table 2.1. Determination of the Molar Mass of $[Co(NH_3)_6][Co(CO_3)_3]$.

Mass of crystals (g)	Abs[a] (472 nm)	Molarity[a] (M)	Moles (mole)	Molar mass (g/mole)
7.85×10^{-3}	0.0468	7.81×10^{-4}	1.95×10^{-5}	402
3.55×10^{-2}	0.2134	3.56×10^{-3}	8.91×10^{-5}	399
3.61×10^{-2}	0.2146	3.58×10^{-3}	8.95×10^{-5}	403
3.71×10^{-2}	0.2230	3.72×10^{-3}	9.30×10^{-5}	399
4.74×10^{-2}	0.2847	4.78×10^{-3}	1.18×10^{-4}	399
8.84×10^{-2}	0.5299	8.84×10^{-3}	2.21×10^{-4}	400

[a] For sample dissolved in 25.0 mL of aqueous HCl.

Table 2.2. Determination of the Equivalent Weight of $[\mathrm{Co(NH_3)_6}][\mathrm{Co(CO_3)_3}]$.

Mass of crystals (g)	$\mathrm{HCl}_{\mathrm{initial}}$ (mole)	NaOH (mole)	$\mathrm{HCl}^{+}_{\mathrm{excess}}$ (mole)	$\mathrm{HCl}_{\mathrm{used}}$ (mole)	Eq. weight
0.0079	2.00×10^{-3}	1.89×10^{-3}	1.89×10^{-3}	1.10×10^{-4}	65.45
0.0450	4.00×10^{-3}	3.33×10^{-3}	3.33×10^{-3}	6.73×10^{-4}	66.82
0.0884	9.75×10^{-3}	8.45×10^{-3}	8.45×10^{-3}	1.30×10^{-3}	68.00
0.1080	1.05×10^{-2}	8.87×10^{-3}	8.87×10^{-3}	1.63×10^{-3}	66.26

X-ray Crystallography. A 0.32 × 0.06 × 0.05 mm crystal was mounted with silastic adhesive on a glass fiber. Precession photographs (CuKα) gave preliminary lattice constants and showed absences consistent with the monoclinic space group $P2_{1/C}$. The crystal was then mounted on an automated diffractometer (Bruker P4/RA/SMART 1000 CCD)[18] equipped with MoKα radiation for the remaining studies. Least-squares analysis centered with MoKα radiation (λ = 0.71073 Å) yielded the following unit cell information; a = 17.8070 Å, b = 10.5466 Å, c = 13.7297 Å, β = 104.482°, V = 2496.5 $Å^3$, ρ = 2.129 g/cm^{-3}(density of the unit cell), Z = 8 (molecules in the unit cell) and μ = 2.716 mm^{-1} (linear absorption coefficient of the unit cell).

Intensity data were collected by the θ - 2θ scan method with Zr-filtered MoKα radiation. A symmetric scan of 0.3° plus an allowance for spectral dispersion was used with a scan rate of 0.3° per 30 second. Of the 12698 data examined with $2\theta \leq 51.40°$, 3048 data with $I > 2\sigma I$ (I is the intensity) were used throughout the solution and refinement of the structure using direct methods (SHELXL-93).[19] Full matrix isotropic least-squares final refinement resulted in discrepancy factors of $R_1 = \sum /Fo/ - /Fc// /\sum /Fo/ = 0.0407$ and $wR_2 = [\sum w(Fo^2 - Fc^2)^2/\sum w(Fo^4)]^{1/2} = 0.0998$.

Production of $Co(OH_2)_6^{3+}$ from $[Co(NH_3)_6][Co(CO_3)_3]$. The following procedure was used to determine the amount of $Co(OH_2)_6^{3+}$ produced when the green crystals dissolve in acid (equation 2.1). A weighed amount of $[Co(NH_3)_6][Co(CO_3)_3]$ crystals was dissolved in 20 mL of 2.50 M $HClO_4$ at ice temperature, stirred for 1½ hours till no carbon dioxide evolved, and then diluted to 25.0 mL before removing the precipitate. The precipitate $Co(NH_3)_6(ClO_4)_3$ was removed by centrifugation and 5.0 mL of the solution was transferred to a 50 mL Erlenmeyer flask, and ~ 0.10 g (6.67×10^{-4} mole) of NaI was added. The sample was diluted to 25.0 mL and titrated with 2.50×10^{-3} M $Na_2S_2O_3$. The thiosulfate solution was added slowly while swirling the flask to mix the two solutions until the solution turned pale yellow. Then 10 drops of starch solution was added and the titration was continued with stirring until the solution turned colorless. Based on equation (2.7) and (2.8) the moles of $Co(OH_2)_6^{3+}$ in 5.0 mL of stock solution equals the moles of $S_2O_3^{2-}$ added at the end point. The results are shown in Table 2.4.

$$2Co(OH_2)_6^{3+} + 2I^- \longrightarrow 2Co(OH_2)_6^{2+} + I_2 \qquad (2.7)$$

$$I_2 + 2S_2O_3^{2-} \longrightarrow 2I^- + S_4O_6^{2-} \qquad (2.8)$$

From this work, the maximum yield of $Co(OH_2)_6^{3+}$ produced from $[Co(NH_3)_6][Co(CO_3)_3]$ was ~ 90 %. Based on general experience, the yield is best at higher acidity (> 1.00 M) and lower temperature (< 5 °C). The normal temperature was 0 °C in this work. It should be noted from Table 2.4 that when the powder of $[Co(NH_3)_6][Co(CO_3)_3]$ obtained when excess $Co(NH_3)_6^{3+}$ is used, the yield of aqueous cobalt(III) reduces tremendously to ~ 70 %.

The spectrum of the $Co(OH_2)_6^{3+}$ produced from $[Co(NH_3)_6][Co(CO_3)_3]$ was measured on the Cary spectrophotometer. The results, summarized in Table 2.3, give average extinction coefficient values of 40.0 ± 0.5 and 35.0 ± 0.4 $M^{-1}cm^{-1}$ at 400 and 605 nm, respectively, based on the cobalt(III) concentration determined by iodiometry.

Table 2.3. Determination of the Yield and Extinction Coefficient of $Co(OH_2)_6^{3+}$.

	1[a]	2[b]	3[a]	4[a]
$[Co(NH_3)_6][Co(CO_3)_3]$, g[c]	0.0481	0.0601	0.0613	0.1202
$S_2O_3^{2-}$, mL	8.38	8.68	10.86	21.40
$10^3[Co(OH_2)_6^{3+}]$, M (theory)	4.80	6.00	6.10	12.00
$10^3[Co(OH_2)_6^{3+}]$, M (found)	4.19	4.34	5.43	10.70
% Yield	87.1	72.3	89.0	91.7
$\varepsilon_{605\ nm}$, M^{-1} cm^{-1} [d]	35.5	35.0	35.2	34.5
$\varepsilon_{400\ nm}$, M^{-1} cm^{-1} [d]	40.2	39.2	40.0	40.5

[a] Prepared from different batches of green crystals. [b] Prepared from the green powder. [c] Dissolved in 20.0 mL of 2.5 M $HClO_4$ at ice temperatures and diluted to 25.0 mL. [d] In 2.0 M $HClO_4$.

Results

X-ray Crystallograpy; A perspective view of the local coordination environment of the cobalt(III) center of hexaamminecobalt(III) *tris*(carbonato)cobaltate(III) with the atom labelling scheme is shown in Figure 2.1. The compound consists of a $Co(NH_3)_6^{3+}$ cation and a $Co(CO_3)_3^{3-}$ anion. The anion has six O atoms from three chelate carbonato ligands coordinated to cobalt(III) in a distorted octahedral geometry, while the cation has six N atoms from the six NH_3 groups coordinated in an octahedral geometry. A summary of the coordination distances and angles in $Co(CO_3)_3^{3-}$ is given on the illustration in Figure 2.2. The complete set of values is given in Appendix 2.1 and 2.2.

Some interatomic distances and angles for $Co(CO_3)_3^{3-}$ and some analogous carbonato cobalt(III) complexes are presented in Table 2.4. In $Co(CO_3)_3^{3-}$, the average lengths of the Co-O, O-C and C=O bonds are similar to those in other cobalt(III) complexes.[20-25] It should be noted that the average terminal C=O bond length (1.233 Å) in $Co(CO_3)_3^{3-}$ is less than the average bond length in the K and Na carbonates (1.285 Å),[26,27] indicating that the former has a bond order of 2.

A common feature of all the carbonato cobalt(III) complexes in Table 2.4 is the distorted angles in the chelate ring. The angles O-Co-O and O-C-O are ~70° and ~110°, respectively, compared to undistorted values of 90° and 120°, respectively. The reason for this distortion is not obvious, because both angles could be expanded towards the undistorted values without changing to Co-O or C-O distances. It would appear that the controlling feature is the Co-O-C angle, which is 90°, but would contract to 75° if the other angles were undistorted.

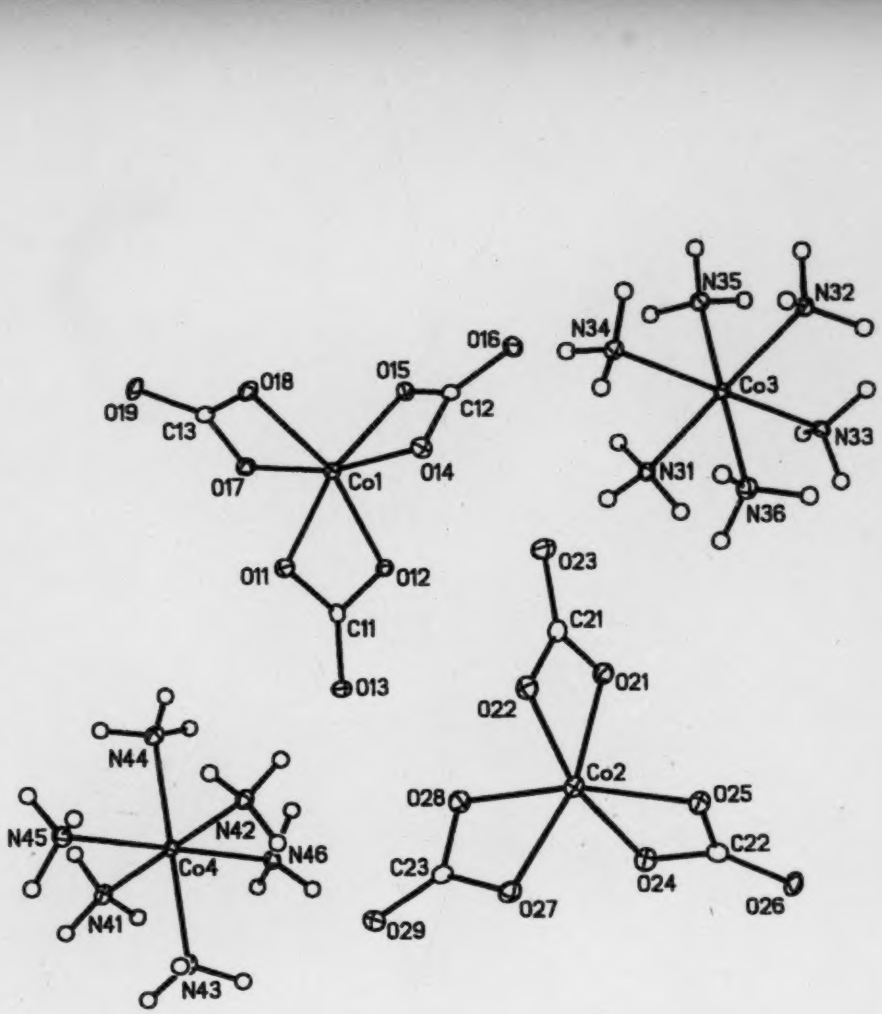
N35
N32
N34
Co3
N33
N31
N36
O16
O15
O18
O19
C13
C12
O17
Co1
O14
O11
O12
C11
O13
O23
C21
O21
O22
N44
Co2
O28
O25
N42
N46
N45
Co4
C22
C23
O24
N41
O27
O26
O29
N43

Figure 2.1. Perspective view of the asymmetric unit of $[Co(NH_3)_6][Co(CO_3)_3]$ showing the atom labeling scheme. Two crystallographically-independent units of each of $Co(NH_3)_6^{3+}$ and $Co(CO_3)_3^{3-}$ are present. Non-hydrogen atoms are represented by Gaussian ellipsoids at the 20 % probability level. Hydrogen atoms are shown with arbitrarily small thermal parameters

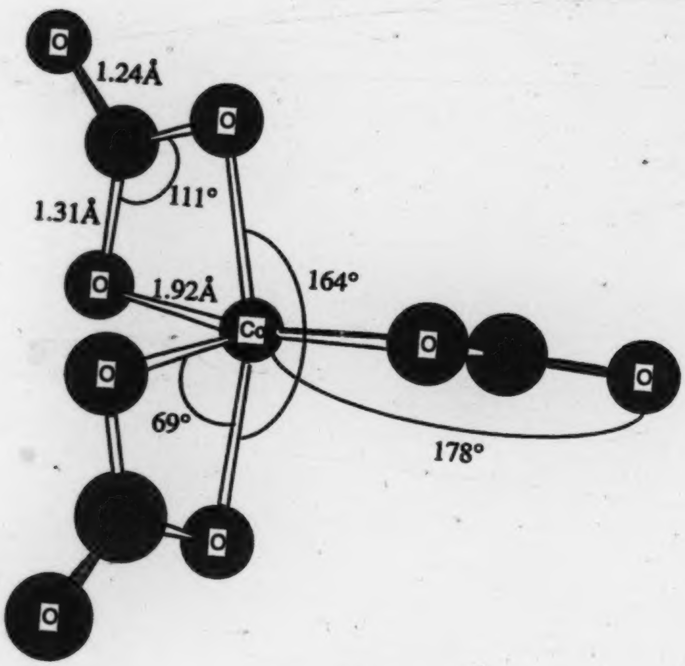
O
1.24Å
O
111°
1.31Å
O
1.92Å
164°
Co
O
O
69°
178°
O
O
O

Figure 2.2. Structure of the $Co(CO_3)_3^{3-}$ anion showing distorted angles and distances.

Table 2.4. Comparative Values of Distances and Angles of Various Cobalt(III) Carbonato Complexes.

Compound Ion[a]	Distance Co-O Å	Angle O-Co-O Degree	Angle Trans-O-Co-O Degree	Angle O-C-O Degree
$[Co(CO_3)_3]^{3-}$ [b]	1.915(3)	68.89(12)	164.14(13)	111.0
$[Co(NH_3)_4(CO_3)]^{+}$ [c]	1.905(11)	70.5(5)	-	110.4
$[Co(en)_2(CO_3)]^{+}$ [d]	1.907(2)	68.2(1)	-	109.9
$[Co(EDDA)(CO_3)]^{-}$ [e]	1.902(7)	69.16(12)	167.84(11)	-
$[Co(tren)_2(CO_3)]^{+}$ [f]	1.886(5)	68.19(12)	165.75(12)	-
$[Co(CO_3)(trien)]^{+}$ [g]	1.909(4)	68.7(2)	165.7(2)	110.2
$[Co(CO_3)L_3]^{+}$ [h]	1.932(11)	70.9(4)	166.4(5)	-

[a] en is ethylenediamine, EDDA is ethylenediaminediacetato, tren is trimethylenediamine, trien is triethylenetetramine, and L_3 is (2R,5R,8R,11R)-1,7-dibenzyl-2,5,8,11-tetraethyl-1,4,7,10-tetraazacylododecane. [b] This work. [c] Reference 20. [d] Reference 21. [e] Reference 22. [f] Reference 23. [g] Reference 24. [h] Reference 25.

The other complexes that have been isolated and characterized that contain three chelating carbonato ligands include $[Co(NH_3)_6][Sm(CO_3)_3(H_2O)]\bullet 4H_2O$,[28] $K_4[UO_2(CO_3)_3]$,[29] $[(NH_4)_4][UO_2(CO_3)_3]$,[30] and $[La_2(CO_3)_3]\bullet 8H_2O$.[31] The single-crystal X-ray diffraction study of $[Co(NH_3)_6][Sm(CO_3)_3(H_2O)]\bullet 4H_2O$ reveals a zig-zag chain structure of 9-coordinate samarium(III) centers bridged by μ-η^2:η^1 carbonato ligands.[28] Each samarium is coordinated by three bidentate carbonato ligands, two monodentate carbonato ligands from the adjacent unit in the chain, and a water ligand. The bond lengths of the chelated ligands in the Sm(III) complex are similar to those in $Co(CO_3)_3^{3-}$. The Sm-O bond length (average 2.45 Å) is ~ 0.54 Å longer than the Co-O bond length in $Co(CO_3)_3^{3-}$ as expected from the difference in ionic radii of octahedral low-spin cobalt(III) and 9-coordinate Sm(III).[32]

It is interesting to note that the carbonato chelate in the Sm(III) complex shows angle distortion similar to those of the Co(III) complexes. The Sm-O-C and O-C-O angles are 98.2° and 111.3°, respectively. The O-Sm-O angle is 52.3°, but it is not obvious what the ideal angle would be in this irregular 9-coordinate system. Again it is not clear why the O-Sm-O angle is compressed from 90°, unless there is some constraint applied by the Sm-O-C angles.

$Co(OH_2)_6^{3+}$ Production; For general studies and applications of aqueous cobalt(III), it would be advantageous to be able to prepare solutions with the widest possible range of [Co(III)] and [H^+]. The major limitation in this goal is that higher [Co(III)] and lower [H^+] favor oligomerization and reduction by water of aqueous cobalt(III), as described in detail in Chapter 3. These chemical reactions are the major limitations to the scope of the rather slow electrolytic method of preparation.

To illustrate the scope of the present method under routine conditions, the results of several sample preparations are summarized in Table 2.5. In these experiments a known mass of the green crystals was stirred for ~ 1 hour in a modest volume (V_o) of moderately concentrated (H_o, M) perchloric acid at ice temperature. Then the solutions were diluted with water to the final volume (V_{II}) and the Co(III) and H^+ concentrations were determined in aliquots of the final solutions, as described above.

Discussion

The synthesized and fully characterized salt, $[Co(NH_3)_6][Co(CO_3)_3]$, is formed as dark green, needle-like crystals. The material is stable at room temperature and is extremely insoluble in water, alcohol, acetone and acetonitrile. It serves as a reliable source of the strongly oxidizing aqueous cobalt(III) ion. The crystalline salt reacts with aqueous $HClO_4$, to give CO_2 (g), $Co(NH_3)_6(ClO_4)_3$ (s) and $Co(OH_2)_6^{3+}$ (aq). The solid $Co(NH_3)_6(ClO_4)_3$ is easily separated from the solution by centrifugation. Solutions of cobalt(III) at a range of initial concentrations and acidities were conveniently prepared by this method.

For most of the samples in Table 2.5, the yield of Co(III) is 85-90 %. The major exception is one run with a yield of 44.9 %. In this case, all of the crystals did not dissolve after the normal 1 hour period. This is also indicated by the fact that the final acidity (H_{II}) of 0.663 M is much higher than the calculated value of 0.409 M. The latter

Table 2.5. Representative Results for the Preparation of Aqueous Cobalt(III) from Crystalline $[Co(NH_3)_6][Co(CO_3)_3]$.

Initial Solutions			Final Solutions			Calculated		
Mass	V_o[a]	H_o[a]	V_{II}[b]	H_{II}[b]	Co^{3+}[b]	H_{II}[c]	% Co^{3+}[d]	$[Co^{3+}]/[H^+]$[e]
g	mL	M	mL	M	M	M		
0.1123	2.00	1.78	6.0	0.320	0.0405	0.313	86.6	0.126
0.2784	5.00	2.07	10.0	0.585	0.0566	0.617	81.3	0.097
0.2785	5.00	2.07	10.0	0.590	0.0616	0.617	88.5	0.104
0.3482	5.00	2.07	10.0	0.552	0.0741	0.513	85.1	0.134
0.3940	8.00	2.21	16.0	0.693	0.0526	0.736	85.4	0.076
0.4176	5.00	2.07	10.0	0.663	0.0469	0.409	44.9	0.071
0.4432	8.00	2.21	12.0	0.880	0.0819	0.919	88.7	0.093
0.4510	9.40	2.37	12.0	1.264	0.0854	1.293	90.9	0.068
0.5103	8.00	2.21	8.0	1.230	0.1320	1.253	82.8	0.107
0.5869	12.0	2.21	24.0	0.670	0.0541	0.738	88.5	0.081

[a] The volume and initial H^+ concentration of the solution in which the given mass of green crystals was dissolved. [b] The volume to which the initial solution was diluted and the H^+ and Co(III) concentrations determined by analysis. [c] The calculated H^+ concentration in the final solution, assuming 6 moles of H^+ are consumed per mole of reactant. [d] The yield of Co(III) based on that found in the final solution and the mass of the sample. [e] The ratio of Co(III) to H^+ in the final solution.

value predicts a final acidity of 0.82 M before dilution, and this, plus experience with other samples, indicate that this acidity needs to be ≥ 1 M for the dissolution of the green crystals. For the other samples, the final $[H^+]$ is, on average, with ± 4.8 % of that predicted. One unexpected feature is that the calculated $[H^+]$ is often slightly higher than that observed. One would expect the opposite if all the crystals had not dissolved, or if some cobalt(III) was lost due to oxidation of water.

The representative solutions presented in Table 2.5 reveal that solutions containing up to ~ 0.14 M Co(III) and down to 1.1-1.2 M $HClO_4$, before dilution, have been prepared. It was also noted that the final acidity, before dilution, should be ≥ 1 M for all of the green crystals to dissolve. With this limitation of the acidity after reaction, and using the known reaction stoichiometry and molar mass of $[Co(NH_3)_6][Co(CO_3)_3]$, it can be shown that the maximum concentration of cobalt(III) that can be prepared from a solution of initial acidity of H_o is given by equation (2.9)

$$[\mathrm{Co(III)}]_{\max} = \frac{H_o - 1}{6.00} \qquad (2.9)$$

Thus, for samples such as those in Table 2.5, with $H_o = 2.0$ M, $[\mathrm{Co(III)}]_{\max} \approx 0.17$ M. In principle, increasing H_o allows $[\mathrm{Co(III)}]_{\max}$ to be increased, however there are no doubt limits on the stability of more concentrated solutions with $[H^+] \approx 1$ M.

Other useful relationships for the preparation and analysis of the solutions can be developed. The final acidity after reaction ($H_f \geq 1$ M) is given by

$$H_f = \frac{V_I H_o - 15m}{V_I} \tag{2.10}$$

where V_o is the solution volume (mL) and m is the mass (g) of the sample of green crystals. Simple rearrangement gives the value of m for a chosen V_o, H_o and H_f as

$$m = \frac{V_o(H_o - H_f)}{15} \tag{2.11}$$

and the theoretical molar concentration of Co(III) is

$$[\mathrm{Co(III)}] = \frac{2.5m}{V_o} \tag{2.12}$$

This method of preparation of aqueous cobalt(III) has several advantages over the earlier methods. It provides good control of the final acidity, compared to the acidification of cobalt(III) carbonate solution. The solid starting material is easier to prepare and far more stable than $Co_2(SO_4)_3 \bullet 18H_2O$. This method is takes around 1½ hours as compared to electrolysis, which has been outlined in detail on page 2 of Chapter 1, and has a relatively high ratio of $Co(OH_2)_6^{3+}$ to acid concentration of 0.134 (maximum) as compared to 0.017 for electrolysis.[8,11-12] This simply means that one can access solutions with a wider range of cobalt(III) and H^+ concentrations.

The extinction coefficients 40.0 and 35.0 $M^{-1}cm^{-1}$ at 400 and 605 nm, respectively, determined in this study for $Co(OH_2)_6^{3+}$ compare well with those from earlier studies,[7-13] using different synthetic methods. As noted in Chapter 1, the earlier values range from 39 to 41 $M^{-1}cm^{-1}$ at 400 nm, and from 32.6 to 35 $M^{-1}cm^{-1}$ at 605 nm.[7-13] Weiser[9] reported extinction coefficients of 6.0 and 3.05×10^3 $M^{-1}cm^{-1}$ at 320 and 250 nm, respectively, for cobalt(III) (2.0×10^{-5} to 4.0×10^{-3} M) solutions and acidity of (> 0.4 M at 25 °C or 0.1 M at 0 °C). In the present work, 6.6 and 3.0×10^3 $M^{-1}cm^{-1}$ at 325 and 250 nm, respectively, were obtained under comparable conditions of > 0.3 M H^+ and 0.04 to 7.7×10^{-4} M cobalt(III). Baxendale and Wells[7] also reported a value of 2.97×10^3 $M^{-1}cm^{-1}$ at 250 nm, in agreement with ~ 3.0×10^3 $M^{-1}cm^{-1}$ found by Weiser[9] and in this work. The extinction coefficients at 325 nm is significant because any slight increase would imply formation of species other than cobalt(III) i.e. the dimers to be discussed in Chapter 3.

References

(1) Mori, M.; Shibata, M.; Kyuno, E.; Adachi, T. *Bull. Chem. Soc. Jpn.* **1956**, *28*, 883.

(2) Bauer, H. F.; Drinkard, W. C. *J. Amer. Chem. Soc.* **1960**, *82*, 5031.

(3) Bauer, H. F.; Drinkard, W. C. *Inorg. Synth.* **1966**, *8*, 202.

(4) McCutcheon, T. P.; Schuele, W. J. *J. Amer. Chem. Soc.* **1953**, *75*, 1845.

(5) Gillard, R. D.; Mitchell, P. R.; Price, M. G. *J. Chem. Soc. Dalton* Trans. **1972**, 1211.

(6) Nakamoto, K.; Fujita, J. Tanaka, S.; Kobayashi, M. *J. Amer. Chem. Soc.* **1957**, *79*, 4906.

(7) Baxendale, J. H.; Wells, C. F. *Trans. Faraday Soc.* **1957**, *53*, 800.

(8) Hargreaves, G.; Sutcliffe, L. H. *Trans. Faraday Soc.* **1955**, *51*, 786.

(9) Weiser, D. W. *Ph. D. Thesis*, University of Chicago, **1956**.

(10) Habib, H. S.; Hunt, J. P. *J. Amer. Chem. Soc.* **1966**, *88*, 1668.

(11) Ferrer, M.; Llorca, J.; Martinez, M. *J. Chem. Soc. Dalton Trans.* **1992**, 229.

(12) Pelizzetti, E.; Mentasti, E.; Pramauro, E. *J. Chem. Soc. Dalton Trans.* **1976**, 23.

(13) Davies, G.; Warnqvist, B. *Coord. Chem. Rev.* **1970**, *5*, 349.

(14) Liteplo, M. P.; Endicott, J. F. *Inorg. Chem.* **1971**, *10*, 1420.

(15) Schlessinger, G. G. *Inorganic Laboratory Preparations*; Chemical Publishing Company Inc.; New York, New York, **1962**; pg. 176.

(16) Dixon, N. E.; Jackson, W. G.; Lancaster, M. J.; Lawrence, G. A.; Sargeson, A. M. *Inorg. Chem.* **1981**, *20*, 470.

(17) Hofman-Bang, N.; Wulff, I. *Acta Chem. Scand.* **1955**, *9*, 1230.

(18) Programs for diffractometer operation, data collection, data reduction and absorption correction were those supplied by Bruker.

(19) Sheldrick, G. M. SHELXL-93. Program for crystal structure determination. University of Göttingen; Germany **1993**.

(20) Barclay, G. A.; Hoskins, B. F. *J. Chem. Soc.* **1962**, 586.

(21) Bigoli, F.; Lanfranchi, M.; Leporati, E.; Pellinghelli, M. A. *Cryst. Struct. Comm.* **1980**, *9*, 1261.

(22) Egan, T. J.; Baldwin, D. A.; Denner, L. *Acta Cryst.* **1995**, *C51*, 1994.

(23) Zhu, H.-L.; Chen, X.-M. *Acta Cryst.* **1999**, *C55*, 2010.

(24) Masuda, H.; Masuda, C.; Jitsukawa, K.; Eigana, H. *Bull. Chem. Soc. Jpn.* **1994**, *67*, 3000.

(25) Tsuboyama, S.; Fujimoto, J.; Hanabira, S; Yasuda, N.; Kobayashi, K.; Sakurai, T.; Tsuboyama, K. *J. Chem. Soc. Dalton Trans.* **1996**, 45.

(26) Palmer, D. A.; Van Eldik, R. V. *Chem. Rev.* **1983**, *83*, 651.

(27) Zemann, J. *Fortschr. Mineral.* **1981**, *59*, 95.

(28) Clark, D. L; Donohoe, R. J.; Gordon J. C.; Gordan, P. L.; Kenogh, D. W.; Scott, B. L.; Tait, C. D. *J. Chem. Soc. Dalton Trans.* **2000**, 1975.

(29) Anderson, A.; Chieh, D. E.; Tong, J. P. K. *Can. J. Chem.* **1980**, *58*, 1651.

(30) Graziani, R.; Bombier, E. *J. Chem. Soc. Dalton Trans.* **1972**, 2059.

(31) Shinn, D. B.; Eick, H. A. *Inorg. Chem.* **1968**, 7, 1340.

(32) Huheey, J. E.; Keiter, E. A.; Keiter, R. L. *Inorganic Chemistry Principles of Structure and Reactivity;* Harper Collins; New York, New York, 4th Ed, **1993**; pg. 116-117.

CHAPTER 3. Decomposition of Hexaaquacobalt(III) in Perchloric Acid

Introduction

As will be apparent from the summary below, the extent of hydrolysis of aqueous cobalt(III) ions has been debated for some time, with a lot of disagreement about the species existing in solution, and a paucity of good equilibrium data. This is largely a consequence of the experimental preparation difficulties, and the instability of $Co(OH_2)_6^{3+}$ in aqueous solution.

It seems to be well established that some binuclear and/or polynuclear hydrolyzed complex(es) form at relatively high concentrations of $Co(OH_2)_6^{3+}$ (> 10^{-3}-10^{-2} M) and low acidities ($[H^+]$ < 0.4 M) at temperatures greater than about 10 °C. Hargreaves and Sutcliffe[1] determined that the electronic spectrum was independent of cobalt(III) for the concentration range 3.0–30 × 10^{-3} M in 1.0–6.0 M $HClO_4$. From this they concluded that no polynuclear cobalt(III) species are formed for $[H^+] > 1.0$ M.

However in a subsequent kinetic study of the oxidation of water by cobalt(III), Baxendale and Wells[2] proposed that cobalt(III) is present as a μ–oxo dimer with a possible structure shown below in solutions of < 0.1 M acidity and ≥ 10^{-3} M total cobalt(III).

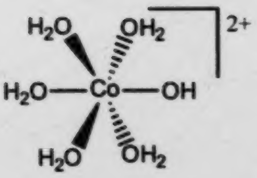

Monomer

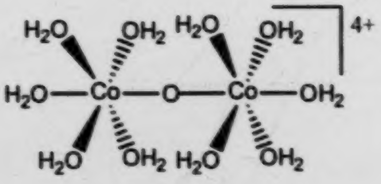

Dimer

For the kinetic runs the concentration ranges were 0.4-3.0 × 10^{-3} M Co(III), 4.19-8.27 × 10^{-2} M $HClO_4$ in 0.10 M $NaClO_4/HClO_4$. They found that the rate depended on $[Co(III)]^{3/2}$ and $[H^+]^{-2}$. Their proposed mechanism is reproduced in equation (3.1)-(3.4).

$$Co(OH_2)_6^{3+} \overset{K_1}{\rightleftarrows} Co(OH_2)_5OH^{2+} + H^+ \tag{3.1}$$

$$2Co(OH_2)_5OH^{2+} \overset{K_2}{\rightleftarrows} [(H_2O)_5Co-O-Co(OH_2)_5]^{4+} + H_2O \tag{3.2}$$

$$[(H_2O)_5Co-O-Co(OH_2)_5]^{4+} \overset{K_3}{\rightleftarrows} [HO(H_2O)_4Co-O-Co(OH_2)_4OH]^{2+} + 2H^+ \tag{3.3}$$

$$Co(OH_2)_5OH^{2+} + [HO(H_2O)_4Co-O-Co(OH_2)_4OH]^{2+} + 5H_2O \xrightarrow{k_4} 3Co(OH_2)_6{}^{2+} + 2OH^- + HO_2{}^{\bullet} \tag{3.4}$$

The first three steps were proposed to be rapidly maintained equilibria, with the last step as rate controlling. Therefore the rate of disappearance is given by equation (3.5)

$$\begin{aligned} -\frac{\partial[Co(III)]}{\partial t} &= k_4[Co(H_2O)_5OH^{2+}][HO(H_2O)_4Co-O-Co(OH_2)_4OH^{2+}] \\ &= \frac{K_3k_4[(H_2O)_5Co-O-Co(OH_2)_5{}^{4+}]^{3/2}}{K_2{}^{1/2}[H^+]^2} \end{aligned} \tag{3.5}$$

It was assumed further that $K_2 \geq K_3$ so that the cobalt(III) is present predominantly as $[(H_2O)_5Co\text{-}O\text{-}Co(OH_2)_5]^{4+}$, and then (3.5) becomes (3.6)

$$-\frac{\partial[\mathrm{Co(III)}]}{\partial t}=\frac{K_3k_4\left(\frac{1}{2}[\mathrm{Co(III)}]\right)^{3/2}}{K_2^{1/2}[\mathrm{H}^+]^2}=\frac{0.353K_3k_4[\mathrm{Co(III)}]^{3/2}}{K_2^{1/2}[\mathrm{H}^+]^2} \qquad (3.6)$$

where [Co(III)] is the total cobalt(III).

In light of this proposal, Sutcliffe and Weber[3] reexamined the spectra of cobalt(III) perchlorate solutions in 0.06-4.50 M H^+ at 2.3-9.4 × 10^{-3} M Co(III) and μ = 1.0-4.50 M $NaClO_4/HClO_4$. Absorbance readings at 330 nm were taken when the absorption reached a maximum. The observed extinction coefficient at 330 nm increases with increasing $Co(OH_2)_6^{3+}$ concentration and with decreasing acid concentration. Sutcliffe and Weber[3] attributed the increase in absorbance at 330 nm to rapid hydrolysis (3.1) followed by slow formation of the dimer and gave the tentative mechanism shown in (3.7)-(3.8), where $CoOH^{2+}$ is $Co(OH_2)_5OH^{2+}$.

$$\mathrm{Co(OH_2)_6}^{3+} + \mathrm{CoOH}^{2+} \rightleftarrows [(\mathrm{H_2O})_5\mathrm{Co-O-Co(OH_2)_5}]^{4+} + \mathrm{H_2O} + \mathrm{H}^+ \qquad (3.7)$$

and / or

$$2\mathrm{CoOH}^{2+} \rightleftarrows [(\mathrm{H_2O})_5\mathrm{Co-O-Co(OH_2)_4OH}]^{3+} + \mathrm{H_2O} + \mathrm{H}^+ \quad \text{(slow)} \qquad (3.8)$$

Weiser[4] made a detailed study of the absorption spectrum of aqueous cobalt(III) in the range 220-900 nm for solutions at various concentrations of cobalt(III) (2×10^{-5} - 4×10^{-3} M) and acidities, (2×10^{-3} to 7 M $HClO_4$). Weiser found that the spectrum of cobalt(III) was independent of the $HClO_4$ concentration for $[H^+] > 0.4$ M at 25 °C or > 0.1 M at 0 °C. He reported absorption maxima at 602 and 402 nm with extinction coefficients of 34.8 and 40.5 $M^{-1}cm^{-1}$, and assigned this spectrum to $Co(OH_2)_6^{3+}$. At lower acidities (2.2×10^{-3} – 2.4×10^{-2} M H^+), Weiser claimed that another species forms with no well defined absorption maxima below 400 nm for [Co(III)] in the range of 0.45×10^{-3} to 3.5×10^{-3} M. This species has a reasonably constant extinction coefficient of ~ 150 $M^{-1}cm^{-1}$ (based on total cobalt(III)) at 402 nm. Ultimately Weiser proposed that this species was a dimer of composition $[(H_2O)_5Co\text{-}O\text{-}Co(OH_2)_5]^{4+}$ which is formed essentially irreversibly from monomeric species.

Aqueous cobalt(III) solutions are known to oxidize water by the overall reaction (3.9).

$$4Co(OH_2)_6^{3+} + 2H_2O \longrightarrow 4Co(OH_2)_6^{2+} + O_2 + 4H^+ \qquad (3.9)$$

Bawn and White[5] studied the kinetics of this reaction for cobalt(III) sulfate and perchlorate solutions in ~ 0.1 to 0.8 M perchloric acid. The reaction was monitored volumetrically by reaction with iron(II). Bawn and White concluded that the reaction was between first- and second-order in Co(III) and the rate decreased with increasing acidity. To conform to these kinetics, they suggested that two types of rate-determining reactions occurred, one involving a monomeric cobalt(III) species (3.10) and (3.11),

$$\mathrm{Co(OH_2)_6}^{3+} + \mathrm{OH}^- \longrightarrow \mathrm{Co(OH_2)_6}^{2+} + \mathrm{HO}^\bullet \tag{3.10}$$

and / or

$$\mathrm{Co(OH_2)_5OH}^{2+} + \mathrm{OH}^- \longrightarrow \mathrm{Co(OH_2)_5OH}^{+} + \mathrm{HO}^\bullet \tag{3.11}$$

and another involving a dimeric species of the type $[(H_2O)_5Co\text{-}O\text{-}Co(OH_2)_5]^{4+}$.

Weiser[4] also studied the rate of oxidation of water by cobalt(III) at 2.2 × 10^{-3} to 0.14 M H^+ and 0.47 × 10^{-3} to 4.8 × 10^{-3} M cobalt(III). For $[H^+] \leq 0.024$ M, the initial absorbance at 402 nm was higher than predicted for $Co(OH_2)_6^{3+}$ and gave an extinction coefficient of ~150 $M^{-1}cm^{-1}$ per cobalt(III). However, the growth of this absorbance was not monitored because instrumental limitations prevented absorbance readings being taken before about 300 s. It was noted that the absorbance at 402 nm reached a maximum after ~ 400 s for 0.78 × 10^{-3} M Co(III) in 0.063 M H^+. An approximate kinetic analysis indicated that the $Co(OH_2)_6^{3+}$ disappeared with a rate law that is second-order in [Co(III)] and inverse third-order in $[H^+]$, and this pathway produces the species with the extinction coefficient of ~ 150 $M^{-1}cm^{-1}$. The latter species disappears by a two-term rate law; one term is just first-order in the species and the other also is first-order in [Co(III)] and inverse second-order in $[H^+]$.

Similar studies were done by Weiser[4] at much higher acidities (0.10-7.0 M) and higher [Co(III)] (1.0 × 10^{-2} – 8.0 × 10^{-2} M). There was also cobalt(II) present in these runs at the 0.02 to 0.22 M level, and it was found that cobalt(II) did not affect the rate. It was concluded that the rate of disappearance of cobalt(III) has two terms, k_1[Co(III)] and $k_2[\mathrm{Co(III)}]^2[H^+]^{-1}$. The graphical analysis of the data is somewhat complex and gave rather erratic values of k_1 between 0.9×10^{-6} and 9.3×10^{-6} s^{-1}. However, the dominant k_2 pathway gave fairly constant values of k_2 between 2.9×10^{-3} and 4.6×10^{-3} s^{-1}.

Further observations of Weiser relate to the pathway for the oxidation of water. It was observed that the photo-catalyzed reaction is inhibited by cobalt(II). This result and the overall dependence of the quantum yield on concentrations are consistent with the hydroxy radical being formed from the photo-activated cobalt(III), $(Co(OH_2)_6^{3+})^*$, as shown in Scheme 3.1. The third step produces the inhibition by cobalt(II).

Scheme 3.1

$$Co(OH_2)_6^{3+} + h\nu \longrightarrow (Co(OH_2)_6^{3+})^*$$

$$(Co(OH_2)_6^{3+})^* + H_2O \longrightarrow Co(OH_2)_6^{2+} + OH^\bullet + H^+$$

$$Co(OH_2)_6^{2+} + OH^\bullet + H^+ \longrightarrow Co(OH_2)_6^{3+} + H_2O$$

$$Co(OH_2)_6^{3+} + OH^\bullet \longrightarrow \text{products}$$

Since the thermal reaction is not affected by cobalt(II), one can infer that the thermal pathway does not involve the hydroxy radical in any rate-controlling steps.

As observed by Davies and Warnqvist[6] the common features of the studies by Weiser[4] and by Bawn and White[5] on the $Co(OH_2)_6^{3+}$-water reaction seem to be:

(a) a term in the rate law second-order in $Co(OH_2)_6^{3+}$ and proportional to $[H^+]^{-2}$, (according to Weiser,[4] proportional to $[H^+]^{-1}$ at higher acidity);

(b) another term approximately first order in $Co(OH_2)_6^{3+}$, which seems to be irreproducible, and to depend on the history of the solution.[4]

The former, main term (a) of the rate law can be explained by a rate-determining step involving two monomeric cobalt(III) species, e.g. two $Co(H_2O)_5(OH)^{2+}$ ions, which form a dimeric complex.

Anbar and Pecht[7] have suggested hydrogen peroxide formation from water by the concerted reduction of two $Co(OH_2)_6^{3+}$ ions. They put forward two possible mechanisms. The first mechanism involves the interaction of two $Co(OH_2)_6^{3+}$ species to form the dimer (3.12). Then the dimer undergoes internal molecular conversion to a binuclear peroxy complex of $Co(OH_2)_6^{2+}$ (3.13), which hydrolyses into H_2O_2 and $2Co(OH_2)_6^{2+}$ (3.14) and finally steps (3.15) and (3.16) would follow:

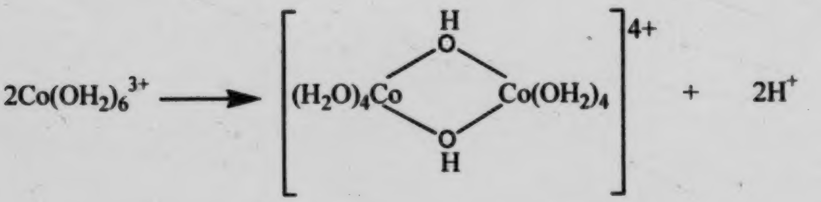
2Co(OH2)6 3+
H
O
(H2O)4Co
Co(OH2)4
O
H
4+
+
2H+

(3.12)

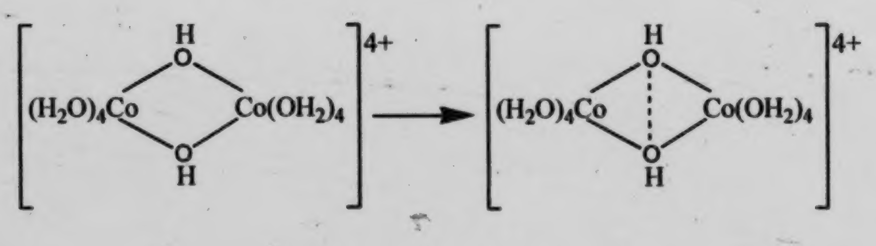
H
O
(H2O)4Co
Co(OH2)4
O
H
4+
H
O
(H2O)4Co
Co(OH2)4
O
H
4+

(3.13)

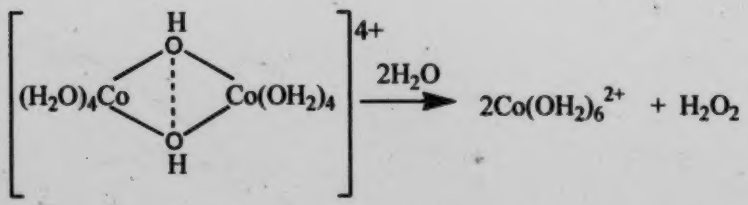
H
O
(H2O)4Co
Co(OH2)4
O
H
4+
2H2O
2Co(OH2)6 2+
+ H2O2

(3.14)

$$H_2O_2 + Co(H_2O)_6^{3+} \rightarrow Co(H_2O)_6^{2+} + H^+ + HO_2^\bullet \qquad (3.15)$$

$$HO_2^\bullet + Co(H_2O)_6^{3+} \rightarrow Co(H_2O)_6^{2+} + H^+ + O_2 \qquad (3.16)$$

The second mechanism involves the attack of $Co(OH_2)_6^{3+}$on $[Co(OH_2)_4OH]_2^{4+}$ (3.17) followed by formation of $HO_2^\bullet$ radical (3.18), which reacts with or terminates the reaction as shown in equations (3.19) and (3.20), respectively.

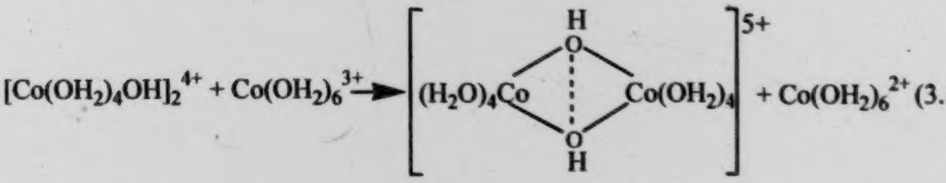

[Co(OH2)4OH]2 4+ + Co(OH2)6 3+
H
O
(H2O)4Co
Co(OH2)4
O
H
5+
+ Co(OH2)6 2+

(3.17)

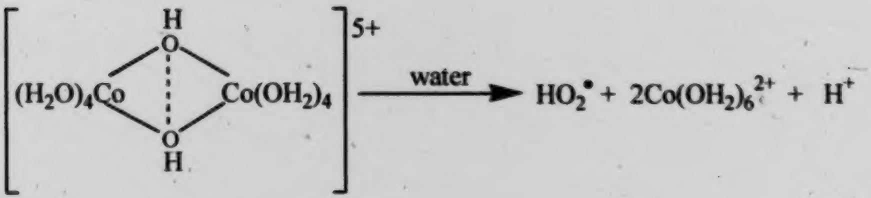

H
O
(H2O)4Co
Co(OH2)4
O
H
5+
water
HO2• + 2Co(OH2)6 2+ + H+

(3.18)

$$HO_2^\bullet + Co(H_2O)_6^{3+} \rightarrow O_2 + H^+ + Co(H_2O)_6^{2+} \qquad (3.19)$$

or

$$2HO_2^\bullet \rightarrow H_2O_2 + O_2 \qquad (3.20)$$

Wells[8] argued that the findings of Anbar and Pecht[7] hardly furnished quantitative support for his idea that cobalt(III) would exist, at equilibrium, mainly as a dimer in highly acidic perchlorate solution. In their ^{18}O distribution study, Anbar and Pecht[7] found

"< 3.1 % dimeric cobalt(III)" at 0.6 M $Co(OH_2)_6^{3+}$ in 6 M $HClO_4$ at room temperature. This corresponds to an overall dimerization quotient, K_D, of ≤ 0.03 M^{-1} for the equilibrium in equation (3.21).

$$2\text{Co(III)} \xrightleftharpoons{K_D} [\text{Co(III)}]_2 \qquad (3.21)$$

K_D may be a function of acidity and ionic strength, but if neither dimeric nor monomeric $Co(OH_2)_6^{3+}$ hydrolyzes appreciably in the acidity range 0.1-6 M,[8] then K_D will be within an order of magnitude of the above mentioned maximum value. If this is the case, then less than 1 % cobalt(III) would be dimeric at 3.0×10^{-3} M $Co(OH_2)_6^{3+}$ and $[H^+] \approx 0.1$ M. An increase in K_D proportional to the inverse of the square of the hydrogen ion activity would give $K_D \leq 2 \times 10^{-2}$ M^{-1} at $[H^+] \approx 0.1$ M, which correspond to ≥ 60 % monomeric Co(III) at 3×10^{-3} M $Co(OH_2)_6^{3+}$. In short, Anbar and Pecht's findings do not support the idea that cobalt(III) exists, at equilibrium, mainly as a dimer in highly acidic perchlorate solutions.

In this study of the reaction of cobalt(III) with water, the solutions of aqueous cobalt(III) at a range of initial concentrations and acidities were conveniently prepared by the reaction in equation (3.22).

$$\begin{aligned}[\text{Co(NH}_3)_6][\text{Co(CO}_3)_3] + 6\text{HX(aq)} &\longrightarrow \text{Co(OH)}_6^{3+}\text{(aq)} + \\ &[\text{Co(NH}_3)_6]\text{X}_3\text{ (s)} + 3\text{CO}_2\text{(g)} + 3\text{X}^-\end{aligned} \qquad (3.22)$$

The advantages of this preparative method for cobalt(III) are discussed in detail in Chapter 2. The kinetic method has been applied in determining the nature of the hydrolyzed and dimeric states of aqueous cobalt(III).

Experimental

Preparation of $Co(OH_2)_6^{3+}$. Approximately 0.12 g (3.0×10^{-4} mole) to 0.31 g (7.8×10^{-4} mole) of $[Co(NH_3)_6][Co(CO_3)_3]$ crystals were dissolved in 1.5-6.0 mL of 2.0-3.21 M $HClO_4$ at ice temperature. The solution was stirred for 1½ hours until no more carbon dioxide evolved and it was then diluted to 12.0 mL with ice cold water. The precipitate of $Co(NH_3)_6(ClO_4)_3$ was removed by centrifugation and the $Co(OH_2)_6^{3+}$ stock solution was kept in ice. The concentration of the $Co(OH_2)_6^{3+}$ stock solution was determined in a 0.50 cm path-length cell by spectrophotometry using an extinction coefficient of 35 $M^{-1}cm^{-1}$ at 605 nm.[4] The excess acid was determined by reacting 1.0 mL of stock solution with 2.0 mL of 2.0 M NaCl to reduce Co(III) as in equation (3.23).

$$2Co(OH_2)_6^{3+} + 2Cl^- \longrightarrow 2Co(OH_2)_6^{2+} + Cl_2(g) \qquad (3.23)$$

Then the solution was boiled to remove chlorine and carbon dioxide (formed by equation 3.22), cooled to room temperature, and titrated with 0.100 M analytical grade NaOH.

Solutions Used in Kinetics Studies. The required concentration of $Co(OH_2)_6^{3+}$ in 1.0-2.0 M acid was kept at 0 °C and a second solution containing the required amounts of $LiClO_4$ and $HClO_4$ was maintained at a higher temperature. The volumes of the two solutions (6.00 mL at 0 °C and 9.00 mL at 40 °C) determined this temperature, so that when they were mixed the temperature would be close to 25 °C. The reaction commenced when the two solutions were mixed (zero time). The reaction was monitored on the 8451A Diode Array spectrophotometer at a wavelength range of 300-700 nm and a spectrum was taken on the Cary 219 spectrophotometer for accurate determination of $[Co(OH_2)_6^{3+}]$ ($> 1.4 \times 10^{-3}$ M) from the absorbance at 605 nm.

Results

The spectrum of 2.8×10^{-2} M $Co(OH_2)_6^{3+}$ in 1.00 M H^+ in Figure 3.1 shows two major peaks at 400 and 605 nm. The absorbance of this solution is stable for an initial 2.4×10^3 seconds (40 minutes) and then starts to decrease gradually at both 400 and 605 nm. In 0.45 M H^+ the spectrum in Figure 3.2 shows three significant absorbance changes at three wavelengths. At 605 nm, the absorbance is fairly constant for the first 1.5×10^3 seconds and then slowly decreases. At 400 nm, the absorbance initially increases slightly, and then slowly decreases. At 325 nm, there is rapid increase in the absorbance, reaching a maximum after 1.5×10^3 seconds, and then a slow decrease.

Analysis of Absorbance-Time Curves. The variations of absorbance with time for acidic aqueous solutions of cobalt(III) has been examined in detail at 325 and 605 nm. For the samples to be discussed, the concentration conditions fall generally into two

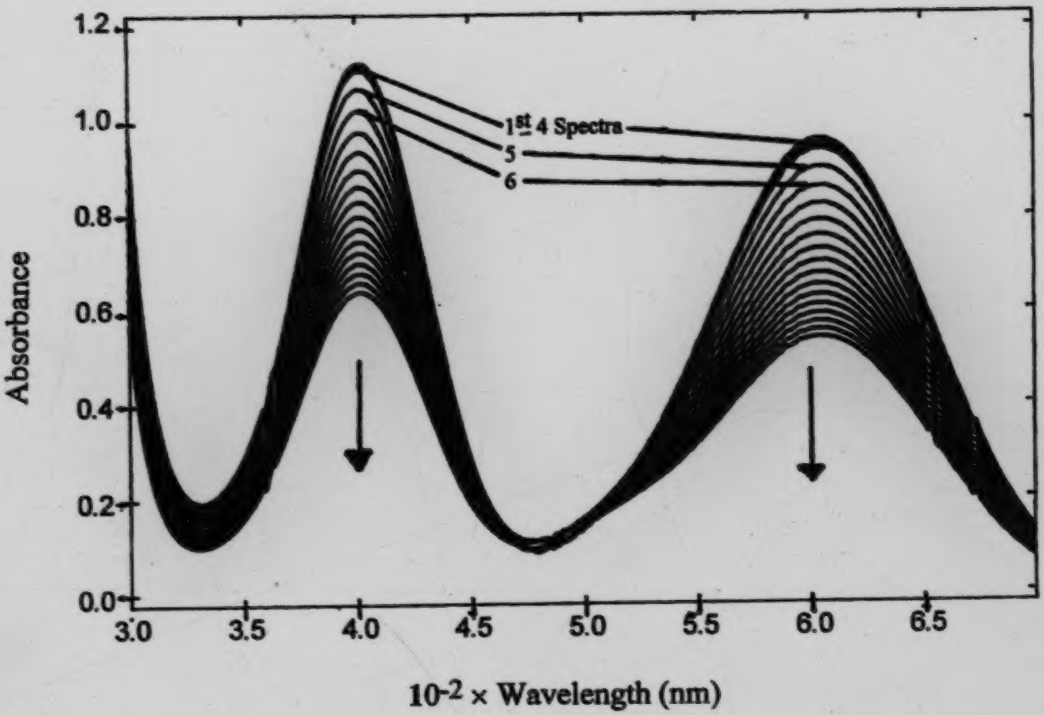

Figure 3.1. The spectrum of 2.8×10^{-2} M $Co(OH_2)_6^{3+}$ in 1.00 M $HClO_4$ at 25 °C. Time separation for the spectra is 10 minutes.

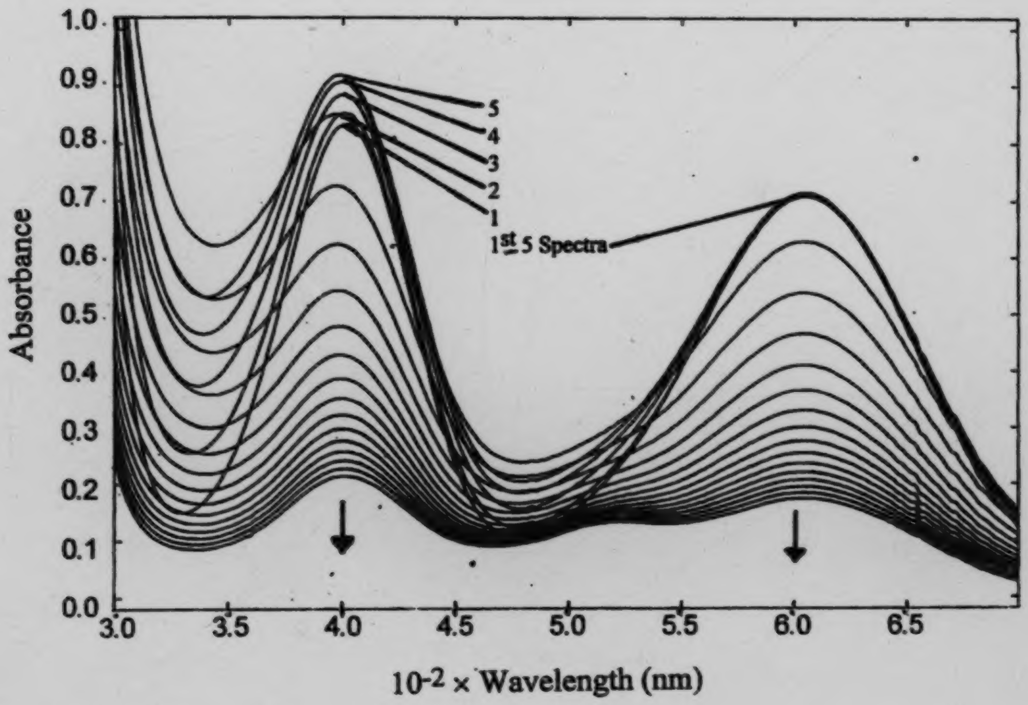

Figure 3.2. The spectrum of 2.09×10^{-2} M $Co(OH_2)_6^{3+}$ in 0.45 M $HClO_4$/0.55 M $LiClO_4$ at 25 °C. Time separation for the spectra is 5 minutes.

categories: low [Co(III)] ($1.1 \times 10^{-3} - 3.3 \times 10^{-3}$ M) and low [H^+] ($2.4 \times 10^{-2} - 1.2 \times 10^{-1}$ M); high [Co(III)] (9.0×10^{-3} – 34.0×10^{-3} M) and high [H^+] (0.11–0.45 M). The conditions have been dictated, at least in part, by a desire to have [Co(III)] << [H^+] so that the H^+ resulting from hydrolysis of $Co(OH_2)_6^{3+}$ does not seriously affect the concentration of free H^+. Otherwise the [H^+] would be changing significantly as the Co(III) is converted to Co(II).

The general pattern of the absorbance-time curves is illustrated in Figures 3.3-3.5 for the full 20×10^3 s of each run, and in Figures 3.6-3.8 for the initial 2×10^3 s only. The longer time-scale mainly illustrates the behavior of the decrease in absorbances after the maximum. It appears qualitatively from the half-times that this process gets slower as the [Co(III)] decreases (Figures 3.3 and 3.4) and clearly gets faster as the [H^+] decreases. The shorter time-scale presentation illustrates the details of the initial stages of the reaction. In Figure 3.6, it is apparent that the rate and extent of the absorbance increase at 325 nm increases with increasing [Co(III)], and an apparent induction period is clear from the run with 1.2×10^{-3} M Co(III). The same runs observed at 605 nm in Figure 3.7 show a parallel pattern, but the absorbance increase is much smaller, and is not even observed at 1.2×10^{-3} M Co(III). The runs at higher [Co(III)] and varying [H^+] in Figure 3.8 show that the absorbance increase at 325 nm is faster and larger at lower [H^+]. The induction period is apparent only for the run at the highest [H^+].

The overall impression from these qualitative observations is that the absorbance changes occur in at least three stages. The first stage causes small changes in absorbance. The next stage produces an absorbance increase that is quite large at 325 nm. The last stage is the reduction of cobalt(III) species and causes an absorbance decrease. The last

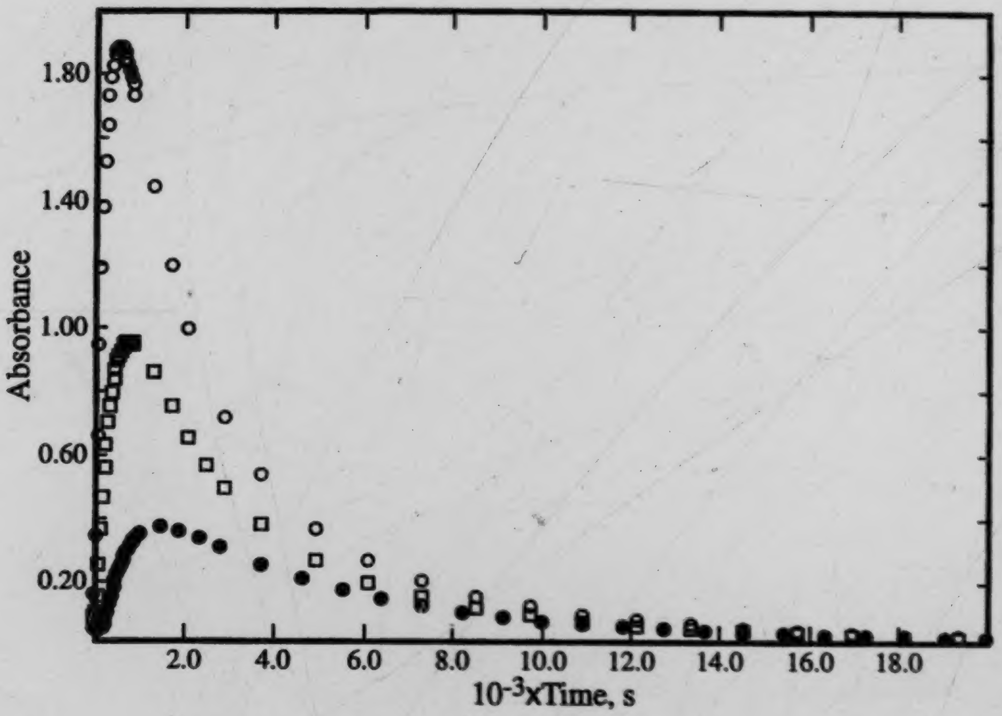

Figure 3.3. Variation of the absorbance at 325 nm with time for solutions of 3.30×10^{-3} M (O), 2.20×10^{-3} M (□), and 1.20×10^{-3} M (●) $Co(OH_2)_6^{3+}$ in 0.080 M $HClO_4$/0.92 M $LiClO_4$ at 25 °C.

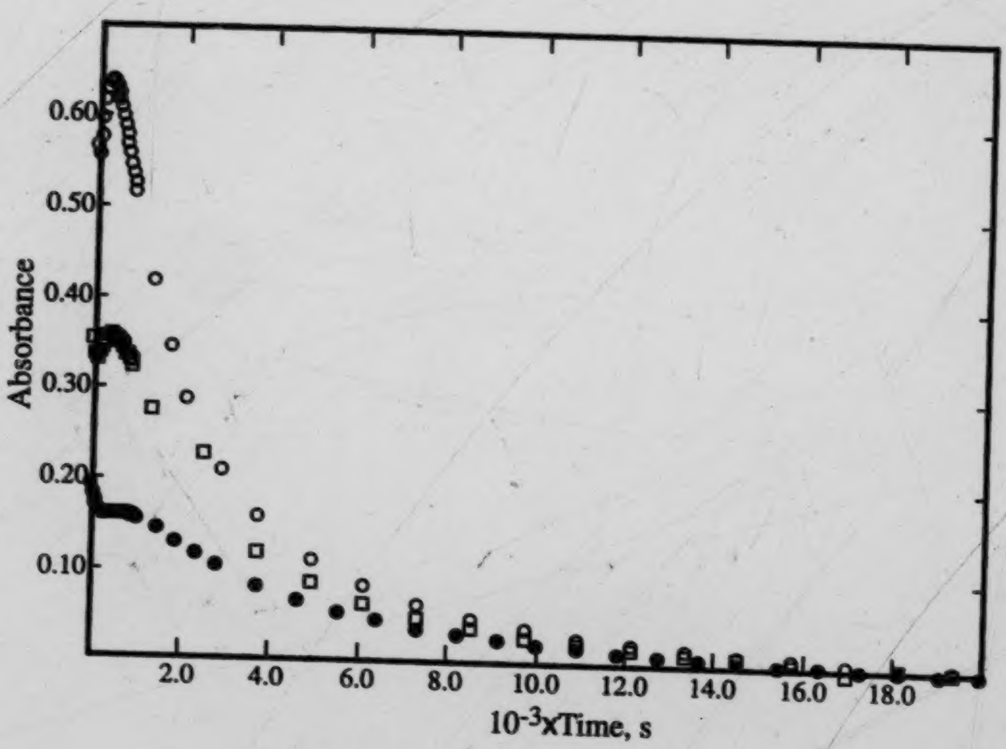

Figure 3.4. Variation of the absorbance at 605 nm with time for solutions of 3.30 × 10^{-3} M (O), 2.20 × 10^{-3} M (□), and 1.20 × 10^{-3} M (●) $Co(OH_2)_6^{3+}$ in 0.080 M $HClO_4$/0.92 M $LiClO_4$ at 25 °C.

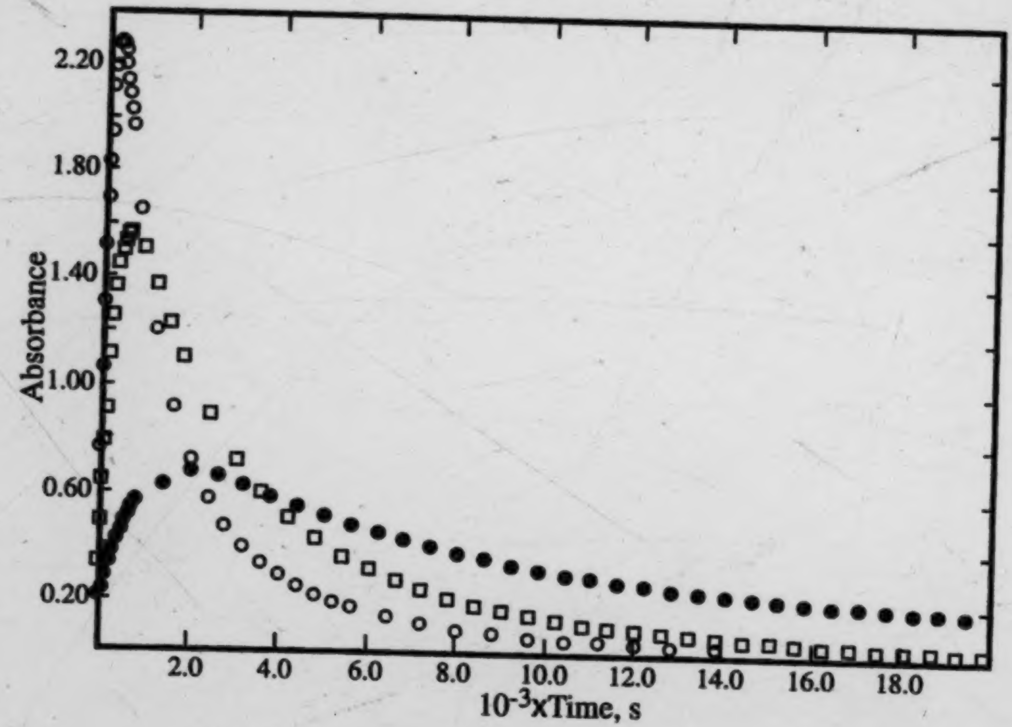

Figure 3.5. Variation of the absorbance at 325 nm with time for solutions of 1.82 × 10^{-2} M $Co(OH_2)_6^{3+}$ in 0.11 M (O), 0.20 M (□), and 0.45 M (●) H^+ in 1.0 M $HClO_4/LiClO_4$ at 25 °C.

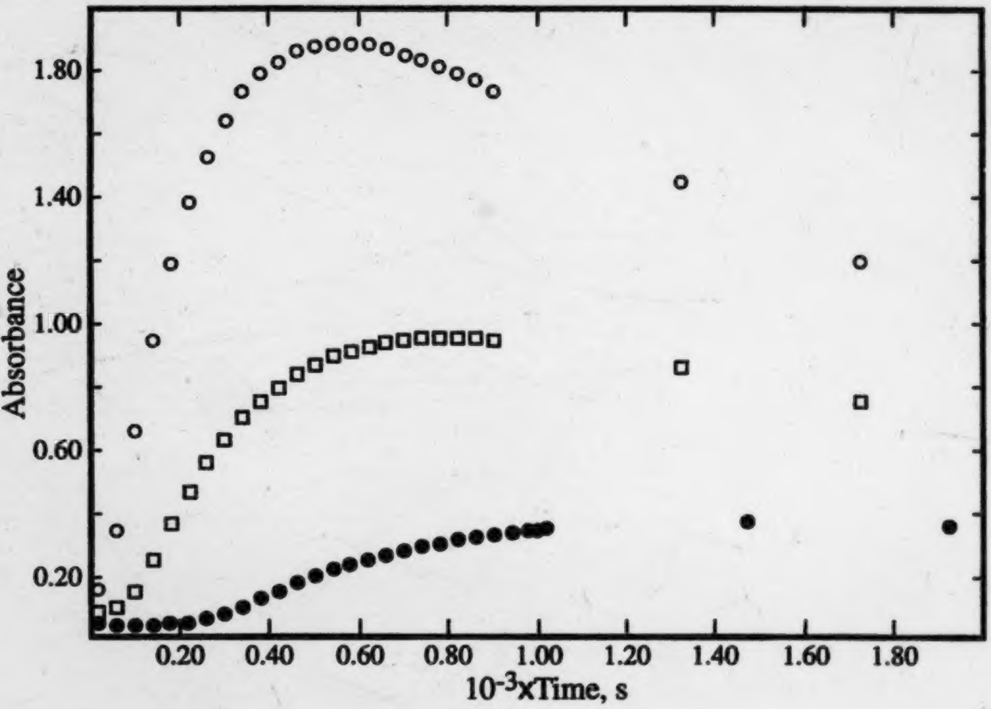

Figure 3.6. Variation of the absorbance at 325 nm with time for solutions of 3.30×10^{-3} M (O), 2.20×10^{-3} M (□), and 1.20×10^{-3} M (●) $Co(OH_2)_6^{3+}$ in 0.080 M $HClO_4$/0.92 M $LiClO_4$ at 25 °C.

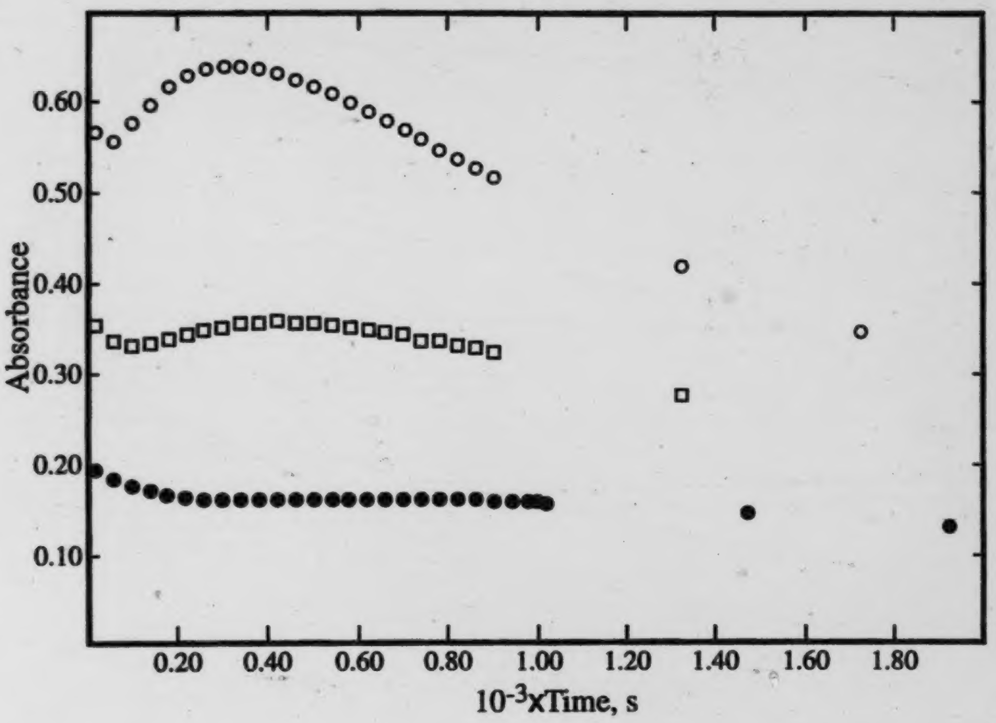

Figure 3.7. Variation of the absorbance at 605 nm with time for solutions of 3.30 × 10^{-3} M (O), 2.20 × 10^{-3} M (□), and 1.20 × 10^{-3} M (●) $Co(OH_2)_6^{3+}$ in 0.080 M $HClO_4$/0.92 M $LiClO_4$ at 25 °C.

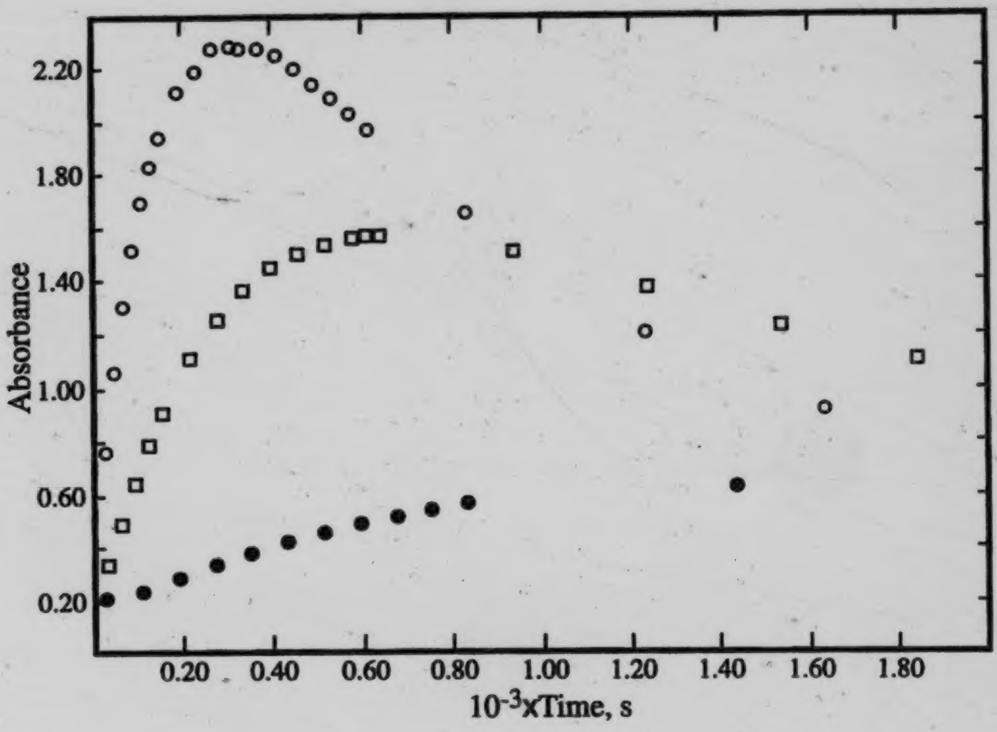

Figure 3.8. Variation of the absorbance at 325 nm with time for solutions of 1.82×10^{-2} M $Co(OH_2)_6^{3+}$ in 0.11 M (O), 0.20 M (□), and 0.45 M (●) H^+ in 1.0 M $HClO_4/LiClO_4$ at 25 °C.

two stages are always rather well separated in time, but the first stage is clearly manifested only when the conditions are such that the second stage is slow.

In order to provide a quantitative analysis of the results, it appears that one needs a model of the general form of equation (3.24)

$$A \longrightarrow B \longrightarrow C \longrightarrow D \qquad (3.24)$$

where A is the equilibrium mixture of $Co(OH_2)_6^{3+}$ and $Co(OH_2)_5(OH)^{2+}$, whose proportions will depend on $[H^+]$, B and C are probably hydroxyl-bridged oligomers, and D is $Co(OH_2)_6^{2+}$. The supposition about B and C is based on the known chemistry of aqueous iron(III) and chromium(III).[9,10] It would be expected that the dependence of the rates of formation of B and C on the [Co(III)] would indicate if these are dimers, trimers or higher oligomers. It should be noted that equation (3.24) may be a simplification in that both A and B may also oxidize water.

A model that provides a quantitative explanation of the observations obviously should fit the observed changes in rates for the different stages with changes in [Co(III)] and $[H^+]$. It should also give constant extinction coefficients for the intermediates that are independent of the [Co(III)]. One also might hope that the extinction coefficients are independent of $[H^+]$, although this involves the assumption that B and C are not undergoing hydrolytic equilibria at the acidities used.

The analysis of the observations began with the data at 325 nm because the observed changes there are the most dramatic and therefore easier to assess qualitatively. The general method is to construct model schemes, based on the ideas described above and then use numerical integration methods to determine if the particular model will fit the observations under a range of concentration conditions. The modeling will require input guesses for the extinction coefficients of the species involved and rate constants for the various steps. It has been assumed that $Co(OH_2)_6^{3+}$ is not a highly reactive oxidant for water at high acidity. This is because of the stability of dilute solutions of cobalt(III) ($< 5 \times 10^{-3}$ M) in strong acid (> 1 M H^+).

Following standard practice in mechanistic studies, the simplest model that seems consistent with the qualitative observations will be examined first. The model involves only dimeric species, the first being a monohydroxy bridged dimer ($[Co(\mu\text{-}OH)Co]^{5+}$) and the second a dihydroxy dimer ($[Co(\mu\text{-}OH)_2Co]^{4+}$). The latter species undergoes redox decomposition to cobalt(II) and H_2O_2. The H_2O_2 is rapidly oxidized by monomeric cobalt(III) as described in Chapter 4. The reaction pathways are summarized in Scheme 3.2, where non-reacting water ligands have been omitted for clarity.

Scheme 3.2

$$2Co(OH_2)^{3+} \xrightarrow{k_1} [(H_2O)Co(\mu - OH)Co]^{5+} + H^+$$

$$[(H_2O)Co(\mu - OH)Co]^{5+} \xrightarrow{k_2} [Co(\mu - OH)_2Co]^{4+} + H^+$$

$$[Co(\mu - OH)_2Co]^{4+} \xrightarrow{k_3} 2Co^{2+} + H_2O_2$$

$$2Co(OH_2)^{3+} + H_2O_2 \xrightarrow{k_4} 2Co^{2+} + O_2 + 2H^+ + 2H_2O$$

In order to possibly model the small initial absorbance change under some conditions, it will be assumed that $Co(OH_2)^{3+}$ and $[Co(\mu\text{-}OH)Co]^{5+}$ have similar extinction coefficients and that the increase in absorbance at 325 nm is due to $[Co(\mu\text{-}OH)_2Co]^{4+}$.

The model leads to the following set of differential equations to describe the time dependence of the concentrations.

$$\partial\frac{[Co(OH_2)^{3+}]}{\partial t} = -2k_1[Co(OH_2)^{3+}]^2 - 2k_4[H_2O_2][Co(OH_2)^{3+}][H^+]^{-1} \tag{3.25}$$

$$\partial\frac{[Co(\mu-OH)Co^{5+}]}{\partial t} = k_1[Co(OH_2)^{3+}]^2 - k_2[Co(\mu-OH)Co^{5+}] \tag{3.26}$$

$$\partial\frac{[Co(\mu-OH)_2Co^{4+}]}{\partial t} = k_2[Co(\mu-OH)Co^{5+}] - k_3[Co(\mu-OH)_2Co^{4+}] \tag{3.27}$$

$$\partial\frac{[H_2O_2]}{\partial t} = k_3[Co(\mu-OH)_2Co^{4+}] - k_4[Co(OH_2)^{3+}][H_2O_2][H^+]^{-1} \tag{3.28}$$

The rate law for the last step is based on the results in Chapter 4, with $k_4 = 26.4 \pm 0.5\ s^{-1}$. When the runs at 0.08 M H^+ and 2.2×10^{-3}, 2.7×10^{-3} and 3.3×10^{-3} M Co(III) were fitted to this model, they gave extinction coefficient values (ε, $M^{-1}\ cm^{-1}$) for $[Co(\mu\text{-}OH)_2Co]^{4+}$ of 380, 428 and 470, respectively. The observed and calculated curves are compared in Figure 3.9. Although the values are not constant, their variation perhaps is not beyond what might be expected for this simple model.

For comparison purposes, an average extinction coefficient (ε) of 426 $M^{-1}\ cm^{-1}$ was used to calculate the curves in Figure 3.10. This shows that this ε value does not

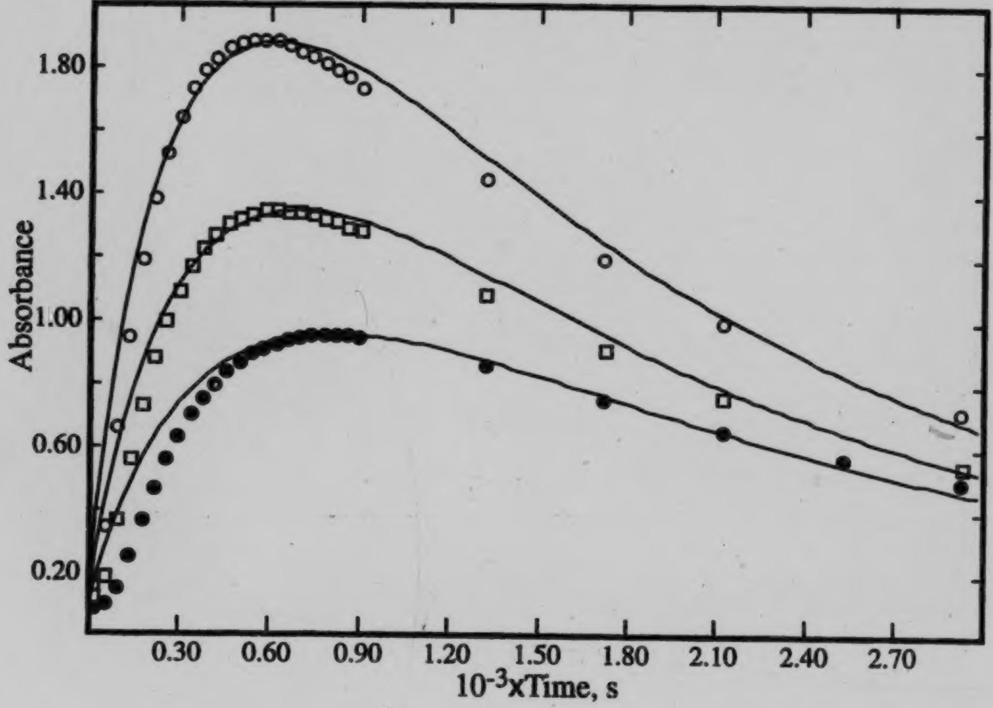

Figure 3.9. Variation of the observed and calculated absorbance at 325 nm with time for solutions of 3.30×10^{-3} M (O), 2.70×10^{-3} M (□) and 2.20×10^{-3} M (●) $Co(OH_2)_6^{3+}$ in 0.080 M $HClO_4$/0.92 M $LiClO_4$ at 25 °C.

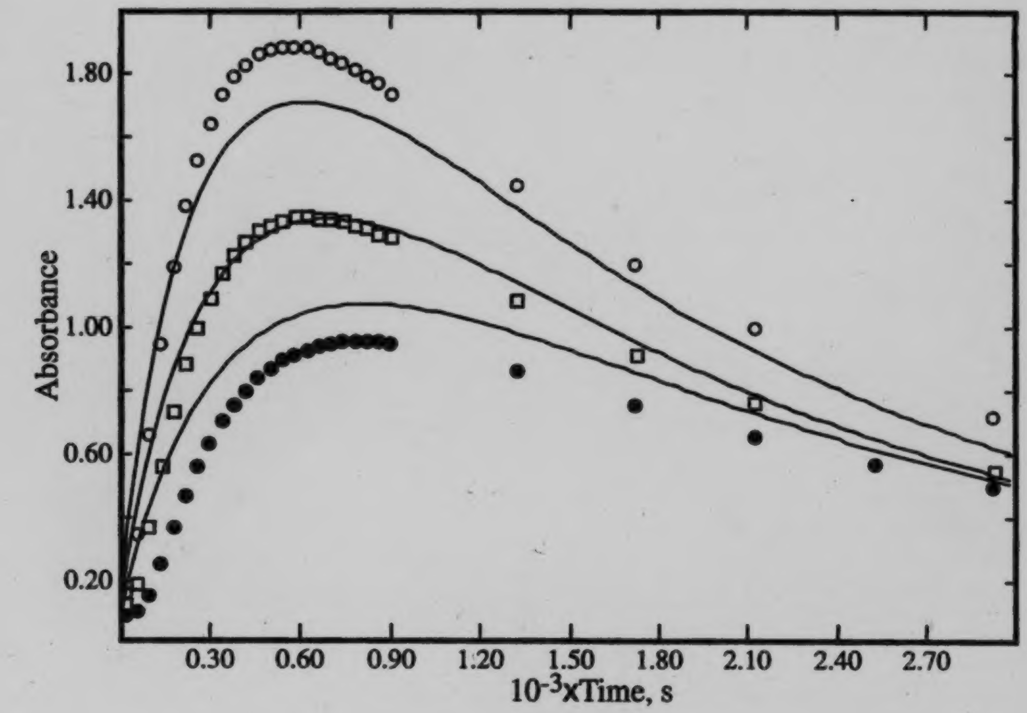

Figure 3.10. Variation of the observed and calculated (fitted using an average ε_3 value of 426 M^{-1} cm^{-1}) absorbance at 325 nm with time for solutions of 3.30 × 10^{-3} M (O), 2.70 × 10^{-3} M (□) and 2.20 × 10^{-3} M (●) $Co(OH_2)_6^{3+}$ in 0.080 M $HClO_4$/0.92 M $LiClO_4$ at 25 °C.

give an adequate fit for the highest and lowest [Co(III)] so that there is a significant problem with this model. When the runs at lower acidity (0.0235 and 0.040 M H^+) and lower Co(III) (1.05×10^{-3} and 1.23×10^{-3} M) were fitted, they seemed most consistent with $[H^+]^{-2}$ and $[H^+]^{-1}$ dependences for k_1 and k_2, respectively.

What was most encouraging was that, when the data at much different conditions, (18.2×10^{-3} M Co(III) in 0.11 or 0.20 M H^+, and 26.0×10^{-3} M Co(III) in 0.45 M H^+) were examined, the absorbance-time profiles were well reproduced. However, the ε were 415, 330 and 210 M^{-1} cm^{-1}, respectively. The observed and calculated curves are shown in Figure 3.11. In general, these observations seem to confirm the inverse $[H^+]$ dependence and indicate that the formation of the major chromophore has a $[Co(III)]^2$ dependence. The expressions for k_1 and k_2 that fit the data are $3.5 \times 10^{-3}[H^+]^{-2}$ and $3.2 \times 10^{-3}[H^+]^{-1}$, respectively. However the variation in the ε values remains a problem. There is a further problem in that this model does not properly reproduce the extent of the "induction period" at the start of the reaction with low [Co(III)] and high $[H^+]$.

The variation in ε values implies that other models should be tried to obtain a consistent fit of the data and to shed more light on the "induction period". One possibility is to change Scheme 3.2 to make the first step reversible with a rate constant k_{-1}. Then it is only necessary to modify the first two differential equations describing the system to (3.29) and (3.30).

$$\partial\frac{[Co(OH_2)^{3+}]}{\partial t} = -2k_1[Co(OH_2)^{3+}]^2 + k_{-1}[(H_2O)Co(\mu-OH)Co]^{5+} - \\ 2k_4[H_2O_2][Co(OH_2)^{3+}][H^+]^{-1} \qquad (3.29)$$

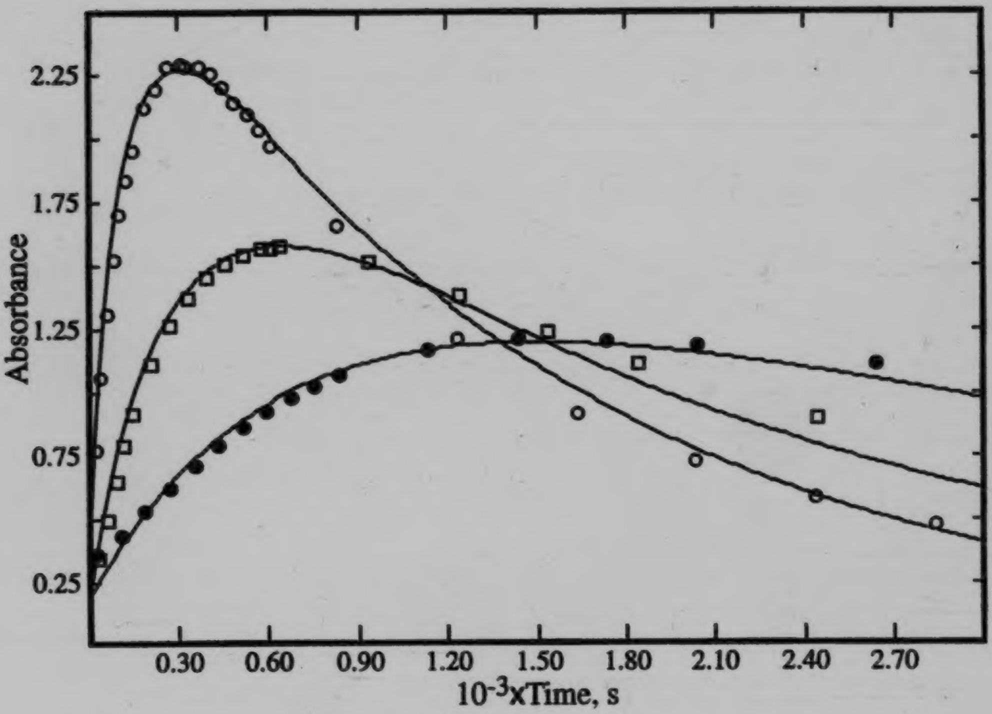

Figure 3.11. Variation of the observed and calculated absorbance at 325 nm with time for solutions of 18.2×10^{-3} M Co(III) in 0.11 M H^+ (O), 18.2×10^{-3} M Co(III) in 0.20 M H^+ (□) and 26.0×10^{-3} M Co(III) in 0.45 M H^+ (●) in 1.0 M $HClO_4$/$LiClO_4$ at 25 °C.

$$\frac{\partial[[(H_2O)Co(\mu-OH)Co]^{5+}]}{\partial t}=k_1[Co(OH_2)^{3+}]^2$$
$$-(k_{-1}+k_2)[[(H_2O)Co(\mu-OH)Co]^{5+}] \qquad (3.30)$$

This might have the effect of reducing the amount of the dihydroxy dimer at low total Co(III), and possibly reproduce the induction period if formation of the monohydoxy dimer precursor is rate limiting at low Co(III) concentration. It should be noted that making the k_2 step reversible will not help in this regard because it is unimolecular and does not depend on the Co(III) concentration.

Another obvious modification to Scheme 3.2 is to assume that the monohydroxy dimer has a significant absorbance. However, this would seem to remove all possibility of modeling the induction period. If the dimer models do not work, then it would seem logical to propose a trimer as the major chromophere. Extension of Scheme 3.2 then leads to Scheme 3.3 as a possibility, where $[(Co)_3(\mu\text{-}OH)_3{}^{6+}]$ is the trimer.

Scheme 3.3

$$2Co(OH_2)^{3+}\xrightarrow{k_1}[Co(\mu-OH)Co]^{5+}+H^+$$

$$[Co(\mu-OH)Co]^{5+}\xrightarrow{k_2}[Co(\mu-OH)_2Co]^{4+}+H^+$$

$$Co(OH_2)^{3+}+[Co(\mu-OH)_2Co]^{4+}\xrightarrow{k_3}\text{trimer}+H^+$$

$$\text{trimer}\xrightarrow{k_4}2Co^{2+}+Co^{3+}+H_2O_2+H^+$$

$$2Co(OH_2)^{3+}+H_2O_2\xrightarrow{k_5}2Co^{2+}+O_2+2H^++2H_2O$$

This model leads to the following set of differential equations to describe the time dependence of the concentrations.

$$\begin{aligned}\partial\frac{[\mathrm{Co(OH_2)^{3+}}]}{\partial t} &= -2k_1[\mathrm{Co(OH_2)^{3+}}]^2 - 2k_5[\mathrm{H_2O_2}][\mathrm{Co(OH_2)^{3+}}][\mathrm{H^+}]^{-1} \\ &\quad - k_3[\mathrm{Co(\mu-OH)_2Co^{4+}}][\mathrm{Co(OH_2)^{3+}}] + k_4[\mathrm{trimer}]\end{aligned} \tag{3.31}$$

$$\partial\frac{[[\mathrm{(H_2O)Co(\mu-OH)Co}]^{5+}]}{\partial t} = k_1[\mathrm{Co(OH_2)^{3+}}]^2 - k_2[[\mathrm{(H_2O)Co(\mu-OH)Co}]^{5+}] \tag{3.32}$$

$$\begin{aligned}\partial\frac{[\mathrm{Co(\mu-OH)_2Co^{4+}}]}{\partial t} &= k_2[[\mathrm{(H_2O)Co(\mu-OH)Co}]^{5+}] \\ &\quad - k_3[\mathrm{Co(\mu-OH)_2Co^{4+}}][\mathrm{Co(OH_2)^{3+}}]\end{aligned} \tag{3.33}$$

$$\partial\frac{[\mathrm{trimer}]}{\partial t} = k_3[\mathrm{Co(\mu-OH)_2Co^{4+}}][\mathrm{Co(OH_2)^{3+}}] - k_4[\mathrm{trimer}] \tag{3.34}$$

$$\partial\frac{[\mathrm{H_2O_2}]}{\partial t} = k_4[\mathrm{trimer}] - k_5[\mathrm{Co(OH_2)^{3+}}][\mathrm{H_2O_2}][\mathrm{H^+}]^{-1} \tag{3.35}$$

Modification to this model, similar to those described for the dimer may also be explored.

Discussion

This work has established that some binuclear and/or polynuclear hydrolyzed complex(es) form for conditions of $[\mathrm{Co(III)}] > 10^{-3}$ and $[\mathrm{H^+}] \leq 0.45$ M at 25 °C. The evidence for this comes from the spectrophotometric measurements (see Figures 3.2-3.11), that show an absorbance increase at 325 nm on the time scale of minutes and that the maximum absorbance increases with increasing cobalt(III) concentration, and with decreasing H^+ concentration.

Similar observations have been made in the study of the hydrolysis behavior of aqueous Fe(III). Vosburgh and co-workers[10,11] observed an isosbestic point in dilute Fe(III) solutions at about 273 nm, attributed to $Fe(OH_2)_6^{3+}$ and $Fe(OH_2)_5OH^{2+}$. The isosbestic point disappeared at high concentrations of Fe(III), consistent with the appearance of a third species, $[Fe(OH_2)_4(OH)]_2^{4+}$. Some anologous oligomers have been isolated in studies of aqueous Cr(III).[9,12-14] Ion-exchange techniques were used to separate and identify the species $[Cr(\mu\text{-}OH)(OH_2)_4]_2^{4+}$ (blue) and $[Cr_3(\mu\text{-}OH)_3(OH_2)_{11}(OH)]^{5+}$ (green) from solutions of Cr(III).

This study indicates that the rate of rise in absorbance shown in Figures 3.3-3.11 is second-order in [Co(III)] and inverse second-order in $[H^+]$. The absorbance decay is essentially independent of the [Co(III)], but is first-order in the concentration of the intermediate species and inverse first-order in H^+ concentration.

The $[H^+]^{-2}$ and $[H^+]^{-1}$ dependence for the absorbance increase and decrease, respectively, may be accounted for by hydrolysis equilibria for $Co(OH_2)_6^{3+}$ and the oligomers. If K_1 and K_2 represent the equilibrium constants for these hydrolyses, respectively, and k_1 and k_2 are rate constants for the absorbance increase and decrease, respectively. The rate for the initial rise is given by (3.36)

$$\frac{-\partial[\mathrm{Co(OH_2)}^{3+}]}{\partial t} = k_1\left(\frac{K_1[\mathrm{Co(III)_T}]}{K_1+[\mathrm{H^+}]}\right)^2 \qquad (3.36)$$

where $[\mathrm{Co(III)_T}] = [\mathrm{Co(OH_2)_6}^{3+}] + [\mathrm{Co(OH_2)_5OH}^{2+}]$. The rate for the subsequent decrease is given by (3.37)

$$\frac{-\partial[\mathrm{dimer}]}{\partial t} = k_2\left(\frac{K_2[(\mathrm{dimer})_\mathrm{T}]}{K_2+[\mathrm{H^+}]}\right) \qquad (3.37)$$

where $[(\mathrm{dimer})_\mathrm{T}] = [(\mathrm{H_2O})\mathrm{Co}(\mu\text{-OH})\mathrm{Co}^{5+}] + [\mathrm{Co}(\mu\text{-OH})\mathrm{CoOH}^{4+}]$. The calculated values for k_1K_1 and k_2K_2 that fit the data are 3.5×10^{-3} $\mathrm{s^{-1}}$ and 3.2×10^{-3} M $\mathrm{s^{-1}}$, respectively. Weiser[4] calculated the rate constant for the decomposition of the Co(III) dimer at 330 nm to be 2.9 - 4.6×10^{-3} M $\mathrm{s^{-1}}$, which is comparable to the value (3.2×10^{-3} M $\mathrm{s^{-1}}$) estimated in this study at 325 nm.

Other researchers[2-7] have made similar observations suggesting that Co(III) forms dimers/polymers in aqueous perchloric acid. For the purpose of comparison to some of the earlier work, it is possible to calculate an observed extinction coefficient (ε_{obs}) from the maximum absorbance divided by the total cobalt(III) concentration. Sutcliffe and Weber[3] reported a value of ε_{obs} at 330 nm of 62 $\mathrm{M^{-1}}$ $\mathrm{cm^{-1}}$ for a run in 0.330 M $\mathrm{H^+}$ with 18.6×10^{-3} M Co(III) for Co(III) dimer species. In the present work, a value of 62 $\mathrm{M^{-1}}$ $\mathrm{cm^{-1}}$ at 325 nm is obtained under comparable conditions of 0.300 M $\mathrm{H^+}$ and 18.0×10^{-3} M Co(III). It should be noted that although there is slight difference in wavelengths and acid concentrations, these values are in good agreement.

Weiser[4] reported values of ε_{obs}, but they are based on the absorbance determined by extrapolation of the decay back to zero time. This seems to be based on the assumption that the absorbance rise is essentially instantaneous. Although the present work has shown that this assumption is not correct, for purpose of comparison, one can still reproduce Weiser's method of analysis. Weiser obtained rather constant values for ε_{obs} of ~ 150 M^{-1} cm^{-1} at 402 nm for conditions such as 3.5×10^{-3} M Co(III) in 0.024 M $HClO_4$. From his tabulation of one complete spectrum one can interpolate a value of ~ 380 M^{-1} cm^{-1} at 325 nm. For a run from the present study with 1.05×10^{-3} M Co(III) in 0.0235 M H^+, the extrapolation gives an ε_{obs} of ~ 220 M^{-1} cm^{-1} at 325 nm. Given the different concentrations of Co(III) and uncertainties in the extrapolations, this value seems consistent with Weiser's observations.

Baxendale and Wells[2], observed a general increase in absorbance below 500 nm that gave a shoulder at 400 nm with ε_{obs} of 78.1 M^{-1} cm^{-1} in 0.1 M H^+ and 8.8×10^{-3} M Co(III) at ionic strength of 1.82 M $HClO_4/NaClO_4$. In this study, under comparable conditions of 0.11 M H^+ and 18×10^{-3} M Co(III), at ionic strength of 1.0 M $HClO_4/LiClO_4$, the ε_{obs} is 74.1 M^{-1} cm^{-1}at 400 nm, in excellent agreement with that of Baxendale and Wells. However, the present kinetic observations and those of Weiser do not agree with the proposals of Baxendale and Wells that Co(III) is present predominantly as the dimer, even at high acidities, and that the rate is three-halves-order in [Co(III)].

References

(1) Hargreaves, G.; Sutcliffe, L. H. *Trans. Faraday Soc.* **1955**, *51*, 786.

(2) Baxendale, J. H.; Wells, C. F. *Trans. Faraday Soc.* **1957**, *53*, 800.

(3) Sutcliffe, L. H.; Weber, J. R. *J. Inorg. Nucl. Chem.* **1960**, *12*, 281

(4) Weiser, D. W. *Ph. D. Thesis*, University of Chicago, **1956**.

(5) Bawn, C. E. H.; White, A. G. *J. Chem. Soc.* **1951**, 331.

(6) Davies, G.; Warnqvist, B. *Coord. Chem. Rev.* **1970**, 5, 349.

(7) Anbar, M.; Pecht, I. *J. Amer. Chem. Soc.* **1967**, *89*, 2553.

(8) Wells, C. F. *Disc. Faraday Soc.* **1968**, *46*, 197.

(9) Baes, C. F. Jr.; Mesmer, R. M. *The Hydrolysis of Cations*; Wiley Interscience; Toronto, Ontario, Canada, **1976**; pg. 229 and 211.

(10) Siddall, T. H., III; Vosburgh, W. C. *J. Amer. Chem. Soc.* **1951**, *73*, 4270.

(11) Milburn, R. M.; Vosburgh, W. C. *J. Amer. Chem. Soc.* **1955,** *77*, 1352.

(12) Laswick, J. A.; Plane, R. A. *J. Amer. Chem. Soc.* **1959,** *81*, 3564.

(13) Spiccia, L.; Marty, W.; Giovali, R. *Inorg. Chem.* **1988**, *27*, 2660.

(14) Stunzi, H.; Marty, W. *Inorg. Chem.* **1983**, *22*, 2145.

CHAPTER 4. Reaction of Hydrogen Peroxide with Hexaaquacobalt(III) Perchlorate

Introduction

The probable production of hydrogen peroxide in the reaction between $Co(OH_2)_6^{3+}$ and water in Chapter 3, prompted a further investigation of the reaction between hydrogen peroxide and $Co(OH_2)_6^{3+}$.

The kinetics of this reaction were studied by Baxendale and Wells,[1] who followed the decrease of cobalt(III) concentration as a function of time at 230 nm. The concentration ranges for the kinetics were: $[Co(III)] = 4.9$ to 9.2×10^{-5} M; $[H_2O_2] = 1.0$ to 50.0×10^{-4} M; $[HClO_4] = 0.5$ to 2.0 M, at an ionic strength of 2.0 M ($NaClO_4$). The concentration range available to Baxendale and Wells[1] was restricted because of the rapidity of the reaction. The rate was found to be first-order in the concentrations of Co(III) and H_2O_2 and inverse first-order in $[H^+]$. Baxendale and Wells[1] observed a rapid fall in the initial absorbance during the reaction of Co(III) with H_2O_2. They proposed that an intermediate complex $[Co(OH_2)_6^{3+}\bullet HO_2^-]$ is formed that is in rapid and reversible equilibrium with Co(III) and H_2O_2. They suggested that, if cobalt(III) is in monomeric form, then the inverse dependence on $[H^+]$ can arise from any or all of the reactions in equations (4.1) to (4.6);

$$H_2O_2 \underset{}{\overset{K_p}{\rightleftarrows}} HO_2^- + H^+ \qquad (4.1)$$

$$Co(OH_2)_6^{3+} + HO_2^- \overset{K_c}{\rightleftarrows} [Co(OH_2)_6^{3+} \bullet HO_2^-] \tag{4.2}$$

$$[Co(OH_2)_6^{3+} \bullet HO_2^-] \xrightarrow{k_1} Co(OH_2)_6^{2+} + HO_2^{\bullet} \tag{4.3}$$

$$Co(OH_2)_6^{3+} + HO_2^- \xrightarrow{k_3} Co(OH_2)_6^{2+} + HO_2^{\bullet} \tag{4.4}$$

$$Co(OH_2)_6^{3+} \overset{K_a}{\rightleftarrows} Co(OH_2)_5OH^{2+} + H^+ \tag{4.5}$$

$$Co(OH_2)_5OH^{2+} + H_2O_2 \xrightarrow{k_2} Co(OH_2)_6^{2+} + HO_2^{\bullet} \tag{4.6}$$

If the equilibria are established rapidly, the rate of reaction is given by equation (4.7);

$$\frac{-\partial[Co(III)]}{\partial t} = \frac{b[Co(III)]_T[H_2O_2]_T}{g} \tag{4.7}$$

where $[Co(III)]_T = [Co(OH_2)_6^{3+}] + [Co(OH_2)_5OH^{2+}] + [Co(OH_2)_6^{3+} \bullet HO_2^-]$, $b = k_1K_cK_p + k_3K_p + k_2K_a$ and $g = K_cK_p[H_2O_2]_T + K_p + K_pK_a + [H^+]$. All three pathways {(4.1-3), (4.1 and 4.4) and (4.5-4.6)} lead to the observed rate law if $[H^+] >> K_cK_p[H_2O_2]_T$, K_pK_a and knowing that $[H^+] >> K_p = 10^{-12}$ M. The assumed conditions are true for the range of $[H^+]$ and $[H_2O_2]$ used. We used the published data to calculate that $b = 25.3$ s^{-1} at 25 °C and that ΔH^* and ΔS^* are 25.5 ± 0.4 kcal mol^{-1} and 33.3 ± 1.5 cal mol^{-1} K^{-1}, respectively.

Davies et al.[2] reinvestigated the reaction by monitoring the disappearance of cobalt(III) between 240 and 605 nm, depending on the [Co(III)], using stopped-flow and Cary model 14 spectrophotometers. Absorbance measurements were used to determine the cobalt(III) and cobalt(II) concentrations ($\varepsilon_{605\ \mathrm{nm}} = 35$ and $\varepsilon_{509\ \mathrm{nm}} = 4.8\ \mathrm{M^{-1}\ cm^{-1}}$, respectively). The concentration ranges used were: [Co(III)] = 0.62-6.7 × 10^{-3} M; constant $[H_2O_2] = 2.32 \times 10^{-2}$ M; $[HClO_4] = 0.15$-1.50 M, in 3.0 M $NaClO_4/HClO_4$. The observations showed no evidence for complex formation. The reaction rate was assumed to be first-order in $[H_2O_2]$ and was shown to be first-order in [Co(III)] and to be inverse first-order in $[H^+]$. The second-order rate constant is given by $k_{2obs} = a + b/[H^+]$, where only an upper limit of $a \leq 2\ \mathrm{M^{-1}\ s^{-1}}$ could be determined, and $b = k_2K_a = 23\ \mathrm{s^{-1}}$. The rate law and value of b agree with those found by Baxendale and Wells.

Davies[3] suggested the mechanism for the reaction shown in equations (4.5) and (4.8) to (4.10).

$$\mathrm{Co(OH_2)_6}^{3+} + \mathrm{H_2O_2} \xrightarrow{a} \mathrm{Co(OH_2)_6}^{2+} + \text{other products} \tag{4.8}$$

$$\mathrm{Co(OH_2)_5OH}^{2+} + \mathrm{H_2O_2} \xrightarrow{k_2} \mathrm{Co(OH_2)_6}^{2+} + \text{other products} \tag{4.9}$$

$$\mathrm{Co(OH_2)_6}^{3+} + \text{other products} \xrightarrow{\text{fast}} \mathrm{Co(OH_2)_6}^{2+} + \mathrm{O_2} \tag{4.10}$$

"Other products" presumably include radical species, since cobalt(III) is a one-electron oxidant and hydrogen peroxide needs to lose two electrons in order to be converted to oxygen. The step (4.10), involving the reaction between aquacobalt(III) complexes and highly reactive "other products", is assumed to be at least ten times faster than either steps (4.8) or (4.9). The assumption also is made that acid-base equilibria involving hydrogen peroxide can be ignored because $H_3O_2^+$ is a very strong acid ($pK_a = -3$) and

H_2O_2 is a very weak acid (pK_a = 12) so that such equilibria will be insignificant in the acidity range of the study. This mechanism predicts that $b = k_2K_a$.

Davies et al.[2] noted that the kinetic simplicity of the reaction between hydrogen peroxide and $Co(OH_2)_6^{3+}$ contrasts sharply with the more complex kinetics observed in the reactions of cobalt(III) with chloride ion[4,5] and malic[6] and thiomalic[7] acids, where the formation and disappearance of intermediate complexes have been monitored spectrophotometrically. The kinetic and spectrophotometric observations suggest that any intermediate complexes formed with H_2O_2 are present at undetectably low concentration levels.

The oxidation of hydrogen peroxide by aqueous cobalt(III) has been studied in the present work in 1.0 M $HClO_4/LiClO_4$ in order to establish the kinetics under the same conditions as those used for the oxidation of water.

Experimental

Preparation of Stock $KMnO_4$. The potassium permanganate (Shawinigan) solution was standardized with sodium oxalate (Baker). A sample (0.150 g, 5.31×10^{-3} mole) of dry sodium oxalate was added to 120 mL of water containing 6.25 mL of concentrated sulfuric acid (BDH). The mixture was stirred till all the oxalate had dissolved and the solution was cooled to 25-30 °C in a water bath. About 90-95 % of the required quantity of MnO_4^- solution was added from a burette at a rate of 25-35 mL per minute to the oxalate solution while stirring slowly. The solution was heated to 55-60 °C and the titration was completed by adding MnO_4^- solution till a faint pink coloration persisted for 30 seconds. The concentration of [MnO_4^-] was calculated using equation (4.11).

$$[MnO_4^-] = \frac{5 \times \text{moles of } C_2O_4^{2-}}{2 \times \text{Vol. of } MnO_4^- \text{ (L)}} \tag{4.11}$$

Preparation of Stock H_2O_2. The stock H_2O_2 (ACP) solution was standardized by titration with $KMnO_4$. A 4.0 mL aliquot of the stock solution was acidified with 2.0 mL of 0.2 M sulfuric acid (BDH) and titrated with MnO_4^-. The [H_2O_2] was calculated using equation (4.12).

$$[H_2O_2] = \frac{2[MnO_4^-] \times \text{Vol. of } MnO_4^- \text{ (L)}}{5 \times \text{Vol. of } H_2O_2 \text{ (L)}} \tag{4.12}$$

Kinetic Measurements. The ionic strength in the reaction of $Co(OH_2)_6^{3+}$ and H_2O_2 was maintained at 1.0 M with $LiClO_4$ and $HClO_4$. This reaction was carried out on stopped-flow and Cary 219 spectrophotometers under first and second-order conditions, with the [H_2O_2] higher than [$Co(OH_2)_6^{3+}$].

For the stopped-flow measurement, a new solution of aqueous $Co(OH_2)_6^{3+}$ was made from the stock solution stored at 0 °C in 2.0 M $HClO_4$ (preparation in Chapter 3) after every four runs at < 0.1 M acid concentration. This was done to minimize the presence of oligomers of aqueous cobalt(III) in the reactant solution. The actual concentration of $Co(OH_2)_6^{3+}$ was determined immediately before starting and after the reaction from the absorbance at 605 nm of a sample from each new solution. The disappearance of $Co(OH_2)_6^{3+}$ was monitored at 246 nm. The absorbance-time data (256 points per trace) were collected on an MS-DOS 486 computer and at least 140 points for each trace were analyzed by least-squares to give the first-order and second-order rate constants. The observed rate constants were averaged for 6 to 8 runs. The temperature (± 0.5 °C) of the cell housing was regulated by circulation of thermostatted water.

For conditions of $[H^+] > 0.28$ M and $[H_2O_2] < 1.75 \times 10^{-3}$ M the reaction was slow enough so that it could be monitored on the Cary 219 spectrophotometer in a 1.00 cm path-length cell at 246 nm. At least 30 points for each trace were analyzed by least-squares to give the first-order rate constant. The temperature (± 0.5 °C) of the cell housing was regulated by circulation of thermostatted water.

First-order Analysis. From the overall reaction in equation (4.13)

$$H_2O_2 + 2Co(OH_2)_6^{3+} \rightarrow 2Co(OH_2)_6^{2+} + O_2 + 2H^+ \qquad (4.13)$$

A generic reaction can be developed from equation (4.13) given in equation (4.14)

$$A \; + \; 2B \longrightarrow 2C \qquad (4.14)$$

The data collected under pseudo-first-order conditions ([A] >> [B]) can be analyzed by the first-order rate equation (4.15)

$$-\frac{\partial[\mathrm{B}]}{\partial t} = 2k_{2obs}[\mathrm{A}][\mathrm{B}] = k_{1obs}[\mathrm{B}] \qquad (4.15)$$

which gives equation (4.16) as the integrated rate law

$$[\mathrm{B}] = [\mathrm{B}]_0 \mathrm{e}^{-k_{1obs}t} \qquad (4.16)$$

where [B] is the concentration at any time, t, $[\mathrm{B}]_0$ is the initial concentration and k_{1obs} is the pseudo-first-order rate constant. In the present case A = H_2O_2, B = $Co(OH_2)_6^{3+}$ and C = $Co(OH_2)_6^{2+}$. The disappearance of B was monitored, therefore the property being observed is designated as I and its proportionality constant with concentration is ε. Then the initial absorbance in a 1.00 cm path-length cell is

$$I_0 = \varepsilon_\mathrm{B}[\mathrm{B}]_0 \qquad (4.17)$$

and at any time I is given by (4.18)

$$I = \varepsilon_\mathrm{B}[\mathrm{B}] \qquad (4.18)$$

Substitution for [B] and $[\mathrm{B}]_0$ in terms of ε_B, I and I_0 into equation (4.16) yields (4.19)

$$\frac{I}{\varepsilon_\mathrm{B}} = \frac{I_0}{\varepsilon_\mathrm{B}} \mathrm{e}^{-k_{1obs}t} \qquad (4.19)$$

Equation (4.19) reduces to

$$I = I_0 e^{-k_{1obs}t} \tag{4.20}$$

Equation (4.20) can be used to fit the values of I with t by least-squares to obtain k_{1obs}. There is no need to know the initial concentrations or extinction coefficients.

Second-order Analysis. For second-order conditions for reaction (4.14), the stoichiometry relationship $[A]_0 - [A] = 2[B]_0 - 2[B]$ gives equation (4.21)

$$-\frac{\partial[B]}{\partial t} = 2k_{2obs}[A][B] = 2k_{2obs}\left([A]_0 - 2[B]_0 + 2[B]\right)[B] \tag{4.21}$$

where [A] and [B] represent the concentrations at any time, t, $[A]_0$ and $[B]_0$ are the initial concentrations and k_{2obs} is the second-order rate constant. Rearrangement and integration of (4.21) gives equation (4.22)

$$-2k_{2obs}t = \frac{1}{\left([A]_0 - 2[B]_0\right)}\ell n\left(\frac{\left([A]_0 - 2[B]_0 + 2[B]\right)}{[B]} \times \frac{[B]_0}{[A]_0}\right) \tag{4.22}$$

The concentration of B at any time can be solved from equation (4.22) to be

$$[B] = \frac{\left([A]_0 - 2[B]_0\right)}{\frac{[A]_0}{[B]_0}\exp\left\{2\left(2[B]_0 - [A]_0\right)k_{2obs}t\right\} - 2} \tag{4.23}$$

With these expressions for the concentration and Beer's law, one can develop the relationship for the time dependence of the absorbance (I) under various experimental conditions.

For the present experiment, [B] < [A] and [B] is the only absorbing species at 246 nm ($\varepsilon_B = 4.05 \times 10^3$ M^{-1} s^{-1}). Then the initial absorbance in a 1.00 cm path-length cell is

$$I_0 = \varepsilon_B[B]_0 \tag{4.24}$$

so that $[B]_0 = I_0/\varepsilon_B$. Then the absorbance I at any time t is given by equation (4.25), where [B] has been expressed from equation (4.23)

$$I = \varepsilon_B[B] = \left[\frac{\varepsilon_B\left([A]_0 - \dfrac{2I_0}{\varepsilon_B}\right)}{\left(\dfrac{\varepsilon_B[A]_0}{I_0}\right)\exp\left\{2\left(\dfrac{2I_0}{\varepsilon_B} - [A]_0\right)k_{2obs}t\right\} - 2}\right] \tag{4.25}$$

Since ε_B and $[A]_0$ are known, this equation was used to determine least-squares best-fit values for k_{2obs} for the absorbance-time curve for each kinetic run.

Results

The overall reaction is given by equation (4.13). Under pseudo-first-order conditions ($[H^+]$, $[H_2O_2]$ >> [Co(III)]), the absorbance-time curves were analyzed to obtain k_{1obs} (equation (4.20)). Under second-order conditions ($[H^+]$ >> $[H_2O_2]$ > [Co(III)]) the curves were analyzed to obtain k_{2obs} (equation (4.25)). The results are collected in Table 4.1. Overall, the data are consistent with the rate law in equation (4.26)

$$-\frac{\partial[\mathrm{Co(III)}]}{\partial t} = k_{1obs}[\mathrm{Co(III)}] = 2k_{2obs}[\mathrm{H_2O_2}][\mathrm{Co(III)}] = \frac{b\,[\mathrm{H_2O_2}][\mathrm{Co(III)}]}{[\mathrm{H^+}]} \qquad (4.26)$$

where b is a constant as defined by Davies et al.[2,3]

For runs at constant $[H^+]$ under pseudo-first-order conditions, k_{1obs} has a first-order dependence on $[H_2O_2]$, consistent with (4.26) and shown by the plot in Figure 4.1. It should be noted that $k_{2obs} = k_{1obs}/2[H_2O_2]$ from equation (4.26).

The rate law predicts that a plot of k_{2obs} versus $[H^+]^{-1}$ should be linear and this is confirmed by Figure 4.2. Alternatively, this condition predicts that $2k_{2obs}[H^+] = b$ should be a constant, and this is confirmed by the values in the last column in Table 4.1. The final analysis gave the value of b and its standard deviation as 26.4 ± 0.5 s^{-1} in 1.0 M $HClO_4/LiClO_4$ at 25 °C.

It should be noted that 4 out of the original 38 runs have been rejected in the above analysis on the conservative basis[8] that the b value deviated by ≥ 5 standard deviations from the original mean. The data also were fit to a rate law that included an

Table 4.1. Kinetic Data for the Reaction of H_2O_2 with $Co(OH_2)_6^{3+}$] in 1.0 M $LiClO_4$/ $HClO_4$ at 25 °C.

$[H_2O_2]$ (M)	$10^4[Co(OH_2)_6^{3+}]$ (M)	10^2 $[H^+]$ (M)	k_{1obs}[a] (s^{-1})	$10^{-2}k_{2obs}$ (M^{-1} s^{-1})	$2k_{2obs}[H^+]$ (s^{-1})
6.72×10^{-3}	2.60	4.00	9.07	6.75	27.0
1.00×10^{-2}	2.23	4.00	13.8	6.90	27.6
2.00×10^{-3}	2.60	5.00	2.16	5.40	27.0
3.00×10^{-3}	2.60	5.00	3.42	5.70	28.5
4.00×10^{-3}	2.60	5.00	4.44	5.55	27.8
5.00×10^{-3}	2.60	5.00	5.85	5.85	29.3
6.00×10^{-3}	2.60	5.00	6.72	5.60	28.0
7.00×10^{-3}	2.60	5.00	8.05	5.75	28.8
3.84×10^{-3}	2.23	6.00	3.25	4.23	25.4
6.72×10^{-3}	2.60	6.00	5.02	3.74	22.4
6.72×10^{-3}	2.60	6.00	5.25	3.95	26.5
1.00×10^{-2}	2.23	6.00	8.80	4.40	26.4
1.15×10^{-2}	2.23	6.00	9.03	3.93	23.6
1.73×10^{-2}	2.23	6.00	13.7	3.97	23.8
6.00×10^{-4}	2.70	8.00		3.26[b]	30.1
6.00×10^{-4}	2.70	8.00		2.34[b]	22.7

6.72×10^{-3}	2.60	8.00	4.14	3.80	24.7
1.00×10^{-2}	2.23	8.00	6.88	3.44	27.5
6.00×10^{-4}	2.70	12.0		2.24[b]	26.9
6.00×10^{-4}	2.70	12.0		2.41[b]	23.9
6.00×10^{-3}	2.60	12.0	2.53	2.11	25.3
1.00×10^{-2}	2.23	12.0	4.25	2.13	25.5
6.00×10^{-4}	2.70	16.0		1.89[b]	29.5
6.00×10^{-4}	2.70	16.0		1.89[b]	29.4
6.72×10^{-3}	2.60	16.0	2.06	1.53	24.5
6.72×10^{-3}	2.60	20.0	1.64	1.22	24.4
1.00×10^{-2}	2.23	20.0	2.62	1.31	26.2
6.00×10^{-4}	2.70	30.0		1.07[b]	32.1
6.00×10^{-4}	2.70	30.0		0.88[b]	27.9
6.72×10^{-3}	2.60	40.0	0.75	0.56	22.4
6.00×10^{-4}	2.70	60.0		0.45[b]	26.7

---

[a] Determined by first-order analysis. [b] Determined by second-order analysis.

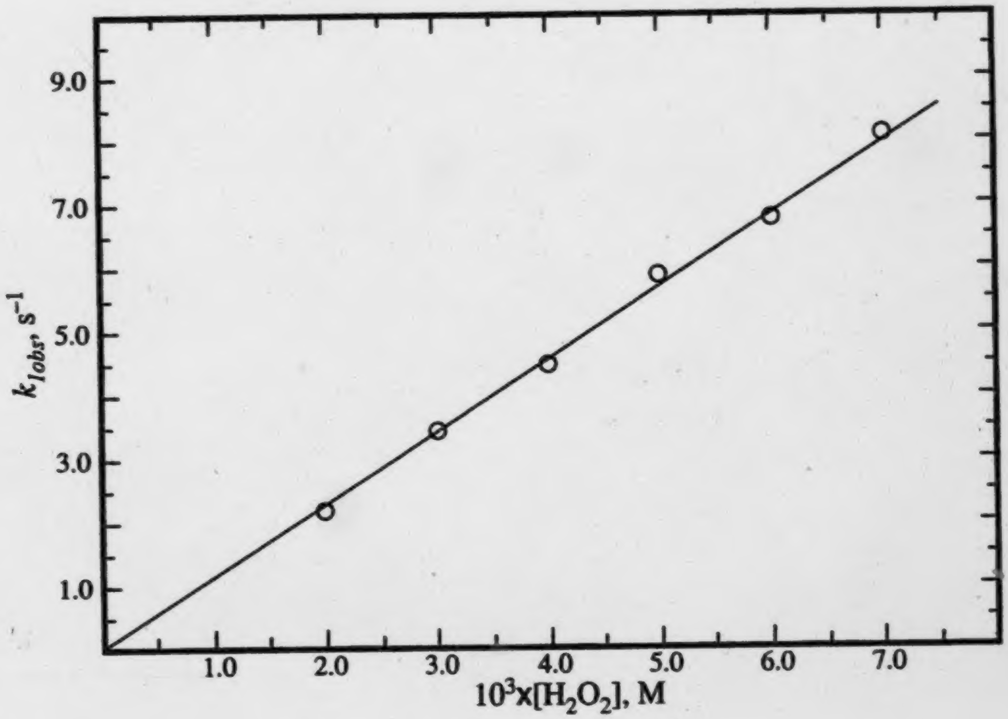

Figure 4.1. Dependence of k_{1obs} on [H_2O_2] with 2.60 × 10^{-4} M $Co(OH_2)_6^{3+}$ and 5.00 × 10^{-2} M $HClO_4$ in 1.0 M $LiClO_4/HClO_4$ at 25 °C.

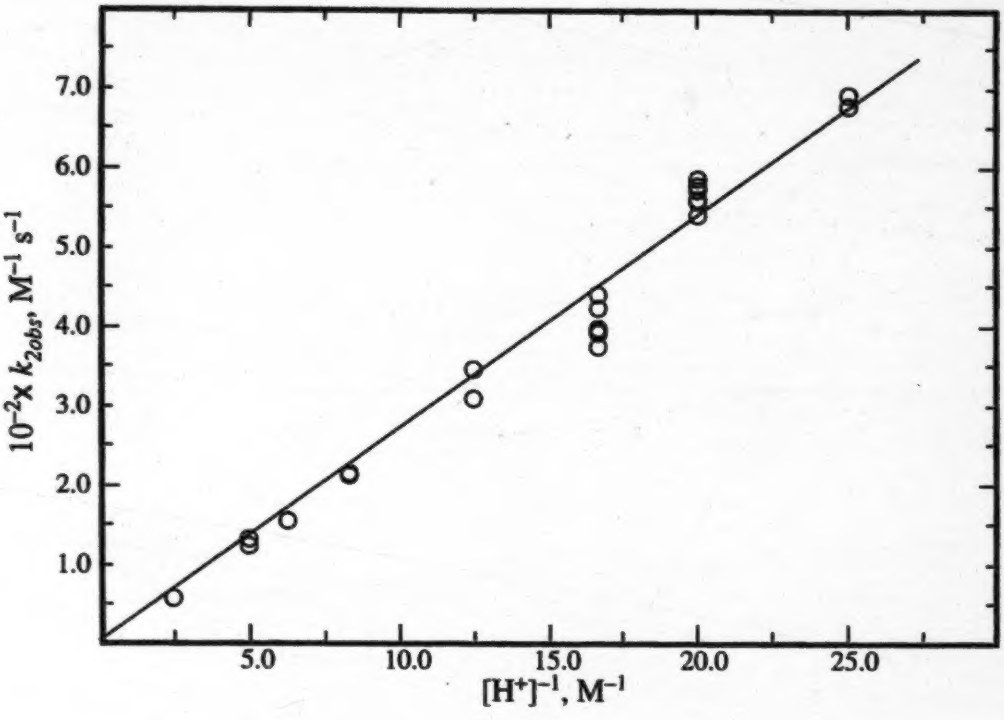

Figure 4.2. Dependence of k_{2obs} on $[H^+]^{-1}$ with 2.23-2.70 × 10^{-4} M $Co(OH_2)_6^{3+}$ and 6.00 – 173 × 10^{-4} M H_2O_2 in 1.0 M $LiClO_4/HClO_4$ at 25 °C.

$[H^+]$ independent term, but this was found to be statistically insignificant because it was 1.3 times smaller than its standard deviation.

Discussion

The rate law for the reaction of $Co(OH_2)_6^{3+}$ with hydrogen peroxide deduced in this work agrees with that of Baxendale and Wells[1] and Davies and Watkins.[2] The value of *b* = 26.4 ± 0.5 s^{-1} (1.0 M $HClO_4$ /$LiClO_4$, 25 °C) may be compared to the values of 25.3 s^{-1} (2.0 M $HClO_4$/$NaClO_4$, 25 °C) found by Baxendale and Wells,[1] and 23 s^{-1} (3.0 M $HClO_4$ /$NaClO_4$, 25 °C) determined by Davies and Watkins[2]. The value of *b* obtained by Baxendale and Wells,[1] is slightly smaller than the values obtained by Davies and Watkins[2] and in this work. The difference could be attributed to the difference in ionic strengths and the medium of reaction (Na^+ versus Li^+ in this work).

In the study of Baxendale and Wells, the reaction was carried out under second-order conditions and the $[Co(OH_2)_6^{3+}]$ was determined directly by using the extinction coefficient of 7.0×10^3 M^{-1} cm^{-1} at 230 nm. This extinction coefficient agrees with that reported by Weiser[9] (7.5×10^3 M^{-1} cm^{-1}). In the study of Davies and Watkins, the $[Co(OH_2)_6^{3+}]$ ($\leq 6.7 \times 10^{-3}$ M) was less than $[H_2O_2]$ (2.3×10^{-2} M), and pseudo-first-order conditions were assumed, so that the determination of $[Co(OH_2)_6^{3+}]$ was not necessary. In the present study, the reaction conditions were both pseudo-first-order and second-order. The cobalt(III) concentrations were determined for each solution used on the stopped-flow by measuring the absorbance of an aliquot from the stock solution at 605 nm and using the extinction coefficient of 35 M^{-1} cm^{-1}.

Baxendale and Wells[1] suggested in their work that the initial fall in the absorbance was due to removal of cobalt(III) by a rapid and reversible reaction with hydrogen peroxide forming $[Co(OH_2)_6{}^{3+}\bullet H_2O^-]$. This was not observed either by Davies and Watkins[2] or in this work. We used Weiser's[9] extinction coefficient for $Co(OH_2)_6{}^{3+}$ at 246 nm ($\varepsilon = 4.1 \times 10^3$ M^{-1} s^{-1}) to calculate the concentration of $Co(OH_2)_6{}^{3+}$ from the initial absorbance of the kinetic solutions. The calculated concentration in most kinetic solutions corresponded to that expected from the concentration of the reactant solution. Any slight fall in absorbance in this work could be attributed to the dead time of the instrument. It should be noted that the hydrogen peroxide concentrations used here were up to four times larger than those of Baxendale and Wells, and the $[H^+]$ was up to 14 times less, so that complex formation should have been even greater under some of our conditions.

The rate controlling process could be simple outer-sphere electron transfer or ligand substitution of H_2O_2 on $Co(OH_2)_5(OH)^{2+}$, followed by inner-sphere electron transfer. If the latter is the case, then one would expect similar rate constants for simple substitution reactions and the redox process. There are several examples in the literature where substitution with an inverse $[H^+]$ dependence has been assigned reaction with $Co(OH_2)_5(OH)^{2+}$. If one takes the literature values of k_2K_a, to make them independent of the uncertain value of K_a, then one finds values of 7.0 s^{-1} (7 °C), 16.0 s^{-1} (7 °C) and 44.0 s^{-1} (25 °C) for malic acid,[6] thiomalic acid[7] and chloride ion,[4,5] respectively. These values are quite similar, after due allowance for temperature differences, to our value of k_2K_a = 26.4 ± 0.5 s^{-1} (25 °C) for H_2O_2. This observation supports an inner-sphere mechanism for oxidation of H_2O_2 by $Co(OH_2)_5(OH)^{2+}$.

The mechanism proposed by Davies and Watkins may be expanded somewhat, as shown in equations (4.5) and (4.27) to (4.30) by being more specific about the "other products". This scheme involves a rapidly maintained equilibrium between $Co(OH_2)_6^{3+}$ and $Co(H_2O)_5(OH)^{2+}$ (equation (4.5)) and oxidation of H_2O_2 by both of these species (equations (4.27) and (4.28)), followed by the fast terminating steps in equation (4.29) and (4.30).

$$H_2O_2 + Co(OH_2)_6^{3+} \xrightarrow{k_1} HO_2^{\bullet} + Co(OH_2)_6^{2+} + H^+ \tag{4.27}$$

$$H_2O_2 + (H_2O)_5Co(OH)^{2+} \xrightarrow{k_2} HO_2^{\bullet} + Co(OH_2)_6^{2+}$$

(4.28)

$$HO_2^{\bullet} + Co(OH_2)_6^{3+} \xrightarrow{k_3} H^+ + O_2 + Co(OH_2)_6^{2+} \tag{4.29}$$

$$HO_2^{\bullet} + (H_2O)_5Co(OH)^{2+} \xrightarrow{k_4} O_2 + Co(OH_2)_6^{2+} \tag{4.30}$$

This mechanism predicts the rate law given by equation (4.31)

$$\begin{aligned}\frac{\partial[\mathrm{Co(II)}]}{\partial t} &= 2[H_2O_2]\left(k_1[Co(OH_2)_6^{3+}] + k_2[Co(OH_2)_5(OH)^{2+}]\right)\\ &= 2\left(\frac{k_1[H^+] + k_2K_a}{K_a + [H^+]}\right)[\mathrm{Co(III)}]_T[H_2O_2] \quad = k_{1obs}[\mathrm{Co(III)}]_T\end{aligned} \tag{4.31}$$

where $[\mathrm{Co(III)}]_T = [Co(OH_2)_6^{3+}] + [Co(H_2O)_5(OH)^{2+}]$. If $K_a << [H^+]$, then the second-order rate constant is given by equation (4.32).

$$k_{2obs} = k_1 + \frac{k_2 K_a}{[\mathrm{H}^+]} \tag{4.32}$$

Therefore a plot of k_{2obs} versus $1/[\mathrm{H}^+]$ should give an intercept of $2k_1$ and slope of $2k_2K_a$. The absence of an intercept in Figure 4.2 indicates that the k_1 pathway is not making a significant contribution.

It should be noted that in Chapter 5, a value of $K_a = 9.5 \times 10^{-3}$ M has been estimated. For the conditions of $[\mathrm{H}^+] < 0.08$ M in this study, it is not strictly true that $[\mathrm{H}^+] >> K_a$. If the data is refitted with $K_a = 9.5 \times 10^{-3}$ M, then one obtains $b = 28.0 \pm 0.5$ s^{-1}. The overall fit is slightly poorer with an approximately 10 % higher overall standard error of the fit. If the value of $K_a = 1.2 \times 10^{-2}$ M of Martinez and co-workers[10] is used, then the overall standard error increased by another 7.5 %. However it cannot be concluded that either of these K_a values is really inconsistent with the kinetics results.

References

(1) Baxendale, J. H.; Wells, C. F. *Trans. Faraday Soc.* **1951**, *53*, 800.

(2) Davies, G.; Watkins, K. O. *J. Phys. Chem.* **1970**, *74*, 3388.

(3) Davies, G. *Coord. Chem. Rev.* **1974**, *14*, 287.

(4) Conocchioli, T. J.; Nancollas, G. H.; Sutin, N. *Inorg. Chem.* **1966**, *5*, 1.

(5) McAuley, A.; Malik, M. N.; Hill, J. *J. Chem. Soc. A*, **1970**, 2461.

(6) Hill, J.; McAuley, A. *J. Chem. Soc. A*, **1968**, 1169.

(7) Hill, J.; McAuley, A. *J. Chem. Soc. A*, **1968**, 2405.

(8) Mortimer, R. D. *Mathematics for Physical Chemistry*; Macmillan Publishing Co.; New York, New York, **1981**; pg. 277.

(9) Weiser, D. W. *Ph.D. Thesis*, University of Chicago, **1956**.

(10) Ferrer, M.; Llorca, J.; Martinez, M. *J. Chem. Soc. Dalton Trans*. **1992**, 229.

CHAPTER 5. Kinetic Studies of the Reduction of Hexaaquacobalt(III) Perchlorate by a Cobaloxime, [Co(dmgBF$_2$)$_2$(H$_2$O)$_2$]

Introduction

Hexaaquacobalt(III) has unique properties when compared to other low-spin d^6 complexes. Both its electron exchange rate[1] and its ligand substitution rate[2] are exceptionally high, relative to other cobalt(III) complexes such as hexaaminecobalt(III). Taube et al.[3] suggested that this might be due to the participation of a low lying, high-spin excited state as an intermediate. However, an effort to observe such an excited state by magnetic susceptibility measurements[3] was unsuccessful.

Navon[4] sought to clarify the above dilemma by studying the temperature dependence of the chemical shift and spin-lattice relaxation time of the ^{59}Co NMR signal of $Co(OH_2)_6^{3+}$. The observations did not produce any clear evidence for a paramagnetic high-spin cobalt(III).

Navon[4] also studied the dependence of the ^{59}Co relaxation rate of $Co(OH_2)_6^{3+}$ (0.03-0.3 M) on the H^+ concentration in the range of 1.0 to 11.0 M at temperatures of 20 and 50 °C. It was seen that the relaxation rate had a sharp increase for $[H^+] \leq 2$ M at 20 °C and for $[H^+] \leq 5$ M at 50 °C . Navon[4] suggested that this increase was due to exchange with $Co(OH_2)_5(OH)^{2+}$ and that more $Co(OH_2)_5(OH)^{2+}$ is formed at the higher temperature. Sutcliffe and Weber[5] reported the temperature dependence (12.5-28.2 °C) of K_a, and did observe an increase in K_a with increasing temperature. Interpolation of their results gives $K_a \sim 1.2 \times 10^{-3}$ at 20 °C and extrapolation gives 6.3×10^{-2} at 50 °C. These values suggest that there would be very little of the hydrolyzed species present for $[H^+] >$

1 M at either temperature. Therefore the above phenomenon observed by Navon could be attributed to dimer formation.

In the case of fast exchange, the contribution to the chemical shift, $\Delta\omega_p$, of exchange with a fraction (f) of $Co(OH_2)_6^{3+}$ in the high-spin state of $Co(OH_2)_6^{3+}$ is given by $\Delta\omega_p = f\Delta\omega_m$; where $\Delta\omega_m$ is the chemical shift of the paramagnetic species (8.71×10^7 rad s^{-1}).[4] Navon[4] estimated from the temperature dependence of the ^{59}Co chemical shift that $\Delta\omega_p/\omega_0 < 20$ ppm and obtained an upper limit of $f < 10^{-4}$. The corresponding lower limit for the difference in the free energies of the low-spin and high-spin states of $Co(OH_2)_6^{3+}$ is > 5.4 kcal mol^{-1}.

There has been a controversy on the value of K_a for reaction (5.1) in the literature.

$$Co(OH_2)_6^{3+} \underset{}{\overset{K_a}{\rightleftarrows}} Co(OH_2)_5OH^{2+} + H^+ \tag{5.1}$$

The values of K_a vary from 0.22 M[6] to 0.009 M[7] at 25 °C. Spectrophotometric measurements have in general yielded estimates close to the lower end of this range,[8-11] whereas estimates from kinetics studies have tended to give values of the order of 0.1 M.[12,13] This has been discussed in detail in Chapter 1. It will be shown in this study that it is possible to estimate a value of K_a at 10 and 15 °C from the rate law for the reaction of $Co(OH_2)_6^{3+}$ with $Co(dmgBF_2)_2(H_2O)_2$.

For the reaction of $Co(OH_2)_6^{3+}$ with various reductants, the second-order rate constant obeys the empirical relationship, $k_{2obs} = a + b/[H^+]$. Consideration of the values of the kinetic parameters a and b for complexation and redox reactions indicates that the rates of reactions of $Co(H_2O)_5(OH)^{2+}$ with such reductants as Br^-, H_2O_2 and oxalic acid are limited by substitution of the reductant at the metal center,[14] whilst the rate with $Fe(OH_2)_6^{2+}$,[15] benzene-1,4-diol,[16,17] and I^- [16] are much faster and must therefore proceed through an outer-sphere electron transfer mechanism.

The kinetics of the reduction of Co(III) by $Os(bipy)_3^{2+}$, $Os(5\text{-Cl-phen})_3^{2+}$, $Fe(5\text{-}NO_2\text{-phen})_3^{2+}$, $Ru(bipy)_3^{2+}$ and $Ru(5\text{-}NO_2\text{-phen})_3^{2+}$ [18] follow a rate law in which the $Co(OH_2)_6^{3+}$ ion is the predominant oxidizing species with the absence of a significant inverse-acid pathway ($[H^+]$ range of 0.5-2.0 M). These reactions proceed by an outer-sphere mechanism. The application of Marcus theory to these reactions yields a self-exchange rate constant of 1×10^{-12} M^{-1} s^{-1} for $Co(OH_2)_6^{3+/2+}$.[18] The directly measured self- exchange rate constant is 5 M^{-1} s^{-1},[19] and is considerably higher than that calculated from the cross-reactions. This anomaly was first noted by Farina and Wilkins[20] for the oxidation of $Co(terpy)_2^{2+}$; the rate constant calculated from Marcus theory is ~ 10^5 times larger than the experimental value. The problem also arises in the oxidation of $Ni(cyclam)^{2+}$, although the authors did not mention it.[21] In this case the calculated and experimental values differ by ~ 10^6. In this study, the reaction of $Co(OH_2)_6^{3+}$ with $Co(dmgBF_2)_2(H_2O)_2$ has been analyzed by Marcus theory.

In spite of extensive earlier investigations, complexes of cobaloximes continue to be actively studied. They hold continued interest not only because of their relationship to the intriguing chemistry of vitamin B_{12}, but also because there is a rich chemistry for this family of complexes. For example, they form alkyl complexes that are stable and isolable, they show enhanced rates of self-exchange, electron-transfer and ligand-exchange reactions compared to simple systems like hexaaminecobalt(III)/(II), and most are known in oxidation states I, II and III.[22,23] Many of these complexes are obtained from Co(II) salts with high formation constants; many bind O_2 or are oxidized by it. However, at high $[H^+]$ (> 0.01M), many of the Co(II) macrocycles rapidly decompose to $Co(OH)_6^{2+}$.[24] These characteristics limit their general utility in certain applications, most notably in reactions that must be carried out in acidic media.

In contrast to such patterns,[25] the complex $Co(dmgBF_2)_2(H_2O)_2$ is remarkably resistant to both reaction with O_2 and decomposition in the presence of acid. This makes it convenient for the study of the kinetics of its reaction with $Co(OH_2)_6^{3+}$, from which the self-exchange rate constant for the Co(II)/Co(III) system may be evaluated.

Experimental

Preparation of $Co(dmgBF_2)_2(H_2O)_2$. About 150 mL of diethyl ether (Caledon), deoxygenated by bubbling argon through it, were added to a 250 mL Erlenmeyer flask containing a mixture of 2.0 g (8.0×10^{-3} mole) of $Co(O_2CCH_3)_2 \bullet 4H_2O$ (Fisher Scientific) and 1.9 g (1.6×10^{-2} mole) of dimethylglyoxime (2,3-butanedione dioxime, $dmgH_2$) (Fisher Scientific). The resulting suspension was stirred for several minutes, and 10.0 mL of boron trifluoride etherate ($BF_3 \bullet OEt_2$, Aldrich) were added from a syringe. The mixture was stirred at room temperature under a slow stream of argon (Praxair) for 6 hours, during which time the desired product precipitated. The brown solid obtained by filtration was washed several times with ice-cold water and methanol (Caledon), and was air dried.[26]

The purity of the $Co(dmgBF_2)_2(H_2O)_2$ was determined from its electronic spectrum at room temperature. Since $Co(dmgBF_2)_2(H_2O)_2$ is not air sensitive, the sample solution was prepared by adding water to a 50 mL volumetric flask containing a weighed amount of $Co(dmgBF_2)_2(H_2O)_2$. The solution was stirred until all the solids dissolved and then transferred to a spectrophotometer cell of 1.00 cm path-length. The electronic spectrum of $Co(dmgBF_2)_2(H_2O)_2$ in water was characterized by absorption maxima at 456, 326 and 260 nm with ε values of 4.04×10^3, 2.06×10^3 and 6.38×10^3 M^{-1} cm^{-1}, respectively. These values are consistent with those reported by Espenson and co-workers[27] with maxima at 456, 328 and 260 nm and ε values of 4.02×10^3, 1.92×10^3 and 5.88×10^3 M^{-1} cm^{-1}, respectively. The values also compare well with those reported by Wang[28] at 454, 326, 260 nm with ε values 4.00×10^3, 2.08×10^3 and 6.57×10^3 M^{-1} cm^{-1}, respectively.

Solutions of $Co(dmgBF_2)_2(H_2O)_2$ Used in Kinetic Study. Stock solutions of $Co(dmgBF_2)_2(H_2O)_2$ were prepared by stirring 8.0 mg of $Co(dmgBF_2)_2(H_2O)_2$ with 50 mL of water for 2 to 3 hour. Then undissolved solids were removed by centrifugation. The concentration was determined by diluting 2.0 mL of the stock solution to 4.0 mL in water and measuring the spectrum in a 1.00 cm path-length cell on the Cary 219 spectrophotometer. The extinction coefficients quoted above were used to calculate the concentration. The solutions of the required concentrations used for the stopped-flow spectrophotometer were made from the stock solution.

Solutions of $Co(OH_2)_6^{3+}$ Used in Kinetic Study. $Co(OH_2)_6^{3+}$ solutions were prepared by procedures given in Chapter 3.

Kinetic Measurements. The absorbance decrease due to oxidation of $Co(dmgBF_2)_2(H_2O)_2$, was monitored on a stopped-flow spectrophotometer (Cantech Scientific Ltd.) at 454 nm, with the temperature of the reactant solutions and observation cell maintained at the desired temperature (± 0.5 °C) by circulation of thermostatted water. The ionic strength was maintained at 1.0 M using $LiClO_4$.

A new solution of $Co(OH_2)_6^{3+}$ was made from the stock solution stored at 0 °C in 2.0 M perchloric acid after every four runs. Immediately before starting and after the reaction, the actual concentration of $Co(OH_2)_6^{3+}$ was determined from the absorbance at 605 nm of a sample from the stopped-flow storage syringe, measured on the Cary 219 spectrophotometer. The cobalt(III) was always in excess and often pseudo-first-order conditions were satisfied ([Co(III)] > 10[Co(II)]), but when this condition was not satisfied a second-order analysis was used.

The absorbance-time data (256 points per trace) were collected on an MS-DOS 486 computer and at least 140 points for each trace were analyzed by least-squares to give the first-order or second-order rate constant depending on the conditions. The observed rate constants were averaged from 6 to 8 runs.

First-order Analysis. The overall reaction is given in equation (5.2)

$$\begin{aligned} &Co(OH_2)_6^{3+} + Co(dmgBF_2)_2(H_2O)_2 \longrightarrow \\ &\qquad\qquad Co(OH_2)_6^{2+} + Co(dmgBF_2)_2(H_2O)_2^{+} \end{aligned} \qquad (5.2)$$

Consider the generic reaction in equation (5.3) developed from equation (5.2)

$$A + B \longrightarrow C + D \tag{5.3}$$

The data collected under pseudo-first-order conditions ([A] >> [B]) can be analyzed by the first-order rate equation (5.4)

$$-\frac{\partial[B]}{\partial t} = k_{2obs}[A][B] = k_{1obs}[B] \tag{5.4}$$

which gives equation (5.5) as the integrated rate law

$$[B] = [B]_0 e^{-k_{1obs}t} \tag{5.5}$$

where [B] is the concentration at any time, *t*, $[B]_0$ is the initial concentration and k_{1obs} is the pseudo-first-order rate constant. In the present case A = $Co(OH_2)_6^{3+}$, B = $Co(dmgBF_2)_2(H_2O)_2$, C = $Co(OH_2)_6^{2+}$ and D = $Co(dmgBF_2)_2(H_2O)_2^+$ and B is the only absorbing species at 454 nm. The disappearance of B was monitored, and the property being observed is designated as *I* and its proportionality constant with concentration is ε. Then the initial absorbance in a 1.00 cm path-length cell is

$$I_0 = \varepsilon_B[B]_0;\ \text{therefore}\ \ [B]_0 = \frac{I_0}{\varepsilon_B} \tag{5.6}$$

and at any time *I* is given by (5.7)

$$I = \varepsilon_B[B];\ \text{therefore}\quad [B] = \frac{I}{\varepsilon_B} \tag{5.7}$$

Substitution for [B] and $[B]_0$ in terms of ε_B, I and I_0 into equation (5.5) yields (5.8)

$$\frac{I}{\varepsilon_B} = \frac{I_0}{\varepsilon_B} e^{-k_{1obs}t} \tag{5.8}$$

which reduces to equation (5.9)

$$I = I_0 e^{-k_{1obs}t} \tag{5.9}$$

Equation (5.9) can be used to fit the variation of I with t by least-squares to obtain k_{1obs}. There is no need to know the initial concentrations or extinction coefficients.

Second-order Analysis. For a second-order reaction (5.3), under the stoichiometry relationship of $[A_0] - [A] = [B_0] - [B]$, the rate of disappearance of B is given by equation (5.10)

$$-\frac{\partial[B]}{\partial t} = k_{2obs}[A][B] = k_{2obs}\left([A]_0 - [B]_0 + [B]\right)[B] \tag{5.10}$$

where [A] and [B] are the concentrations at any time, t, $[A]_0$ and $[B]_0$ are the initial concentrations and k_{2obs} is the second-order rate constant. Rearrangement and integration of (5.10) gives equation (5.11)

$$k_{2obs}t = \frac{1}{[B]_0 - [A]_0}\,\ell n\left(\frac{[A]_0[B]}{[B]_0\left([A]_0 - [B]_0 + [B]\right)}\right) \tag{5.11}$$

The concentration of [B] at any time can be determined from equation (5.11) to be

$$[B] = \frac{\left([B]_0 - [A]_0\right)\dfrac{[B]_0}{[A]_0}\exp\left\{\left([B]_0 - [A]_0\right)k_{2obs}t\right\}}{\dfrac{[B]_0}{[A]_0}\exp\left\{\left([B]_0 - [A]_0\right)k_{2obs}t\right\} - 1} \tag{5.12}$$

With these expressions for the concentration and Beer's law, one can develop the relationship for the time dependence of the absorbance (I) under various experimental conditions.

For this experiment, $[B] < [A]$ and [B] is the only absorbing species at 454 nm ($\varepsilon_B = 4.04 \times 10^3$ M^{-1} s^{-1}). Then the initial absorbance in a 1.00 cm path-length cell is

$$I_0 = \varepsilon_B[B]_0 \tag{5.13}$$

so that $[B]_0 = I_0/\varepsilon_B$. Then the absorbance I at any time t is given by equation (5.14), where [B] has been expressed from equation (5.12)

$$I = \varepsilon_B[B] = \frac{\varepsilon_B\left(\dfrac{I_0^{\,2}}{\varepsilon_B^{\,2}[A]_0} - \dfrac{I_0}{\varepsilon_B}\right)\exp\left\{\left(\dfrac{I_0}{\varepsilon_B} - [A]_0\right)k_{2obs}t\right\}}{\dfrac{I_0}{\varepsilon_B[A]_0}\exp\left\{\left(\dfrac{I_0}{\varepsilon_B} - [A]_0\right)k_{2obs}t\right\} - 1} \qquad (5.14)$$

Since ε_B and $[A]_0$ are known, this equation was used to determine least-squares best-fit values for k_{2obs} for the absorbance-time curve for each kinetic run.

Results

Since the standard reduction potentials of $Co(OH_2)_6^{3+}/Co(OH_2)_6^{2+}$ and $Co(dmgBF_2)_2(H_2O)_2^{+}/Co(dmgBF_2)_2(H_2O)_2$ are 1.86 V and 0.65 V respectively, the equilibrium constant of reaction (5.2) is calculated to be 2.92×10^{20} at 25 °C. Therefore the reverse reaction can be ignored. Under pseudo-first-order conditions $[Co(dmgBF_2)_2(H_2O)_2] < 10[Co(III)]$), the absorbance-time curves were analyzed to obtain k_{1obs} (equation (5.9)). Under second-order conditions ($[Co(dmgBF_2)_2(H_2O)_2] < [Co(III)]$) the curves were analyzed to obtain k_{2obs} (equation (5.14)). The results are collected in Appendix 5.1 and 5.2. Overall, the data are consistent with the rate law in equation (5.15)

$$\begin{aligned}\frac{-\partial[Co(III)]}{\partial t} &= k_{2obs}[Co(dmgBF_2)_2(H_2O)_2][Co(III)] \\ &= k_{1obs}[Co(dmgBF_2)_2(H_2O)_2]\end{aligned} \qquad (5.15)$$

where [Co(III)] is the total concentration of aqueous cobalt(III). The plot of k_{1obs} versus the [Co(III)], shown in Figure 5.1, and the data in Appendix 5.1 show that the rate is first-order in [Co(III)]. The agreement of the rate constants under pseudo-first-order and second-order conditions shows that the rate is first-order in [$Co(dmgBF_2)_2(H_2O)_2$].

The value of k_{2obs} decreases with increasing [H^+] and is consistent with an $[H^+]^{-1}$ dependence as shown in Figure 5.2 for $[H^+] \geq 0.2$ M. The data are given in Appendix 5.2. The results at 20 and 25 °C indicate that there may be a small contribution from an [H^+] independent term, as shown by the intercepts in Figure 5.2. Least-squares analysis gives intercept values of $1.7 \pm 0.2 \times 10^2$ M^{-1} s^{-1} and $1.9 \pm 0.4 \times 10^2$ M^{-1} s^{-1} at 20 and 25 °C, respectively, and inclusion of this contribution gives a 2-3 fold improvement in the standard error of the fits. Further complication in the [H^+] dependence is revealed by a closer examination of the data at 10 and 15 °C. Under these conditions, the cobalt(III) solutions are sufficiently stable to give reproducible kinetics down to 0.021 M H^+. These data reveal a distinct curvature in the plot of k_{2obs} versus $[H^+]^{-1}$, as shown in Figure 5.3. This is consistent with the hydrolysis equilibrium in equation (5.1), which would predict that k_{2obs} should depend on $(K_a + [H^+])^{-1}$ and that the curvature in Figure 5.3 results because K_a is of the magnitude of [H^+] for some runs. Since the [H^+] independent term does not seem to be contributing significantly at 10 and 15 °C, these data were fitted to equation (5.16).

$$k_{2obs} = \left(\frac{b}{K_a + [H^+]}\right) \tag{5.16}$$

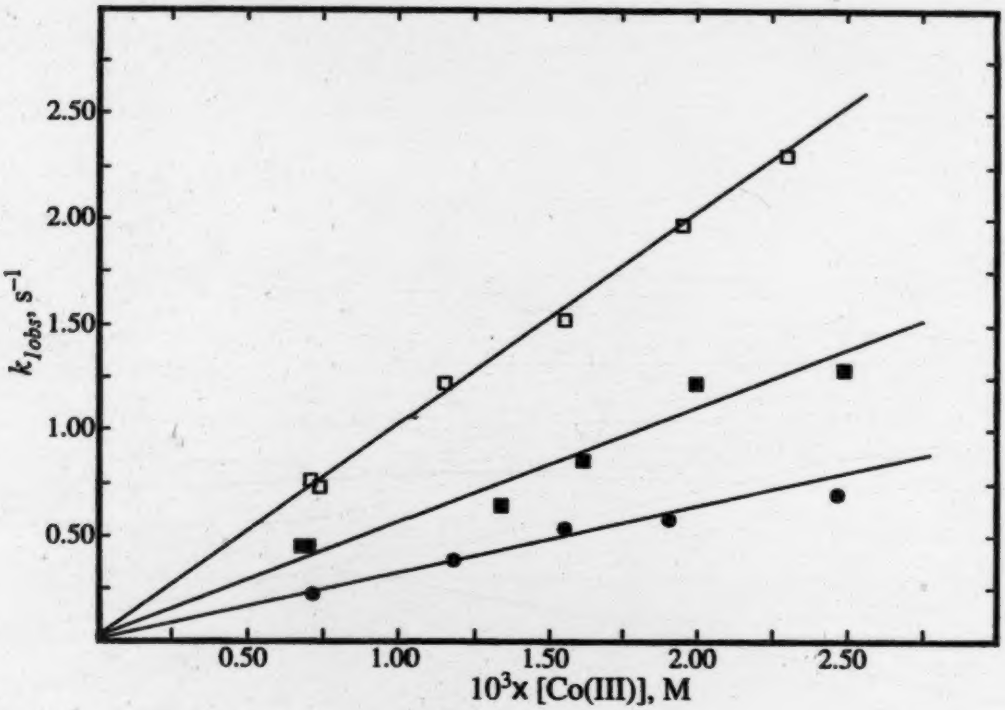

Figure 5.1. Dependence of k_{1obs} on [$Co(OH_2)_6^{3+}$] with 8.25 ×10^{-5} M $Co(dmgBF_2)_2(H_2O)_2$ in 0.60 M $HClO_4$/0.40 M $LiClO_4$ at 10.0 (●), 15.0 (■) and 20.0 °C (□).

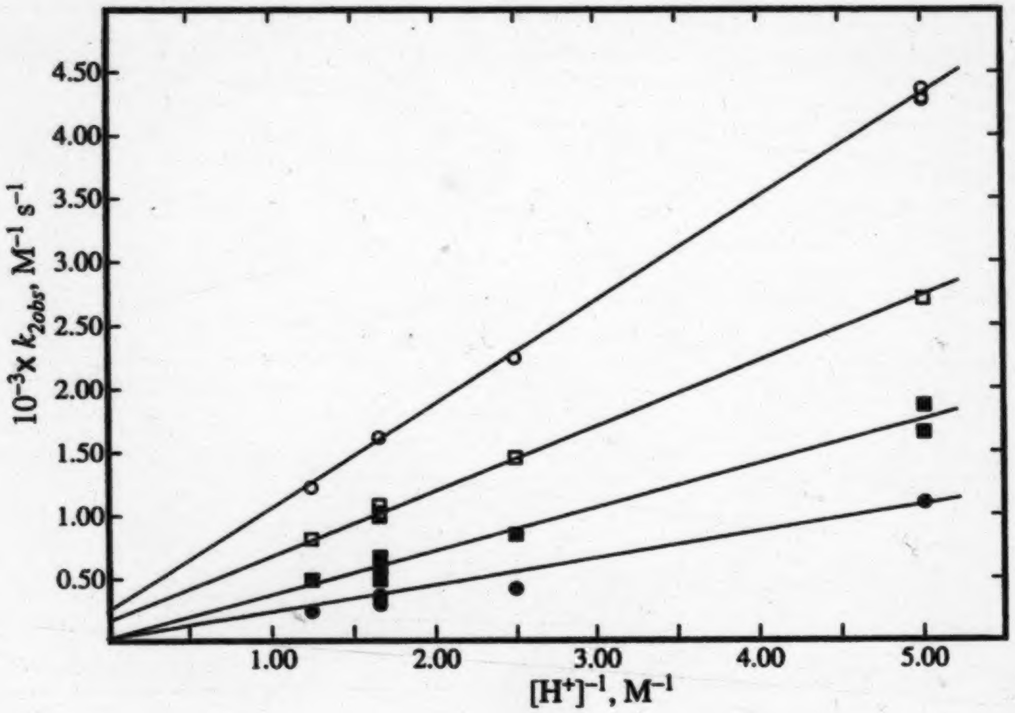

Figure 5.2. Dependence of k_{2obs} on $[H^+]^{-1}$ with 4.29-24.86 $\times 10^{-4}$ M $Co(OH_2)_6^{3+}$ and 5.50-9.00 $\times 10^{-5}$ M $Co(dmgBF_2)_2(H_2O)_2$ for $[H^+] > 0.20$ M in 1.0 M $LiClO_4/HClO_4$ at 10.0 (●), 15.0 (■), 20.0 (□) and 25.0 °C (O).

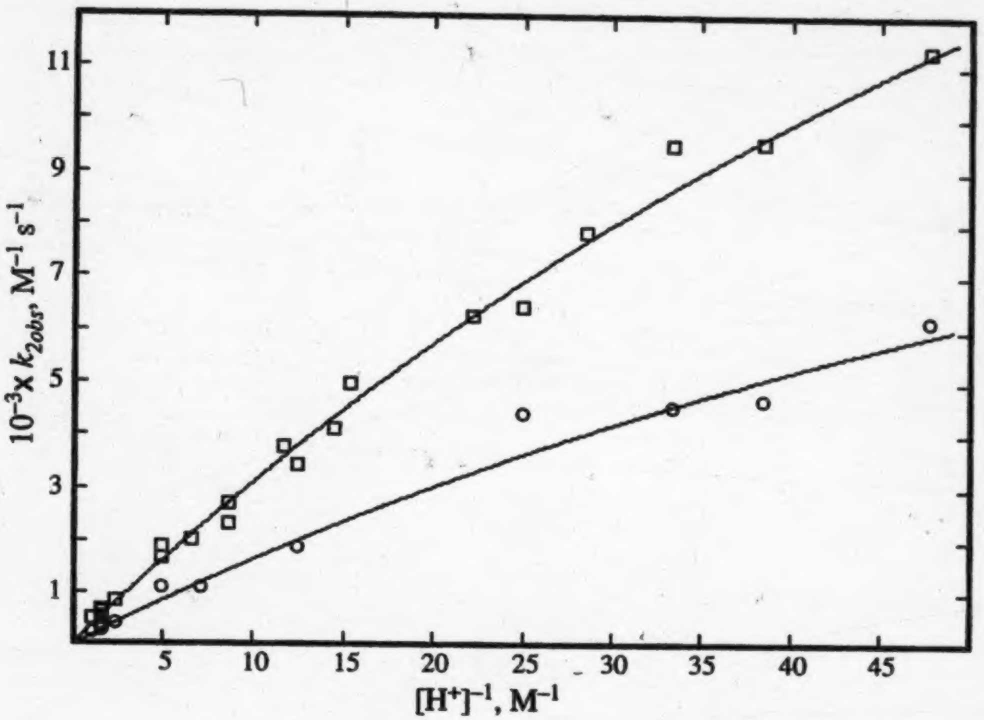

Figure 5.3. Dependence of k_{2obs} on $[H^+]^{-1}$ with 4.94-24.86 $\times 10^{-4}$ M $Co(OH_2)_6^{3+}$ and 5.50-9.00 $\times 10^{-5}$ M $Co(dmgBF_2)_2(H_2O)_2$ for $[H^+] > 0.021$ M in 1.0 M $LiClO_4/HClO_4$ at 15.0 (□) and 10.0 °C (O).

The value of K_a and b are given in Table 5.1. The values of K_a from the two temperatures are quite consistent with each other, but they are not as well defined, in terms of their standard errors, as one might like. Therefore, in the subsequent analysis an average value of $K_a = 9.5 \times 10^{-3}$ M has been assumed at all temperatures.

A more complete representation of the [H$^+$] dependence of k_{2obs} may be given by equation (5.17)

$$k_{2obs} = \left(\frac{a[\mathrm{H}^+] + b}{K_a + [\mathrm{H}^+]}\right) \tag{5.17}$$

The a term corresponds to the [H$^+$] independent contribution when [H$^+$] >> K_a. As already noted, this term makes a minor contribution and can only be evaluated at 20 and 25 °C, with an approximate upper limit of $a \leq 2 \times 10^2$ M^{-1} s^{-1} at 25 °C. If the a term is ignored, then the least-squares analysis of all the data (Appendix 5.1 and 5.2), with K_a = 9.5×10^{-3} M, gives activation parameters for b of $\Delta H^* = 18.1 \pm 0.2$ kcal mol^{-1} and $\Delta S^* = 15.8 \pm 0.9$ cal mol^{-1} K^{-1} and $b = 9.85 \times 10^2$ s^{-1} at 25 °C. If the a term is included and approximated by activation parameters of $\Delta H^* = 27$ kcal mol^{-1} and $\Delta S^* = 42$ cal mol^{-1} K^{-1} (estimated from the a values; $1.7 \pm 0.2 \times 10^2$ M^{-1} s^{-1} and $1.9 \pm 0.4 \times 10^2$ M^{-1} s^{-1} at 20 and 25 °C, respectively), then one obtains for b that $\Delta H^* = 17.6 \pm 0.2$ kcal mol^{-1}, $\Delta S^* = 14.0 \pm 0.9$ cal mol^{-1} K^{-1} and $b = 9.2 \times 10^2$ s^{-1} at 25 °C. Clearly the value for b is not greatly affected by the assumptions made about a.

Table 5.1. Kinetic Parameters for the Reaction of $Co(OH_2)_6^{3+}$ with $Co(dmgBF_2)_2(H_2O)_2$.

T (°C)	$10^{-2}b$ (s^{-1})	10^3K_a (M)
10	1.82 ± 0.09	9.83 ± 2.6
15	3.36 ± 0.10	9.17 ± 2.1
20	6.09 ± 0.10	9.5[a]
25	9.23 ± 0.14	9.5[a]

[a] Value fixed based on results from 10 and 15 °C.

Reaction Mechanism

The experimental rate law is consistent with the usual mechanism for oxidation by aqueous cobalt(III), as shown in Scheme 5.1, where $Co(OH)_6^{3+}$ and $Co(H_2O)_5(OH)^{2+}$ are represented by $Co(OH_2)^{3+}$ and $Co(OH)^{2+}$.

Scheme 5.1

$$Co(OH_2)^{3+} \underset{}{\overset{K_a}{\rightleftarrows}} Co(OH)^{2+} + H^+$$

$$Co(OH_2)^{3+} + Co(dmgBF_2)_2(H_2O)_2 \xrightarrow{k_1} Co(OH_2)^{2+} + Co(dmgBF_2)_2(H_2O)_2^{+}$$

$$Co(OH)^{2+} + Co(dmgBF_2)_2(H_2O)_2 \xrightarrow{k_2} Co(OH)^{+} + Co(dmgBF_2)_2(H_2O)_2^{+}$$

The total cobalt(III) concentration is given by

$$[Co(III)]_T = [Co(OH_2)^{3+}] + [Co(OH)^{2+}] \tag{5.18}$$

and if the K_a step is a rapidly maintained equilibrium, then

$$[Co(OH_2)^{3+}] = \frac{[H^+][Co(III)]_T}{K_a + [H^+]}$$
$$[Co(OH)^{2+}] = \frac{K_a[Co(III)]_T}{K_a + [H^+]} \tag{5.19}$$

If $Co(dmgBF_2)_2(H_2O)_2$ is represented by CoL, then the rate of disappearance of CoL is given by

$$\frac{-\partial[\text{CoL}]}{\partial t} = k_1[\text{Co(OH}_2)^{3+}][\text{CoL}] + k_2[\text{Co(OH)}^{2+}][\text{CoL}] \qquad (5.20)$$

Then substitution from equation (5.19) in (5.20) and collection of terms gives

$$\frac{-\partial[\text{CoL}]}{\partial t} = \left(\frac{k_1[\text{H}^+] + k_2K_a}{K_a + [\text{H}^+]}\right)[\text{Co(III)}]_\text{T}[\text{CoL}] \qquad (5.21)$$

Comparison of equation (5.15) and (5.21) shows that

$$k_{2obs} = \left(\frac{k_1[\text{H}^+] + k_2K_a}{K_a + [\text{H}^+]}\right) = \frac{k_{1obs}}{[\text{Co(III)}]_\text{T}} \qquad (5.22)$$

Comparison of (5.17) and (5.22) shows that this mechanism is compatible with the experimental rate law, with $a = k_1$ and $b = k_2K_a$. As already noted, k_1 is poorly defined by the data, but k_2K_a is the dominant term and is well defined. It should also be noted that the experimental ΔH^* and ΔS^* are really composite values of $\Delta H_2^* + \Delta H_a^\circ$ and $\Delta S_2^* + \Delta S_a^\circ$, where ΔH_a° and ΔS_a° are the standard enthalpy and entropy change for K_a.

The rate law in equation (5.21) could also be derived with the assumption that $Co(dmgBF_2)_2(H_2O)_2$ was undergoing hydrolysis. The K_a would be the hydrolysis constant for this species and k_1 and k_2 would be rate constants for the reaction of the aqua and hydroxy forms with $Co(OH_2)_6^{3+}$. Alternatively, one might assume that $Co(dmgBF_2)_2(H_2O)_2$ is largely protonated under the experimental conditions, and it reacts with $Co(OH_2)_6^{3+}$ through the protonated and conjugated base forms. However, neither of these alternatives is consistent with the observation in Chapter 6 that the reaction of $Fe(bipy)_3^{3+}$ with $Co(dmgBF_2)_2(H_2O)_2$ shows no dependence on $[H^+]$ in the range 0.3×10^{-2} to 1.5×10^{-2} M.

Discussion

In order to determine if Marcus theory can be applied to estimate self-exchange rates in this system, it is first of all necessary to determine whether the electron-transfer is proceeding by an inner-sphere or an outer-sphere mechanism. The theory is only applicable to the latter case.

Since $Co(dmgBF_2)_2(H_2O)_2$ is a low-spin d^7 system and is substitution labile, it is possible for $Co(H_2O)_5(OH)^{2+}$ to react through an inner-sphere bridged intermediate of the form $[(H_2O)_5Co\text{-}(OH)\text{-}Co(dmgBF_2)_2(H_2O)]^{2+}$. Formation of the intermediate involves substitution on $Co(dmgBF_2)_2(H_2O)_2$ and the rate constant for this can be estimated from the solvent exchange rate (k_{ex}). The latter is too fast to measure by standard NMR methods over the temperature range of liquid water, but values of $\sim 2 \times 10^5$ s^{-1} have been measured in H_3CCN and $(H_3C)_2CO$ and predict that the ligand substitution rate constants (k_{sub}) would be of the order of 10^5 M^{-1} s^{-1}.[28] If an inner-sphere mechanism is viable then the value of k_2 (Scheme 5.1) should not be larger than k_{sub}. With $k_2K_a = 9.2 \times 10^2$ s^{-1} and

$K_a = 9.5 \times 10^{-3}$ M one obtains $k_2 = 1 \times 10^5$ M^{-1} s^{-1}. Unfortunately, the values of k_2 and k_{sub} are too similar to provide a justification for ruling out an inner-sphere mechanism.

Since the above arguments cannot eliminate an inner-sphere mechanism, one can assume an outer-sphere mechanism and apply Marcus theory. If a ridiculous result is obtained, it would suggest that the outer-sphere assumption is not valid, and therefore support the inner-sphere alternative. The results of Marcus theory[29] give equation (5.23)

$$k_{12} = \left(k_{11}k_{22}K_{12}f_{12}\right)^{1/2}W_{12} \tag{5.23}$$

where k_{11} and k_{22} are the self-exchange rate constants for the oxidant and reductant, K_{12} is the equilibrium constant for the cross-reaction, i.e. $\log K_{12} = 16.913\Delta E^{\circ}$, and f_{12} and the work term corrections (W_{12} and w_{ij}) have been calculated from the expression in equation (5.24-5.26).[30,31]

$$\ell\mathrm{n}f_{12} = \frac{\left(\dfrac{\ell\mathrm{n}K_{12} + \left(w_{12} - w_{21}\right)}{\mathrm{RT}^2}\right)}{\left(\dfrac{4\ell\mathrm{n}\left(\dfrac{k_{11}k_{22}}{Z^2}\right) + \left(w_{12} - w_{21}\right)}{\mathrm{RT}}\right)} \tag{5.24}$$

where

$$W_{12} = \exp\left[\frac{\left(-w_{12} + w_{21} - w_{11} - w_{22}\right)}{2\mathrm{RT}}\right] \tag{5.25}$$

and

$$w_{ij} = \frac{\left(4.25 \times 10^3\right) Z_i Z_j}{r\left(1 + 0.3285 r \sqrt{\mu}\right)} \tag{5.26}$$

where Z is the collision frequency, taken to be 1.0×10^{11} M^{-1} s^{-1}, r is the sum of the radii of the reactants in Å, μ is the ionic strength, Z_i and Z_j are the charges of the two reactants, and the numerical constants are for water at 25 °C with w_{ij} values in cal mol^{-1}.

For comparison purposes, these calculations will be carried out for both $Co(H_2O)_5(OH)^{2+}$ and $Fe(H_2O)_5(OH)^{2+}$, studied by Espenson et al.[26] The assumed radii are 4.4 Å for $Co(dmgBF_2)_2(H_2O)_2$, 5.0 Å for $Co(H_2O)_5(OH)^{2+}$ and 5.05 Å for $Fe(H_2O)_6^{3+}$ and $Fe(H_2O)_5(OH)^{2+}$. The reduction potentials are known for $Co(dmgBF_2)_2(H_2O)_2^{+/0}$ (0.65 V),[26,31] $Co(OH_2)_6^{3+/2+}$ (1.86 V)[32] and $Fe(OH_2)_6^{3+/2+}$ (0.74 V).[33] The potentials for $Co(OH_2)_5(OH)^{2+/+}$ and $Fe(OH_2)_5(OH)^{2+/+}$ have been estimated from the cycle in Scheme 5.2, where M is Fe or Co.

Scheme 5.2

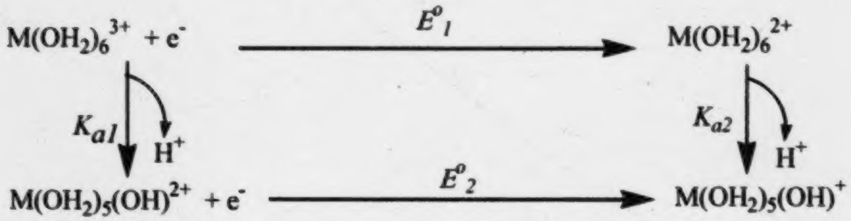

From Scheme 5.2, the E^o_2 value is given by equation (5.27),

$$E^o{}_2 = E^o{}_1 + \frac{\mathrm{RT}}{\mathrm{F}}\left(\ell\mathrm{n}K_{a2} - \ell\mathrm{n}K_{a1}\right) = E^o{}_1 + 0.059\log\left(\frac{K_{a2}}{K_{a1}}\right) \tag{5.27}$$

where the K_{a1} is 9.5×10^{-3} M for $Co(OH_2)_6^{3+}$ and 2.0×10^{-3} M for $Fe(OH_2)_6^{3+}$.[26] However, K_{a2} for $Co(OH_2)_6^{2+}$ and $Fe(OH_2)_6^{2+}$ are not known. A value of $pK_{a2} = 9$ has been assumed since this is typical for bivalent first row transition metal ions.[34] This method gives the reduction potentials of $Co(OH_2)_5(OH)^{2+/+}$ and $Fe(OH_2)_5(OH)^{2+/+}$ to be 1.45 V and 0.37 V, respectively. The latter value indicates that the cross-reaction between $Co(dmgBF_2)_2(H_2O)_2$ and $Fe(OH_2)_5(OH)^{2+}$ is not spontaneous, but the overall reaction is spontaneous because $Fe(OH_2)_6^{2+}$ is the final product. This can be shown from Scheme 5.3.

Scheme 5.3

$$\begin{tikzcd}
\mathrm{Fe(OH_2)_5(OH)^{2+} + Co(dmgBF_2)_2} \arrow[r, "\Delta G^o{}_4"] \arrow[dr, "\Delta G^o{}_5"] & \mathrm{Fe(OH_2)_5(OH)^{+} + Co(dmgBF_2)_2^{+}} \arrow[d, "-\Delta G^o{}_{Ka2}"', "\mathrm{H}^+"] \\
\mathrm{Fe(OH_2)_6^{3+} + Co(dmgBF_2)_2} \arrow[u, "\Delta G^o{}_{Ka1}"] \arrow[r, "\Delta G^o{}_3"] & \mathrm{Fe(OH_2)_6^{2+} + Co(dmgBF_2)_2^{+}}
\end{tikzcd}$$

The following relationships can be derived from Scheme 5.3

$$\Delta G^o{}_5 = \Delta G^o{}_4 - \Delta G^o{}_{K_{a2}}$$

$$\Delta G^o{}_4 = \Delta G^o{}_3 + \Delta G^o{}_{K_{a2}} - \Delta G^o{}_{K_{a1}}, \qquad (5.28)$$

$$E^o{}_5 = 0.09 - 0.059 \log K_{a1} = 0.25\,\mathrm{V}$$

The self-exchange rate constant for $Co(OH_2)_5(OH)^{2+/+}$ was calculated from Habib and Hunt,[1] to be 1.3×10^2 M^{-1} s^{-1} using $K_a = 9.5 \times 10^{-3}$ M. The self-exchange rate constant for $Fe(OH_2)_5(OH)^{2+/+}$ at 25 °C was calculated to be 3.0×10^3 M^{-1} s^{-1} ($\mu = 0.5$ M $LiClO_4$) from the data at 7.3 °C[35] and 2.0 °C.[36]

With these parameters in hand, the Marcus equation can be used to calculate k_{22}, the self-exchange rate for $Co(dmgBF_2)_2(H_2O)_2{}^{+/0}$; the results are summarized in Table 5.2. The reaction of $Co(dmgBF_2)_2(H_2O)_2$ with $Co(H_2O)_5(OH)^{2+}$ gave $k_{22} = 1.7 \times 10^{-4}$ M^{-1} s^{-1}. This is in reasonable agreement with estimates from other reactions, which range from 6.6×10^{-4} M^{-1} s^{-1} to 8.7×10^{-3} M^{-1} s^{-1}, especially when the approximation of K's and E^o for the $Co(H_2O)_5(OH)^{2+}$ system are considered. This result is consistent with an outer-sphere mechanism for the reaction of $Co(dmgBF_2)_2(H_2O)_2$ with $Co(H_2O)_5(OH)^{2+}$.

Application of the Marcus equation to the reaction of $Co(dmgBF_2)_2(H_2O)_2$ with $Co(OH_2)_6{}^{3+}$ presents a serious anomaly. The calculated rate constant, k_{12}, for this reaction is $\sim 10^7$ M^{-1} s^{-1}. This large value is primarily a consequence of the large driving force for the reaction ($K_{12} \approx 10^{20}$). The problem is that this pathway is making an undetectable contribution to the experimental observations, which give an upper limit of $k_{12} < 2 \times 10^2$ M^{-1} s^{-1} at 25 °C.

Table 5.2. Self-Exchange Rate Constants Calculated by the Marcus Relationship.

Couple	$\log K_{12}$	k_{12} ($M^{-1}\,s^{-1}$)	k_{22} ($M^{-1}\,s^{-1}$)	f_{12}	k_{11} ($M^{-1}\,s^{-1}$)
$Co(dmgBF_2)_2(H_2O)_2$ + $Co(OH_2)_5(OH)^{2+}$[a]	13.53	1.0×10^5	1.7×10^{-4}	1.2×10^{-2}	1.6×10^2
$Co(dmgBF_2)_2(H_2O)_2$ + $Fe(bipy)_3^{3+}$[b]	7.27	1.6×10^6	8.7×10^{-3}	1.7×10^{-1}	8.0×10^6
$Co(dmgH)_2(H_2O)_2^+$ + $Co(sep)_3^{2+}$[c]	10.49	5.5×10^3	(2.0×10^{-3})[d]	5.8×10^{-2}	3.5
$Co(dmgBF_2)_2(H_2O)_2^+$ + $Co(sep)_3^{2+}$[c]	15.05	1.5×10^5	(6.6×10^{-4})[d]	3.5×10^{-3}	3.5
$Co(dmgBF_2)_2(H_2O)_2$ + $Fe(OH_2)_6^{3+}$[e]	1.69	2.9×10^2	1.3×10^2	9.3×10^{-1}	4.2[f]
$Co(dmgBF_2)_2(H_2O)_2$ + $Fe(OH_2)_6^{3+}$[e]	1.69	2.9×10^2	9.4×10^4	9.3×10^{-1}	(6.2×10^{-3})[g]
$Co(dmgBF_2)_2(H_2O)_2$ + $Fe(OH_2)_5(OH)^{2+}$[e]	-4.75	6.2×10^4	4.1×10^{11}	1.3×10^{-1}	3.0×10^3

[a] At 25 °C with $\mu = 1.0$ M $LiClO_4$. [b] In Chapter 6. [c] Reference 37 at 25 °C with $\mu = 0.10$ M. [d] The k_{22} for $Co(dmgBF_2)_2(H_2O)_2^{+/0}$ and $Co(dmgH)_2(H_2O)_2^{+/0}$ recalculated from reference 37. [e] At 25 °C with $\mu = 0.5$ M $LiClO_4$. [f] Reference 38. [g] Determined from a least-squares fit to equation (5.23) with $Z = 1.9 \times 10^{10}\ M^{-1} s^{-1}$ (reference 39).

Anomalous behavior was also reported by Sutin et al.[18] when calculating the self-exchange rate constant for $Co(OH_2)_6^{3+/2+}$ using the Marcus equation for the reduction of Co(III) by $Os(bipy)_3^{2+}$, $Os(5\text{-}Cl\text{-}phen)_3^{2+}$, $Fe(5\text{-}NO_2\text{-}phen)_3^{2+}$, $Ru(bipy)_3^{2+}$ and $Ru(5\text{-}NO_2\text{-}phen)_3^{2+}$. The average self-exchange rate constant was estimated to be 1.0×10^{-12} M^{-1} s^{-1}. Although these reactions proceed by an outer-sphere mechanism, the estimated self-exchange rate constant for $Co(OH_2)_6^{3+/2+}$ is much smaller than the directly measured value of 5 M^{-1} s^{-1}.[19] If the self-exchange rate of 1.0×10^{-12} M^{-1} s^{-1} for $Co(OH_2)_6^{3+/2+}$ is applied in the Marcus equation to the reaction of $Co(dmgBF_2)_2(H_2O)_2$ with $Co(OH_2)_6^{3+}$, then a cross-reaction rate constant (k_{12}) of ~ 0.9×10^2 M^{-1} s^{-1} is estimated, which is consistent with the estimated experimental value in this study $< 2 \times 10^2$ M^{-1} s^{-1}.

On the other hand, application of the Marcus equation to the reaction of iron(III) species with $Co(dmgBF_2)_2(H_2O)_2$ indicates that these oxidants are much more reactive than expected. For $Fe(OH_2)_6^{3+}$,[38] one calculates $k_{22} = 1.3 \times 10^2$ M^{-1} s^{-1} for $Co(dmgBF_2)_2(H_2O)_2^{+/0}$. This is $> 10^4$ times larger than predicted from other systems. The situation is even worse if one follows the suggestions of Hupp and Weaver[39] that k_{11} ~ 10^{-3} M^{-1} s^{-1} or Bernhard and Sargeson[40] who found $k_{11} = 6.2 \times 10^{-3}$ M^{-1} s^{-1} to be most consistent with the Marcus equation for several systems. Then the calculated k_{22} is ~ 9×10^4 M^{-1} s^{-1}. Similarly for $Fe(OH_2)_5(OH)^{2+}$, one calculates an improbably high value of $k_{22} = 4 \times 10^{11}$ M^{-1} s^{-1} for $Co(dmgBF_2)_2(H_2O)_2^{+/0}$. This type of anomaly can be rationalized by assigning an inner-sphere mechanism for both reactions. This is the assignment made by Bakac et al.[26] for $Fe(OH_2)_5(OH)^{2+}$, but they suggested an outer-sphere mechanism for $Fe(OH_2)_6^{3+}$. Both systems could be inner-sphere by iron(III) coordination at a $-BF_2$ group through the intermediates $\mathrm{[(H_2O)_5Fe\text{-}(F_2B)\text{-}Co(dmg)_2(BF_2)(H_2O)_2]^{3+}}$, shown in Scheme 5.4, where L is $\mathrm{H_2O}$.

Scheme 5.4

$$\mathrm{Fe(L)_6{}^{3+} + Co(dmgBF_2)_2(L)_2{}^{0} \rightleftarrows [(L)_5Fe(III) - (F_2B) - Co(II)(dmg)_2BF_2(L)_2]^{3+} + L}$$

$$\mathrm{[(L)_5Fe(III) - (F_2B) - Co(II)(dmg)_2BF_2(L)_2]^{3+} \rightleftarrows [(L)_5Fe(II) - (F_2B) - Co(III)(dmg)_2BF_2(L)_2]^{3+}}$$

$$\mathrm{[(L)_5Fe(II) - (F_2B) - Co(III)(dmg)_2BF_2(L)_2]^{3+} \rightleftarrows Fe(L)_6{}^{2+} + Co(dmgBF_2)_2(L)_2{}^{+}}$$

These pathways might not be available for $\mathrm{Co(OH_2)_6{}^{3+}}$ because of the substitution inertness, but the anomalously slow outer-sphere problem remains.

References

(1) Habib, H. S.; Hunt, J. P. *J. Amer. Chem. Soc.* **1966**, *88*, 1668.

(2) Friedman, H. L.; Taube, H.; Hunt, J. P. *J. Chem. Phys.* **1950**, *18*, 759.

(3) Friedman, H. L.; Hunt, J. P.; Plane, R.A.; Taube, H. *J. Amer. Chem. Soc.* **1951**, *73*, 4028.

(4) Navon, G. *J. Phys. Chem.* **1981**, *85*, 3547.

(5) Sutcliffe, L. H.; Weber, J. R. *Trans. Faraday Soc.* **1956**, *152*, 1225.

(6) Conocchioli, T. J.; Nancollas, G. H.; Sutin, N. *Inorg. Chem.* **1966**, *5*, 1.

(7) Ferrer, M.; Llorca, J.; Martinez, M. *J. Chem. Soc. Dalton Trans.* **1992**, 229.

(8) Taube, H. *J. Gen. Physiol.* **1966**, *49*, 29.

(9) Baxendale, J. H.; Wells, C. F. *Trans. Faraday Soc.* **1957**, *53*, 800.

(10) Patel, R. C.; Endicott, J. F. *J. Amer. Chem. Soc.* **1968**, *90*, 6364.

(11) Fereday, F. J.; Logan, N.; Sutton, D. *Chem. Commun.* **1968**, 271; *J. Chem. Soc. A*, **1969**, 2699.

(12) Conocchioli, T. J.; Nancollas, G. H.; Sutin, N. *J. Amer. Chem. Soc.* **1951**, *73*, 4028.

(13) Hill, J.; McAuley, A. *J. Chem. Soc. A*, **1968**, 1169; 2405.

(14) Bodek, I.; Davies, G. *Coord. Chem. Rev.* **1974**, *14*, 269.

(15) Davies, G. *Inorg. Chem.* **1971**, *10*, 1155.

(16) Davies, G.; Watkins, K. O. *J. Phys. Chem.* **1970**, *74*, 3488.

(17) Pelizzetti, E.; Mentasti, E.; Pramauro, E. *J. Chem. Soc. Dalton Trans.* **1976**, 23.

(18) Macartney, D. H.; Sutin, N. *Inorg. Chem.* **1985**, *24*, 3403.

(19) Bonner, N. A; Hunt, J. P. *J. Amer. Chem. Soc.* **1960**, *82*, 3826.

(20) Farina, R.; Wilkin, R. G. *Inorg. Chem.* **1968**, *7*, 514.

(21) Brodovitch, J. C.; McAuley, A. *Inorg. Chem.* **1981**, *20*, 1667.

(22) Dodd, D.; Johnson, M. D. *J. Organomet. Chem.* **1973**, *52*, 1.

(23) Wong, C. L.; Switzer, J. A.; Balakrishman, K. P.; Endicott, J. F. *J. Amer. Chem. Soc.* **1980**, *102*, 5511.

(24) Endicott, J. F.; Durham, B.; Balakrishman, K. P. *Inorg. Chem.* **1982**, *21*, 2437.

(25) Aden, A.; Espenson, J. H. *Inorg. Chem.* **1972**, *11*, 686.

(26) Bakac, A.; Brynildson, M. E.; Espenson, J. H. *Inorg. Chem.* **1986**, *25*, 4108.

(27) Bakac, A.; Espenson, J. H. *J. Amer. Chem. Soc.* **1984**, *106*, 5197.

(28) Wang, K.; Jordan, R. B. *Inorg. Chem.* **1995**, *34*, 5672.

(29) Marcus, R. A.; Sutin, N. *Biochem. Biophys. Acta* **1985**, *811*, 265.

(30) Zahir, K.; Espenson, J. H.; Bakac, A. *J. Amer. Chem. Soc.* **1988**, *110*, 5059.

(31) Heckam, R. G.; Espenson, J. H. *Inorg. Chem.* **1979**, *18*, 38.

(32) Latimer, W. M. *Oxidation Potentials*; Prentice-Hall; New York, New York, **1952**. Johnson, D. A.; Sharpe, A. G. *J. Chem. Soc.* **1964**, 3490.

(33) Creaser, I. I.; Sargeson, A. M.; Zanella. A. W. *Inorg. Chem.* **1983**, *22*, 4022.

(34) Baes, C. F., Jr.; Mesmer, R. E. *The Hydrolysis of Cations;* Wiley; New York, New York, **1976**; pg. 226.

(35) Jolley, W. H.; Stranks, D. R.; Swaddle, T. W. *Inorg. Chem.* **1990**, *29*, 1948.

(36) Bruce, S. B.; Creutz, C.; Macartney, T. H.; Sham, T. K.; Sutin, N. *Faraday Discuss. Chem. Soc.* **1982**, *74*, 113.

(37) Wang, K.; Jordan, R. B. *Can. J. Chem.* **1996**, *74*, 658.

(38) Silverman, J.; Dodson, R. W. *J. Phys. Chem.* **1952**, *56*, 846.

(39) Hupp, J. T.; Weaver, M. J. *Inorg. Chem.* **1983**, *22*, 2557.

(40) Bernhardt, P.; Sargeson, A. M. *Inorg. Chem.* **1987**, *26*, 4122.

NOTE TO USERS

Page(s) missing in number only; text follows. Page(s) were microfilmed as received.

128

This reproduction is the best copy available.

UMI

CHAPTER 6. Kinetic Studies of *tris*(2,2'-bipyridine)Iron(III) Perchlorate with Cobaloxime, $[Co(dmgBF_2)_2(H_2O)_2]$

Introduction

Cobaloxime complexes are prepared in basic media by mixing an appropriate glyoxime with a cobalt(II) salt under anaerobic conditions.[1] These complexes are generally sensitive to oxidation by oxygen, and the sensitivity depends on the nature of the glyoxime ligand. Electron withdrawing groups in the equatorial ligand plane tend to stabilize the Co(II) oxidation state. For example, a solution of $Co(dmgH)_2$ is oxidized in a few seconds on exposure to air, while $Co(dmgBF_2)_2$, with the strong electron withdrawing $-BF_2$ substituents, can be handled in air without undergoing any oxidation.

The cobalt(II) in cobaloximes has a d^7 low-spin configuration in a distorted octahedral ligand field with the configuration of *d*-electrons shown below

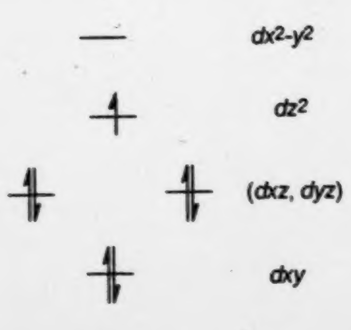

The presence of one unpaired electron is consistent with the observed magnetic moment μ_{eff} = 1.82 B.M. for $Co(dmgH)_2$ in the solid state.[2] The value is only slightly greater than the spin-only value of 1.73 B.M. for one unpaired electron, but distinctly different from that of 3.46 B.M. if Co(II) were high spin.

Studies of $Co(dmgH)_2$ in aqueous solution are somewhat limited by the low solubility. In acidic media, the complex decompose into $Co(OH_2)_6^{2+}$ and $dmgH_2$. The decomposition is nearly first-order in $[H^+]$ so that solutions are stable near *pH* 7.0, but decompose in few seconds at *pH* 4.7.[3] The process is believed to involve protonation of the H---O—H units, since the $Co(dmgBF_2)_2$ derivative, without such units, is much more stable in acidic solution.

X-ray structures of cobaloximes(II) are rare due to the air-sensitive nature of the complexes and difficulty in obtaining single crystals. The bis(pyridine) adduct, $Co(dmgH)_2(py)_2$[4] has $(dmgH)_2$ chelate rings almost coplanar with the Co atom, and the axial Co-N bonds to py (2.25 Å) are 0.37 Å longer than the equatorial Co-N bonds to $dmgH^-$ (1.89Å). The structure of $Co(dmgBF_2)_2(CH_3OH)_2$[5] also shows axial elongation, with $Co\text{-}N_{eq}$ and $Co\text{-}O_{ax}$ (CH_3OH) bond lengths being 1.88 Å and 2.26 Å, respectively. The axial elongation can be attributed to the unpaired electron occupying the slightly antibonding d_{z^2} orbital in these low-spin d^7 complexes.

Cobaloxime(II) complexes are mild reducing agents and undergo oxidation by either inner-sphere or outer-sphere mechanisms, depending on the nature of the oxidant. Oxidation of cobaloxime(II) with $Co(NH_3)_5X^{2+}$ (X = halides and pseudohalides) in aqueous solution[3] was assigned an inner-sphere mechanism because the product is $XCo(dmgH)_2^0$. The rate order of $X = Br^- > Cl^- >> F^-$ indicates a soft acid character for $Co(dmgH)_2$. An inner-sphere mechanism also was suggested for the oxidation of $Co(dmgBF_2)_2(H_2O)_2$ by $Fe(OH_2)_5(OH)^{2+}$.[5] The mechanistic assignment is mainly based on the observed inverse [H^+]-dependence of the reaction rate. The mechanism of this reaction goes through a hydroxide bridged transition state. Espenson and co-workers[5] suggested that the [H^+]-independent pathway for the reaction between $Co(dmgBF_2)_2(H_2O)_2$ and $Fe(OH_2)_6^{3+}$ is expected to go through an outer-sphere mechanism. The calculations in Chapter 5 show that both systems could be inner-sphere possibly by iron(III) coordination at a $-BF_2$ group

Studies on the reduction of various $Co(dmgH)(dmgH_2)XL^+$ and $Co(dmgH)_2XL$ (X = halide or pseudo-halide, L = amine or pyridine) complexes by aqueous V^{2+}, Fe^{2+} and Cr^{2+} have suggested that another possible bridging site in an inner-sphere mechanism could be the oxygen atom(s) of the oxime ligand. These studies were carried out in acidic media ($pH < 4.0$) and the [H^+] dependence is believed to result from the protonation of the $dmgH^-$ ligand described by the equilibrium in equation (6.1).

$$\mathrm{Co(dmgH)(dmgH_2)XL^+} \xrightleftharpoons{K_a} \mathrm{Co(dmgH)_2XL + H^+} \tag{6.1}$$

A general reaction scheme for these systems is shown in Scheme (6.1) where M is Fe, V or Cr.

Scheme 6.1

$$\mathrm{Co(dmgH)(dmgH_2)XL^+ + M^{2+}} \xrightarrow{k_h} \mathrm{Co(dmgH)_2XL^- + H^+ + M^{3+}}$$

$$\mathrm{Co(dmgH)_2XL + M^{2+}} \xrightarrow{k_o} \mathrm{Co(dmgH)_2XL^- + M^{3+}}$$

Then the second-order rate constant is given by equation (6.2)

$$k_2 = \frac{k_o K_a + k_h[\mathrm{H}^+]}{K_a + [\mathrm{H}^+]} \qquad (6.2)$$

An inverse $[H^+]$ dependence of the rate constant indicates that $K_a < [H^+]$. If the protonated form is less reactive than the normal form, this has been taken to suggest an inner-sphere mechanism.

Prince and Segal[6] studied the reduction of $Co(dmgH)_2L_2^+$ (L= NH_3 and $EtNH_2$) by V^{2+}, and found that the rate constant is independent of $[H^+]$ in the range of 0.012 to 0.092 M H^+, but shows an inverse dependence at 0.992 M H^+. The ΔS^* of about -11 cal mol^{-1} K^{-1} for the $[H^+]$ independent pathway for both systems is indicative of an inner-sphere mechanism, since a value of ca. -30 cal mol^{-1} K^{-1} is expected for an outer-sphere mechanism.[7] They proposed that bridging of V^{2+} occurs at the oxygen atom(s) of the $(dmgH)_2$ ligands because the axial NH_3 cannot be a bridging ligand.

However, the V^{2+} reduction of seemingly analogous $Co(dmgH)_2(PhNH_2)_2^+$ has a direct $[H^+]$ dependence that indicates that $K_a >> [H^+]$ giving $k_{obs} = k_o + (k_h[H^+]/K_a)$. On the other hand the $Co(dmgH)_2(py)_2^+$ complex has no $[H^+]$ dependence such that the $k_{obs} = k_o$. In both cases[6] the experiments were carried out at 9.45×10^{-3} and 0.976 M $[H^+]$. Since $PhNH_3^+$ (pK_a 4.7) and pyH^+ (pK_a 5.2) are much stronger acids than NH_4^+ (pK_a 9.25) or $EtNH_3^+$ (pK_a 10.7), it could be argued that $PhNH_2$ and py are poorer electron donors to Co(III). This would make the oxime oxygens less basic so that K_a would be larger, and formation of a bridged complex at the oxime oxygen(s) also would be less favorable than for the NH_3 and $EtNH_2$ complexes. Prince and Segal assigned an outer-sphere mechanism for the k_o pathway based on the ΔS^* values of -31.6 cal mol^{-1} K^{-1} for ($PhNH_2$) and -30.6 cal mol^{-1} K^{-1} for (py), calculated from the k_2 at 9.45×10^{-3} M H^+.

A further complexity of these systems is illustrated by the study of the V^{2+} reductions of $Co(dmgH)_2(Y)(L)$ complexes ($Y = N_3^-, NCS^-, NO_3^-$: L = py, NH_3, $PhNH_2$).[7,8] All these show rates that are essentially independent of $[H^+]$ (3.0×10^{-3} to 1.0×10^{-1} M). However, the Fe^{2+} reductions of some of the same systems ($Y = N_3^-$; L = py, NH_3)[9] have an inverse $[H^+]$ dependence indicative of an inner-sphere mechanism and the kinetics give $K_a = 7.3 \times 10^{-4}$ M (L = py) and 1.9×10^{-3} M (NH_3). The $[H^+]$ independence of the V^{2+} reductions can only be rationalized by equation (6.2) if k_o is essentially equal to k_h. Balasubramanian and Vijayaragharan[8] suggested that this is the case because the rate is controlled by the rate of substitution on $V(H_2O)_6^{2+}$ to form the bridged complex. This process might not be very sensitive to protonation of the oxime if the substitution is at the Y ligand. The upper limit of the rate constant for the substitution can be estimated as < 30 M^{-1} s^{-1}, based on the water exchange rate on $V(H_2O)_6^{2+}$ ($k_{exch} = 89$ s^{-1}; $\Delta H^* = 14.8$ kcal mol^{-1} and $\Delta S^* \approx 0.10$ cal mol^{-1} K^{-1}).[10] For two systems, $Co(dmgH)_2(N_3)(py)$ and $Co(dmgH)_2(NCS)(py)$,[7] reaction with V^{2+} gave respective reduction rate constants of 71 and 284 M^{-1} s^{-1} which exceed the estimated limit for substitution and Balasubramanian and Vijayaragharan assigned outer-sphere mechanisms to these reactions.

Several researchers[11-15] have extensively studied the outer-sphere reduction of Co(III) tetraaza macrocyclic complexes that are structurally similar to cobaloxime(III). In these complexes, the tetraaza ligand forms a square-planar chelate ring binding to the Co cation, with the two axial positions of Co occupied by water ligands. The cross reactions between $Co(N_4)(H_2O)_2^{3+}$ and $Co(N_4')(H_2O)_2^{2+}$ (N_4 and N_4' stand for different tetraaza macrocyclic ligands) complexes were assigned outer-sphere mechanisms because of the bulky nature of the tetraaza macrocyclic ligand.

In the present work we have investigated the kinetics of oxidation of $Co(dmgBF_2)_2(H_2O)_2$ by $Fe(bipy)_3^{3+}$. Magnetically iron(III) is high spin in nearly all its complexes, except those with strong field ligands, such as bipyridine (bipy) in the *tris*(bipyridine)iron(III) complex.

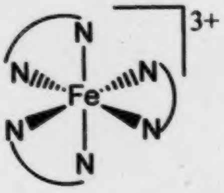

$Fe(bipy)_3^{3+}$

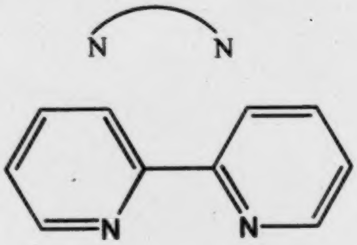

bipy = bipyridine

This low spin complex with a t_{2g}^5 configuration has considerable orbital contributions to its magnetic moment, which is ~ 2.3 B.M. at room temperature. However, the value is temperature dependent, and decreases to ~ 1.9 B.M. at liquid nitrogen temperature (77 K). There is evidence[16] of very high covalence and electron delocalization in low-spin complexes of $Fe(bipy)_3^{3+}$. The $Fe(bipy)_3^{2+}$ formed from the reaction between $Co(dmgBF_2)_2(H_2O)_2$ and $Fe(bipy)_3^{3+}$ is diamagnetic with a low spin electronic configuration of t_{2g}^6.

The purpose of studying this system was to estimate the rate constant for electron exchange of $Co(dmgBF_2)_2(H_2O)_2^0$/ $Co(dmgBF_2)_2(H_2O)_2^+$, by using known information on the kinetics of the electron exchange[17] of $Fe(bipy)_3^{3+}/Fe(bipy)_3^{2+}$.

Experimental

Preparation of *tris*(2,2'-bipyridine)Iron(III). This compound was prepared by addition of 0.20 g (1.3×10^{-3} mole) of 2,2'-bipyridyl (Aldrich) to 0.067 g (4.3×10^{-4} mol) of $Fe(ClO_4)_2$ (Alfa) dissolved in 100 mL of water. The $Fe(bipy)_3(ClO_4)_2$ was separated by filtration and dissolved in 1.0 M sulfuric acid (BDH). Lead(IV) oxide (M&B) powder was added gradually to oxidize $Fe(bipy)_3^{2+}$ to $Fe(bipy)_3^{3+}$. The solution was stirred for 40 minutes at room temperature and filtered through a fine frit to remove the deposited $PbSO_4$ and excess PbO_2. Then solid $NaClO_4$ (BDH) was added to the solution to precipitate $Fe(bipy)_3(ClO_4)_3$. The product was recrystallized from 4 M $HClO_4$ at 0 °C, collected by filtration, washed with a few drops of cold water and methanol (Caledon) and dried in vacuum.[18] The electronic spectrum of the product has a maximum at 620 nm ($\varepsilon = 2.20 \times 10^2$ M^{-1} cm^{-1}) and on reduction with ascorbic acid (BDH) formed $Fe(bipy)_3^{2+}$ with a characteristic band at 520 nm ($\varepsilon = 8.66 \times 10^3$ M^{-1} cm^{-1}). It compares well with the value reported in the literature[19] for $Fe(bipy)_3^{2+}$ at 522 nm ($\varepsilon = 8.85 \times 10^3$ M^{-1} cm^{-1}).

Preparation of $Co(dmgBF_2)_2(H_2O)_2$. The procedure for preparing $Co(dmgBF_2)_2(H_2O)_2$ is given in Chapter 5.

Solutions Used in the Kinetic Study. Solutions of $Fe(bipy)_3^{3+}$ were prepared by dissolving 10.8 mg of $Fe(bipy)_3(ClO_4)_3$ in 2.5 mL of acetonitrile (Fisher Scientific), which had been dried over Molecular Sieve type 4A (BDH) for more than 3 hours. This gave a stock solution with a concentration of 5 × 10^{-3} M $Fe(bipy)_3^{3+}$. Various proportions of this solution were diluted into aqueous 3.0 × 10^{-3} M acid (hydrochloric or nitric) to give 10 mL of solution for stopped-flow measurements.

Solutions of $Co(dmgBF_2)_2(H_2O)_2$ were prepared by dissolving 8.0 mg of $Co(dmgBF_2)_2(H_2O)_2$ in 50 mL of water (stirred for 2 to 3 hours). Then undissolved solids were removed by centrifugation. The concentration was determined by diluting 1.0 mL of the stock solution to 20 mL in water and measuring the spectrum in a 1.0 cm path-length cell. The extinction coefficients quoted in Chapter 5 were used to calculate the concentration. The solutions of the required concentrations used for the stopped-flow spectrophotometer were made from the stock solution.

Kinetic Measurements. The absorbance increase due to formation $Fe(bipy)_3^{2+}$ was monitored on a stopped-flow spectrophotometer (Cantech Scientific Ltd.) at 520 nm. The temperature (± 0.5 °C) was regulated by circulation of thermostatted water. A new solution of $Fe(bipy)_3^{3+}$ was made from the acetonitrile stock solution after every four runs and the $Co(dmgBF_2)_2(H_2O)_2$ was in excess. The data (256 points per trace) were collected on an MS-DOS 486 PC computer and at least 140 points for each trace were analyzed by least-squares to give the second-order rate constant. The reported rate constants are the average from 4 to 8 runs. The analysis was based on formation of $Fe(bipy)_3^{2+}$ ($\varepsilon_{520\ nm} = 8.66 \times 10^3\ M^{-1}\ cm^{-1}$) and the final absorbance of this product gave the initial concentration of $Fe(bipy)_3^{3+}$.

Second-order Analysis. The overall reaction is shown in equation (6.3)

$$\mathrm{Co(dmgBF_2)_2(H_2O)_2} + \mathrm{Fe(bipy)_3}^{3+} \longrightarrow \mathrm{Co(dmgBF_2)_2(H_2O)_2}^{+} + \mathrm{Fe(bipy)_3}^{2+} \quad (6.3)$$

and a generic second-order reaction in equation (6.4) was developed from equation (6.3)

$$\mathrm{A} + \mathrm{B} \longrightarrow \mathrm{C} \qquad (6.4)$$

There is no C present initially and the stoichiometry is 1:1:1, so that mass balance gives $[A] = [A]_0 - [C]$ and $[B] = [B]_0 - [C]$, with the rate law for formation of C expressed by equation (6.5)

$$\frac{\partial[C]}{\partial t} = k_{obs}([A]_0 - [C])([B]_0 - [C]) \qquad (6.5)$$

where [C] represent the concentration at any time, *t*, $[A]_0$ and $[B]_0$ are the initial concentrations and k_{obs} is the second-order rate constant. Rearrangement and integration of (6.5) gives equation (6.6)

$$\ell n\left(\frac{[B]_0 - [C]}{[A]_0 - [C]}\right) + \ell n\left(\frac{[A]_0}{[B]_0}\right) = k_{obs}t([B]_0 - [A]_0) \qquad (6.6)$$

The concentration of C at any time can be solved from equation (6.6) to be

$$[\mathrm{C}] = \frac{[\mathrm{B}]_0\left[\exp\{([\mathrm{B}]_0 - [\mathrm{A}]_0)k_{obs}t\} - 1\right]}{\frac{[\mathrm{B}]_0}{[\mathrm{A}]_0}\exp\{([\mathrm{B}]_0 - [\mathrm{A}]_0)k_{obs}t\} - 1} \qquad (6.7)$$

With this expression for the concentration and Beer's law, one can develop the relationship for the time dependence of the absorbance (I) under various experimental conditions.

In the present case, A = $\mathrm{Co(dmgBF_2)_2(H_2O)_2}$, B = $\mathrm{Fe(bipy)_3^{3+}}$ and C = $\mathrm{Fe(bipy)_3^{2+}}$, which is the only absorbing species at 520 nm ($\varepsilon_C = 8.66 \times 10^3$ $\mathrm{M^{-1}\ s^{-1}}$). The other product, $\mathrm{Co(dmgBF_2)_2(H_2O)_2^+}$, has no absorbance at 520 nm. Under the experimental condition, [B] < [A], the initial absorbance in a 1.00 cm path-length cell is

$$I_0 = \varepsilon_{\mathrm{B}}[\mathrm{B}]_0 \qquad (6.8)$$

and the final absorbance $I_\infty = \varepsilon_C[\mathrm{C}]_\infty = \varepsilon_C[\mathrm{B}]_0$, therefore $[\mathrm{B}]_0 = I_\infty/\varepsilon_C$. At any time, I is given in terms of k_{obs}, I_∞, $[\mathrm{B}]_0$, ε_C and t by equation (6.9)

$$I = \varepsilon_{\mathrm{C}}[\mathrm{C}] = \left(\frac{I_\infty\left[\exp\left\{\left(\frac{I_\infty}{\varepsilon_{\mathrm{C}}} - [\mathrm{A}]_0\right)k_{obs}t\right\} - 1\right]}{\frac{I_\infty}{\varepsilon_{\mathrm{C}}[\mathrm{A}]_0}\exp\left\{\left(\frac{I_\infty}{\varepsilon_{\mathrm{C}}} - [\mathrm{A}]_0\right)k_{obs}t\right\} - 1}\right) \qquad (6.9)$$

Since ε_C and $[\mathrm{A}]_0$ are known, this equation was used to determine least-squares best-fit values for k_{obs} for the absorbance-time curve for each kinetic run.

Results

The reduction of $Fe(bipy)_3^{3+}$ by $Co(dmgBF_2)_2(H_2O)_2$ in 3.0×10^{-3} M H^+ proceeds according to the overall reaction in equation (6.3). Under second-order conditions ($[Co(dmgBF_2)_2(H_2O)_2] > [Fe(bipy)_3^{3+}]$) the curves were analyzed to obtain k_{obs} (equation (6.9)). The results are collected in Table 6.1. Overall, the data are consistent with the rate law in equation (6.10).

$$\frac{-\partial[Fe(bipy)_3^{3+}]}{\partial t} = k_{obs}[Co(dmgBF_2)_2(H_2O)_2][Fe(bipy)_3^{3+}] \qquad (6.10)$$

$[Cl^-]$ and $[H^+]$ Ion Effect. A series of experiments indicated that the rate of oxidation of $Co(dmgBF_2)_2(H_2O)_2$ by $Fe(bipy)_3^{3+}$ depends on the hydrochloric acid concentration. However, further experiments with NaCl demonstrated that k_{obs} increases significantly with increasing $[Cl^-]$, which implies that the linear relationship of k_{obs} versus [HCl] really is due to increases in $[Cl^-]$. The substitution of HCl by HNO_3 demonstrated clearly that k_{obs} does not depend on the $[H^+]$ (Table 6.2) but on the $[Cl^-]$ as shown in Figure 6.1 and data in Table 6.3.

Table 6.1. Dependence of k_{obs} on the Reactant Concentrations for the Reaction of $Fe(bipy)_3^{3+}$ with $Co(dmgBF_2)_2(H_2O)_2$ in 3.0×10^{-3} M HNO_3 and $\mu = 4.1 \times 10^{-2}$ M $HNO_3/NaNO_3$ at 15 °C.

$10^5[Co(dmgBF_2)_2(H_2O)_2]$ (M)	$10^5[Fe(bipy)_3^{3+}]$ (M)	$10^{-6}\,k_{obs}$ ($M^{-1}\,s^{-1}$)
7.83	4.30	1.31
7.86	4.83	1.38
7.86	4.34	1.34
10.40	6.45	1.36

Table 6.2. Dependence of k_{obs} on the HNO_3 Concentration for the Reaction of $Fe(bipy)_3^{3+}$ with $Co(dmgBF_2)_2(H_2O)_2$ in $\mu = 4.1 \times 10^{-2}$ M $HNO_3/NaNO_3$ at 15 °C.

$10^5[Co(dmgBF_2)_2(H_2O)_2]$ (M)	$10^5[Fe(bipy)_3^{3+}]$ (M)	$10^3[HNO_3]$ (M)	$10^{-6}k_{obs}$ ($M^{-1}s^{-1}$)
7.21	5.14	3.00	1.47
7.21	5.11	6.00	1.39
7.86	4.38	6.00	1.29
7.21	5.08	9.00	1.44
7.86	4.55	9.00	1.36
7.21	5.39	12.0	1.31
7.86	4.47	12.0	1.43
7.21	4.91	15.0	1.51
7.86	4.34	15.0	1.34

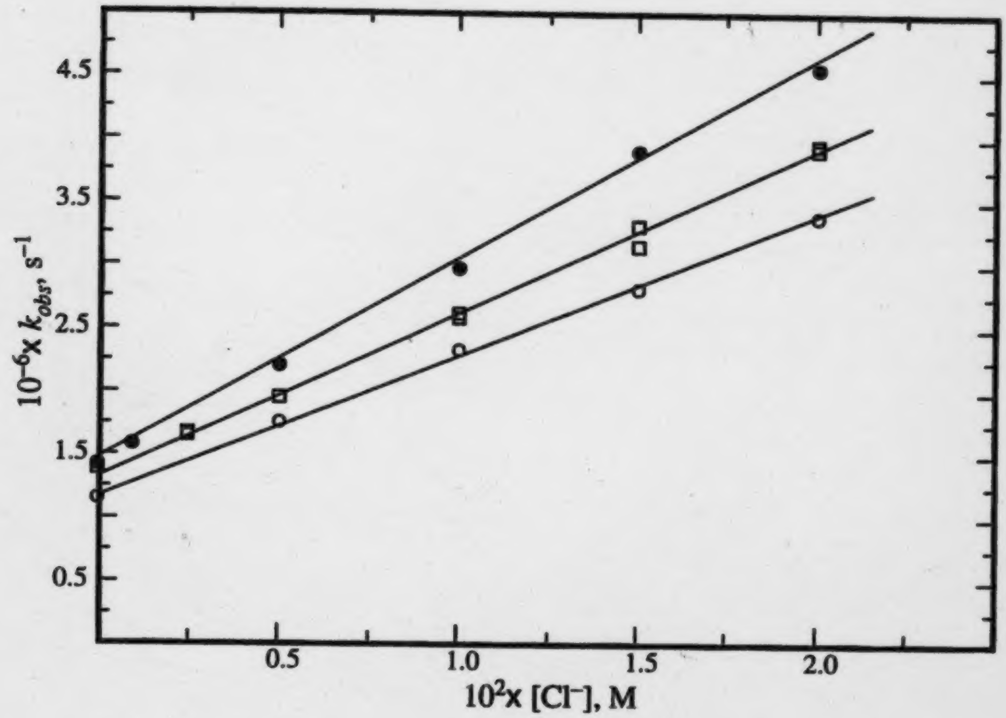

Figure 6.1. Dependence of k_{obs} on [Cl$^-$] with 3.85-6.45 × 10^{-5} M $Fe(bipy)_3^{3+}$, 7.83-10.40 × 10^{-5} M $Co(dmgBF_2)_2(H_2O)_2$ in $\mu = 4.1 \times 10^{-2}$ M $HNO_3/NaNO_3$ at 10.0 (O), 15.0 (□) and 20.0 °C (●).

Table 6.3. Dependence of k_{obs} on Reactant Concentrations and Temperature for the Reaction of $Fe(bipy)_3^{3+}$ with $Co(dmgBF_2)_2(H_2O)_2$ in $\mu = 4.1 \times 10^{-2}$ M $HNO_3/NaNO_3/NaCl$).

T (°C)	$10^5[Co(dmgBF_2)_2(H_2O)_2]$ (M)	$10^5[Fe(bipy)_3^{3+}]$ (M)	10^3[NaCl] (M)	$10^{-6}k_{obs}$ $M^{-1}s^{-1}$
10.0	8.00	4.67	0.00	1.14
10.0	8.00	5.03	5.00	1.75
10.0	8.00	4.80	10.0	2.31
10.0	8.00	4.75	15.0	2.79
10.0	8.00	4.78	20.0	3.36
14.9	10.40	6.45	0.00	1.36
14.9	10.40	6.35	2.50	1.66
14.9	10.40	6.15	5.00	2.16
14.9	10.40	5.89	15.0	3.19
14.9	10.40	5.91	20.0	3.96
15.0	7.83	4.30	0.00	1.31
15.0	7.86	4.83	0.00	1.37
15.0	7.83	4.26	2.50	1.66
15.0	7.86	4.63	2.50	1.64
15.0	7.86	4.73	5.00	1.93

15.0	7.83	3.96	5.00	1.94
15.0	7.83	3.97	10.0	2.57
15.0	7.86	4.76	10.0	2.60
15.0	7.86	4.57	15.0	3.13
15.0	7.83	4.23	15.0	3.29
15.0	7.83	3.92	20.0	3.94
15.0	7.86	4.66	20.0	3.90
20.0	8.00	5.05	0.00	1.40
20.0	8.00	4.92	1.00	1.57
20.0	8.00	4.45	5.00	2.18
20.0	8.00	4.22	10.0	2.95
20.0	8.00	3.87	15.0	3.89
20.0	8.00	3.80	20.0	4.55

Reaction mechanism. A general reaction scheme to account for the $[\mathrm{Cl}^-]$ dependence of k_{obs} is shown in Scheme 6.2.

Scheme 6.2

$$\mathrm{Co(dmgBF_2)_2(H_2O)_2} + \mathrm{Fe(bipy)_3}^{3+} \xrightarrow{k_1} \mathrm{Co(dmgBF_2)_2(H_2O)_2}^{+} + \mathrm{Fe(bipy)_3}^{2+}$$

$$\mathrm{Fe(bipy)_3}^{3+} + \mathrm{Cl}^- \underset{}{\overset{K}{\rightleftarrows}} [\mathrm{Fe(bipy)_3}^{3+} \bullet \mathrm{Cl}^-]$$

$$[\mathrm{Fe(bipy)_3}^{3+} \bullet \mathrm{Cl}^-] + \mathrm{Co(dmgBF_2)_2(H_2O)_2} \xrightarrow{k_2} \mathrm{products}$$

This proposal suggests that the $[\mathrm{Cl}^-]$ dependence arises from formation of an ion-pair between $\mathrm{Fe(bipy)_3}^{3+}$ and Cl^-. Based on Scheme 6.2, the rate of the reaction is given by equation 6.11.

$$\frac{-\partial[\mathrm{Co(II)}]}{\partial t} = \left(k_1[\mathrm{Fe(bipy)_3}^{3+}] + k_2[\mathrm{Fe(bipy)_3}^{3+} \bullet \mathrm{Cl}^-]\right)[\mathrm{Co(dmgBF_2)_2(H_2O)_2}] \quad (6.11)$$

If ion pairing is assumed to be a fast pre-equilibrium and species are represented as $[\mathrm{Fe(bipy)_3}^{3+}] = [\mathrm{Fe}]$, $[\mathrm{Cl}^-] = [\mathrm{X}]$ and $[\mathrm{Fe(bipy)_3}^{3+} \bullet \mathrm{Cl}^-] = [\mathrm{Fe} \bullet \mathrm{X}]$, then $K = \dfrac{[\mathrm{Fe} \bullet \mathrm{X}]}{[\mathrm{Fe}][\mathrm{X}]}$ and $[\mathrm{Fe}]_\mathrm{T} = [\mathrm{Fe} \bullet \mathrm{X}] + [\mathrm{Fe}]$. If $[\mathrm{X}] >> [\mathrm{Fe}]_\mathrm{T}$, these equation can be solved to give $[\mathrm{Fe}] = \dfrac{[\mathrm{Fe}]_\mathrm{T}}{K[\mathrm{X}] + 1}$ and $[\mathrm{Fe} \bullet \mathrm{X}] = \dfrac{K[\mathrm{X}][\mathrm{Fe}]_\mathrm{T}}{K[\mathrm{X}] + 1}$. Then substitution in equation (6.11) gives equation (6.12)

$$\text{Rate} = \left(\frac{k_2K[\text{X}]+k_1}{K[\text{X}]+1}\right)[\text{Fe}]_\text{T}[\text{Co(dmgBF}_2)_2(\text{H}_2\text{O})_2] \qquad (6.12)$$

and the observed second-order rate constant is given by equation (6.13).

$$k_{obs} = \left(\frac{k_2K[\text{X}]+k_1}{K[\text{X}]+1}\right) \qquad (6.13)$$

If $K[\text{X}] << 1$, then equation (6.13) simplifies to equation (6.14)

$$k_{obs} = k_2K[\text{X}]+k_1 \qquad (6.14)$$

This is consistent with the linearity of the plot in Figure 6.1. The value of k_2K and k_1 at 10, 15 and 20 °C are given in Table 6.4. It should be noted that if $[\text{Cl}^-] < 0.02$ M, then the assumption $K[\text{X}] << 1$ in equation (6.13) gives a value of $K \leq 50$ M^{-1}. The K is expected to be ~ 10 M^{-1},[10] which is consistent with the assumption in the rate law.

On the other hand, it is possible for the reaction to go through another pathway, if the ion-pair step in Scheme 6.2 is replaced by the reaction of $\text{Co(dmgBF}_2)_2(\text{H}_2\text{O})_2$ with Cl^- to give $\text{Co(dmgBF}_2)_2(\text{H}_2\text{O})(\text{Cl})^-$ with an equilibrium constant of K_i. The rate law would be identical to that for the ion-pair pathway. The K_i for the Co(II) system value is expected to be less than the value of 0.8 M^{-1} (1.0 M NaClO_4, 25 °C) obtained by Prinsloo et al.[20] for the reaction of Cl^- with a cobalt(III) aquacobalamin$^+$ complex. The present data does not allow a definitive choice between these two reaction pathways.

Table 6.4. Experimental and Extrapolated Kinetic Parameters for the Reaction of $Fe(bipy)_3^{3+}$ with $Co(dmgBF_2)_2(H_2O)_2$ in 3.0×10^{-3} M $HNO_3/3.8 \times 10^{-2}$ M $NaNO_3$.

T (^{O}C)	$10^{-8}k_2K$ ($M^{-2}\,s^{-1}$)	$10^{-6}\,k_1$ ($M^{-1}\,s^{-1}$)
10	1.12 ± 0.12	1.16 ± 0.09
14.9	1.28 ± 0.32	1.37 ± 0.21
15	1.23 ± 0.10	1.37 ± 0.04
20	1.60 ± 0.10	1.40 ± 0.06
25	1.83[b]	1.59[b]

[a] The errors are 95 % confidence limits determined from least-squares analysis at each temperature.

[b] Calculated from the least-squares best fit values of ΔH^* and ΔS^* given in the text.

[H$^+$] dependence. The rate of the reaction of $Fe(bipy)_3^{3+}$ and $Co(dmgBF_2)_2$ does not depend on the H$^+$ ion concentration. This may be contrasted to the [H$^+$] dependence that is observed for the reduction of $Co(dmgH)_2L_2^+$ complexes that were discussed in the introduction. One might have anticipated that the lower oxidation state of cobalt in $Co(dmgBF_2)_2(H_2O)_2$ would favor protonation equilibria such as equation (6.1). However it appears that the strongly electron-withdrawing $-BF_2$ substituents reduce the basicity of the oxygen to the extent that such protonation is not observed, at least up to [H$^+$] = 0.015 M. With the same line of reasoning, one might expect that the $-BF_2$ substituents would enhance the acidity of the water ligands and favor the hydrolysis equilibrium shown in equation (6.15).

$$Co(dmgBF_2)_2(H_2O)_2 \rightleftarrows Co(dmgBF_2)_2(HO)(H_2O)^- + H^+ \qquad (6.15)$$

The lack of an [H$^+$] dependence of the rate indicates that this is not significant, at least for [H$^+$] > 3.0 × 10^{-3} M. This is consistent with the results of Espenson and co-workers[5] who studied the oxidation of $Co(dmgBF_2)_2(H_2O)_2$ by $Fe(OH_2)_6^{3+}$ down to [H$^+$] = 3.1 × 10^{-3} M.

Temperature Dependence. Activation parameters were determined from the temperature dependence of k_1, and k_2K for the reduction of $Fe(bipy)_3^{+3}$ by $Co(dmgBF_2)_2(H_2O)_2$ in 0.3-1.5 × 10^{-2} M HNO_3. The data given in Tables 6.2 and 6.3 were analyzed by the Eyring equation (6.16).

$$\ell n\left(\frac{k_1}{T}\right) = \ell n\left(\frac{\kappa}{h}\right) - \frac{\Delta H^*}{RT} + \frac{\Delta S^*}{R} \qquad (6.16)$$

The results of a least-squares analysis (Appendix 6.1) gave the activation parameters for ΔH^* (kcal mol^{-1}) and ΔS^* (cal mol^{-1} K^{-1}), as 2.22 ± 0.02 and -22.7 ± 0.8 for k_1 and 5.66 ± 0.03 and -1.74 ± 0.12 for k_2K.

Discussion

Some rate constants (k_1) and activation parameters for redox reactions of Fe(bipy)$_3^{3+}$ and the related Fe(phen)$_3^{3+}$ are summarized in Table 6.5. There is a definite trend in ΔS^*, with the values being less negative as the charge on the reductant decreases from +2 to 0 to −1 indicating that higher charged transition state gives more loss of entropy. This may be expected if solvent molecules become more restricted around a more highly charged activated complex.

The electron-transfer reaction studied here must be outer-sphere since Fe(bipy)$_3^{3+}$ has no atoms for bridging and the rates are much faster than the values of the rates for chelate ring opening of the bipyridine ligand.[10] The outer-sphere electron-transfer process for reduction of Fe(bipy)$_3^{3+}$ by Co(dmgBF$_2$)$_2$(H$_2$O)$_2$ consists of three steps:[24] formation of the precursor (ion-pair) complex; irreversible electron transfer; and dissociation of the successor complex to the reaction products. Of these steps, electron transfer is rate determining since precursor formation and successor dissociation are diffusion-controlled processes.[25] For the reaction under consideration, this can be

Table 6.5. Rate and Activation Parameters for the Reduction of $Fe(bipy)_3^{3+}$ and $Fe(phen)_3^{3+}$ by Various Reductants.

Redox Partners	k_i at 25 °C ($M^{-1}\ s^{-1}$)	ΔH^* (kcal mol^{-1})	ΔS^* (cal $mol^{-1}\ K^{-1}$)	Reference
$Fe(phen)_3^{3+}/Fe^{2+}(aq)$	5.8×10^4	0.76	-37.20	23
$Fe(bipy)_3^{3+}/$ $Co(dmgBF_2)_2(H_2O)_2$	1.6×10^6	2.22 ± 0.02	-22.7 ± 0.8	this work
$Fe(phen)_3^{3+}/AH^-$	2.0×10^5	5.02	-17.57	24
$Fe(phen)_3^{3+}/AH^-$	6.8×10^8	1.84	-11.95	24
	6.5×10^8	2.15	-10.99	25

Where, AH_2 and AH^- are ascorbic acid and deprotoned ascorbic acid anions, respectively.

formulated as in Scheme 6.3, where L = H_2O.

Scheme 6.3

$$\mathrm{Co(dmgBF_2)_2(L)_2} + \mathrm{Fe(bipy)_3}^{3+} \overset{K_{os}}{\rightleftarrows} [\mathrm{Co(dmgBF_2)_2(L)_2}^{0} \bullet \mathrm{Fe(bipy)_3}^{3+}]$$

$$[\mathrm{Co(dmgBF_2)_2(L)_2}^{0} \bullet \mathrm{Fe(bipy)_3}^{3+}] \xrightarrow{k_{et}} [\mathrm{Co(dmgBF_2)_2(L)_2}^{+} \bullet \mathrm{Fe(bipy)_3}^{2+}]$$

$$[\mathrm{Co(dmgBF_2)_2(L)_2}^{+} \bullet \mathrm{Fe(bipy)_3}^{2+}] \xrightarrow{\text{fast}} \mathrm{Co(dmgBF_2)_2(L)_2}^{+} + \mathrm{Fe(bipy)_3}^{2+}$$

The measured second-order rate constant, commonly represented as k_{12}, is equal to the product of the precursor complex formation constant and the electron-transfer rate constant, i.e. $k_{12} = K_{os}k_{et}$

The self-exchange rate constant for the $Co(dmgBF_2)_2(H_2O)_2^{+/0}$ was estimated by using equation (6.17) derived from Marcus theory.[26,27]

$$k_{12} = (k_{11}k_{22}K_{12}f_{12})^{1/2}W_{12} \tag{6.17}$$

In this equation, k_{11} and k_{22} are the isotopic exchange or self-exchange rate constants for $Fe(bipy)_3^{3+/2+}$ and $Co(dmgBF_2)_2(H_2O)_2^{+/0}$, respectively, K_{12} is the equilibrium constant for the net reaction and f_{12} and W_{12} are defined in equations (5.24-26) in Chapter 5. Since k_{12} has been measured, k_{11}[28] and K_{12} are known and f_{12} and W_{12} can be reasonably determined from the estimated radii for $Fe(bipy)_3^{3+}$ and $Co(dmgBF_2)_2(H_2O)_2$ of 6.8 Å[29,30] and 4.2 Å,[5] respectively, then the desired value k_{22} can be calculated.

The constant K_{12} for the net reaction was calculated from the electrode potentials of $Fe(bipy)_3^{3+/2+}$ and cobaloximes(III)/(II) by equation (6.18);

$$\log K_{12} = 16.913 \times \Delta E^o \tag{6.18}$$

where ΔE^0 is the difference between the electrode potentials of the oxidant and reductant. The E^0 value (0.74 V) of $Fe(bipy)_3^{3+/2+}$ is taken from Warren's work[31] and E^0 values (0.65 V) for $Co(dmgBF_2)_2(H_2O)_2^{+/0}$ are available from Espenson and co-workers.[5,32] For the $Co(dmgBF_2)_2(H_2O)_2$ plus $Fe(bipy)_3^{3+}$ reaction, $\log K_{12} = 7.27$ and $K_{12} = 1.90 \times 10^7$.

In order to estimate k_{22}, the known values of $k_{11} = 8.0 \times 10^6$ M^{-1} s^{-1} [28] and K_{12} calculated above were used in equation (6.17). Then various values of k_{22} were used to calculate k_{12} from equation (6.17) until the calculated value agreed with the experimental value of k_{12} (k_1 from Scheme 6.2). The value of $k_{22} = 8.7 \times 10^{-3}$ M^{-1} s^{-1} gave a calculated $k_{12} = 1.59 \times 10^6$ M^{-1} s^{-1}, in agreement with experiment. Therefore k_{22} is estimated to be 8.7×10^{-3} $M^{-1}s^{-1}$.

The results of this and related studies are summarized in Table 6.6. This is in reasonable agreement with estimates from other reactions, which range from 1.7×10^{-4} M^{-1} s^{-1} to 8.7×10^{-3} M^{-1} s^{-1}. In a previous study,[33] $Co(sep)_2^{2+}$ was used to reduce $Co(dmgBF_2)_2(H_2O)_2^{+}$ and it was estimated that $k_{22} = 6.6 \times 10^{-4}$ M^{-1} s^{-1}. Ideally, these values should agree, and they do, within the accepted limitations of the theory.[26,27] This result is consistent with an outer-sphere mechanism for the reaction of $Co(dmgBF_2)_2(H_2O)_2$ with $Fe(bipy)_3^{3+}$. It is also interesting to note that these values[33] are

Table 6.6. Self-Exchange Rate Constants for Cobaloxime Systems Calculated by the Marcus Relationship.

Couple	logK_{12}	k_{12} (M^{-1} s^{-1})	k_{11} (M^{-1} s^{-1})	f_{12}	k_{22} (M^{-1} s^{-1})
$Co(dmgBF_2)_2(H_2O)_2$ + $Fe(bipy)_3^{3+}$ [a]	7.27	1.59×10^6	8.0×10^6	1.7×10^{-1}	8.7×10^{-3}
$Co(dmgBF_2)_2(H_2O)_2^+$ + $Co(sep)_3^{2+}$ [b]	15.4	1.50×10^5	3.5	3.5×10^{-3}	6.6×10^{-4}
$Co(dmgBF_2)_2(H_2O)_2$ + $Co(OH_2)_5OH^{2+}$ [c]	13.53	1.0×10^5	1.6×10^2	1.2×10^{-2}	1.7×10^{-4}
$Co(dmgH)_2(H_2O)_2^+$ + $Co(sep)_3^{2+}$ [b]	10.49	5.53×10^3	3.5	5.8×10^{-2}	2.0×10^{-3}

[a] At 25 °C with μ = 0.041 M $HNO_3/NaNO_3$. In calculating the k_{22}, E^o = 1.08 V (vs. NHE, reference 31), and k_{11} is 8.0×10^6 $M^{-1}s^{-1}$ (reference 28) are used for $Fe(bipy)_3^{3+/2+}$. [b] Reference 33 at 25 °C with μ = 0.10 M. Note; k_{22} for $Co(dmgBF_2)_2(H_2O)_2^{+/0}$ and $Co(dmgH)_2(H_2O)_2^{+/0}$ recalculated from reference 33. [c] At 25 °C with μ = 1.00 M $HClO_4/LiClO_4$ in Chapter 5.

similar to the previously estimated value of 2.0 × 10^{-3} M^{-1} s^{-1} from the reaction of $Co(dmgH)_2^+$ with $Co(sep)_2^{2+}$.

This result for k_{22} lies between the experimental values obtained for the self-exchange rate constant of the couples $Co(NH_3)_6^{3+}/Co(NH_3)_6^{2+}$ and $Co(sep)^{3+}/Co(sep)^{2+}$ as indicated in Table 6.7. The self-exchange for $Co(sep)^{3+/2+}$ involves the electron-transfer from the high-spin $Co(sep)^{2+}$ to the low-spin $Co(sep)^{3+}$. Such a spin state change is believed to impose an energy barrier which will contribute to the nonadiabaticity for the $Co(sep)^{3+/2+}$ exchange. However, Swaddle et al.[43] concluded from the activation volume that the electron self-exchange for $Co(sep)^{3+/2+}$ is adiabatic. The large exchange rate with sepulchrate has been attributed by Sargeson et al.[44-46] to the strain in the cage ligand because the Co(III) ion is a bit too small to fit into the cage and Co(II) is a bit too large. As a result, bond length distortion toward the transition state is favorable for $Co(sep)^{3+/2+}$ exchange. This is due to the fact that relaxation of strain which occurs on extension of the Co-N bond during reduction of Co(III) contributes significantly to the driving force (ΔG^o) of the process.[47] The introduction of π conjugated ligands (bipy and phen) on the Co center provides a good orbital overlap causing a significant increase in k_{22}. Also the increase in k_{22} has been ascribed to the fact that such complexes are much closer to the high-low spin cross-over point.[40]

Endicott et al.[35] studied the variation of the self-exchange rates with structure changes for a series of homologous trans-$Co(N4)(H_2O)_2^{3+/2+}$ couples in which both Co(II) and Co(III) are low spin. The self-exchange rate constants were evaluated from the cross-reaction rates among these complexes. Structural studies have shown that the Co-N

Table 6.7. Self-Exchange Rate Constants for Various Co(III)/(II) Complexes at 25 °C.

Reaction	μ (M)	k_{22} ($M^{-1}s^{-1}$)	Reference
$Co(NH_3)_6^{3+/2+}$	1.00	1.0×10^{-7}	34
$Co(Me_6[14]4,11\text{-diene}N_4)(L)_2^{3+/2+}$	1.00	4.5×10^{-5}	35
$Co(en)_3^{3+/2+}$	1.00	8.0×10^{-5}	36
$Co(NH_3)_2(L)_2^{3+/2+}$	0.10	1.6×10^{-4}	37
$Co(dien)_6^{3+/2+}$	1.00	1.9×10^{-4}	38
$Co(dmgBF_2)_2(L)_2^{0/+}$	0.10	3.7×10^{-4}	33
$Co(dmgH)_2(L)_2^{0/+}$	0.10	2.0×10^{-3}	33
$Co(Me_2[14]1,11\text{-diene}N_4\text{-13-one})(L)_2^{3+/2+}$	1.00	4.4×10^{-3}	37
$Co(dmgBF_2)_2(L)_2^{0/+}$	0.04	8.7×10^{-3}	This work
$Co(Me_4[14]\text{tetraene}N_4)(L)_2^{3+/2+}$	1.00	5.0×10^{-2}	35
$Co(L)_6^{3+/2+}$	0.50	3.0×10^{0}	39
$Co(sep)^{3+/2+}$	0.20	5.0×10^{0}	40
$Co(phen)_3^{3+/2+}$	0.10	1.2×10^{1}	41
$Co(bipy)_3^{3+/2+}$	0.10	1.8×10^{1}	42

Where L = H_2O

bond length changes very little between the Co(III) and Co(II) forms of these complexes, but the axial Co-OH_2 bond lengths are 0.38-0.57 Å longer for Co(II) because the unpaired electron occupies the antibonding d_{z^2} orbital. Endicott et al.[35] attributed the variation of the self-exchange rate to the reorganization energies that result from changes (Δd) in Co-OH_2 bond length.

The cobaloxime systems are structurally similar to the $CoN_4(OH_2)_2$ complexes in that the equatorial Co-N bond lengths are 1.87-1.89 Å, and are similar for the Co(III) and Co(II) forms.[48] Only the axial Co-OH_2 bonds lengthen from cobalt(III) to cobalt(II). For the $Co(dmgBF_2)_2$ complex, Co(II)-OH_2 and Co(III)-OH_2 bond lengths can be estimated as 2.28 and 1.97 Å from the Co-O bond lengths in $Co(dmgBF_2)_2(CH_3OH)_2$,[5] and $X(H_2O)Co(dmgH)_2$ (X = halide ions).[48] Therefore, Δd is estimated to be ~ 0.31 Å.

The self-exchange rates decrease in the order $Co(Me_4[14]tetraeneN_4)(L)_2^{3+/2+}$ > $Co(Me_2[14]1,11\text{-}dieneN_4\text{-}13\text{-}one)(L)_2^{3+/2+}$ > $Co(Me_6[14]4,11\text{-}dieneN_4)(L)_2^{3+/2+}$ as the Δd (0.38, 0.43 and 0.57 Å, respectively) becomes larger.[35] If the non-adiabaticity factor is about the same for various Co(III)/Co(II) systems, then the Franck-Condon model predicts that k_{22} should vary inversely with $(\Delta d)^2$ and systems with the same Δd should have the same k_{22}. The Franck-Condon barrier (inner-sphere reorganization energy), described by either classical (harmonic oscillator) or quantum mechanical models, is associated with changes in metal ligand bond length accompanying the electron transfer. Equation (6.19) shows the classical model[35]

$$k_{22}(\mathrm{FC}) = 10^{11} \times \exp\left(-\frac{\Delta G^{*}_{\mathrm{FC}}}{\mathrm{RT}}\right) \qquad (6.19)$$

where

$$\Delta G^{*}_{\mathrm{FC}} = \frac{\mathrm{n}\, f_{II} f_{III}}{2\, f_{II} + f_{III}} (\Delta d)^2 \qquad (6.20)$$

It should be noted that $\Delta G^{*}_{\mathrm{FC}}$ and k_{22}(FC) are the calculated Franck-Condon activation energy and the corresponding self-exchange rate, n is the number of bonds, and f_{II} and f_{III} are the corresponding force constants for stretching the metal-ligand bonds for the Co(II) and Co(III) complexes.

The Δd ~ 0.31 Å for the cobaloximes is similar to that of 0.38 Å for Co(Me$_4$[14]tetraeneN$_4$)(L)$^{3+/2+}$. Therefore the self-exchange rate constant of 5×10^{-2} M^{-1} s^{-1} for the latter system might be expected to be slightly smaller than for cobaloxime. Cobaloxime does not fit this model because it has a value of $k_{22} = 8.7 \times 10^{-3}$ M^{-1} s^{-1}. Thus other electronic (non-structural) factor(s) may contribute to the retardation of cobaloxime(III)/(II) exchange rates calculated by the Marcus relationship.

References

(1) Schrauzer, G. N. *Inorg. Synth.* **1968,** *11*, 61.

(2) Sharp, A. G.; Wakefield, D.B. *J. Chem. Soc.* **1957**, 281.

(3) Adin, A.; Brynildson, M. E.; Espenson, J. H. *Inorg. Chem.* **1972,** *11*, 686.

(4) Fallon, G. D.; Gatehouse, B. M. *Cryst. Struct. Comm.* **1978**, *7*, 263.

(5) Bakac, A.; Brynildson, M. E.; Espenson, J. H. *Inorg. Chem.* **1986**, *25*, 4108.

(6) Prince, R. H. and Segal, M. G. *J. Chem. Soc. Dalton Trans.* **1975**, 1245.

(7) Wilkins, R. G. *Kinetics and Mechanism of Reactions of Transition Metal Complexes*; VCH; New York, New York, **1991**; Chapter 5.

(8) Balasubramanian, G.; Vijayaraghavan, V. R. *Inorg. Chem. Acta* **1981**, *53*, L209.

(9) Balasubramanian, G.; Vijayaragharan, V. R. *Inorg. Chem. Acta* **1980**, *38*, 49.

(10) Jordan, R. B. *Reaction Mechanisms of Inorganic and Organometallic Systems;* Oxford University Press; New York, New York, **1998**; Chapter 3.

(11) Rillema D. P.; Endicott, J. F.; Patel, R. *J. Amer. Chem. Soc.* **1972**, *94*, 394.

(12) Glick, M. D.; Kuszaj, J. M.; Endicott, J. F. *J. Amer. Chem. Soc.* **1973**, *95*, 5097.

(13) Endicott, J. F.; Durham; B.; Glick, M D.; Anderson, T. J.; Kuszaj, J. M.; Schmonsees, W. G.; Balakishnan, K. P. *J. Amer. Chem. Soc.* **1981**, *103*, 431.

(14) Endicott, J. F.; Durham, B.; Kumar, K. *Inorg. Chem.* **1982**, *21*, 2437.

(15) Ramasami, T.; Endicott, J. F. *J. Amer. Chem. Soc.* **1985**, *107*, 389.

(16) Merrithew, P. B.; Lo, C. C.; Modestino, A. J. *Inorg. Chem.* **1973**, *12*, 1927.

(17) Ruff, I.; Zimonyi, M. *Electrochim. Acta* **1973**, *18*, 515.

(18) Kimura, M.; Kaneko, Y. *J. Chem. Soc. Dalton Trans.* **1984**, 34.

(19) Schmid, R.; Kirchner, K.; Franz, L. D. *Inorg. Chem.* **1988**, *27*, 1530.

(20) Prinsloo, F. F.; Breet, E. L. J.; Eldik, R. *J. Chem. Soc. Dalton Trans.* **1995**, 685.

(21) Ford-Smith, M. H.; Sutin, N. *J. Amer. Chem. Soc.* **1961**, *83*, 1830.

(22) Kimura, M. Yamamoto, M.; Yamabe, S. *J. Chem. Soc. Dalton Trans.* **1982**, 423.

(23) Pelizzetti, E. Mentasti, E.; Pramauro, E. *Inorg. Chem.* **1976**, *15*, 2898; **1978**, *17*, 1181.

(24) Sutin, N. *Inorg. Biochem.* **1973**, *2*, 611.

(25) Cannon, R. D. *Electron Transfer Reactions*; Butterworths; London, England, **1980**.

(26) Marcus, R. A.; Sutin, N. *Biochem. Biophys. Acta* **1985**, *811*, 265.

(27) Marcus, R. A. *J. Phys. Chem.* **1963**, *67*, 853.

(28) Doine, H.; Swaddle, T. W. *Can. J. Chem.* **1988**, *66*, 2763.

(29) Chan, M. S.; Wahl, A. C. *J. Phys. Chem.* **1978**, *82*, 2542.

(30) Brunschwig, B.B.; Creutz, C.; Macartney, D. H.; Sham, T. K.; Sutin, N. *Faraday Discuss. Chem. Soc.* **1982**, *74*, 113.

(31) Warren, L. F. *Inorg. Chem.* **1977**, *16*, 2814.

(32) Heckam, R. G.; Espenson, J, H. *Inorg. Chem.* **1979**, *18*, 38.

(33) Wang, K.; Jordan, R. B. *Can. J. Chem.* **1996**, *74*, 658.

(34) Sutin, N. *Prog. Inorg. Chem.* **1983**, *30*, 441.

(35) Endicott, J. F.; Durham, B.; Glick, M. D.; Anderson, T. J.; Kuszaj, J. M.; Schmonsees, W. G.; Balakrishman, K. P. *J. Amer. Chem. Soc.* **1981**, *103*, 1431.

(36) Dwyer, F. P.; Sargeson, A. M. *J. Phys. Chem.*, **1961**, *65*, 1892.

(37) Martinez, P.; Zuluage J.; Noheda P. *Inorg. Chim. Acta* **1992**, *195*, 249.

(38) Ventur, D.; Wieghardt, K.; Nuber, B.; Weiss, J. *Zeit. Anorg. Allge. Chem.* **1987**, *551*, 33.

(39) Habib, H. S.; Hunt, J. P. *J. Amer. Chem. Soc.* **1966**, *88*, 1668.

(40) Sargeson, A. M. *Chem. Br.* **1979**, *15*, 23.

(41) Warren, R. M. L.; Lappin, A. G.; Dev Mehta, B.; Neumann, H. M. *Inorg. Chem.* **1990**, *29*, 4185.

(42) Tsukahara, K.; Yamamoto, Y. *Bull. Chem. Soc. Jpn.* **1981**, *54*, 2642.

(43) Doine, H.; Swaddle, T. W. *Inorg. Chem.* **1991**, *30*, 1858.

(44) Geue, R. J.; Hambley, T. W.; Harrowfield, J. M.; Sargeson, A. M.; Snow, M. R. *J. Amer. Chem. Soc.* **1984**, *106*, 5478.

(45) Geue, R. J.; Hendry, A. J.; Sargeson, A. M. *J. Chem. Soc., Chem. Commun.* **1989**, 1646.

(46) Creaser, I.; Geue, R. J.; Harrowfield, J. M.; Herlt, A. J.; Sargeson, A. M.; Snow, M. R.; Sprinborg, J. *J. Amer. Chem. Soc.* **1982**, *104*, 6016.

(47) Hambley, T. V. *Inorg. Chem.* **1988**, *27*, 2496.

(48) Bresciani-Pahor, N.; Forcolin, M.; Marzilli, L. G.; Randaccio, L.; Summers, M. F.; Toscano, P. J. *Coord. Chem. Rev.* **1985**, *63*,1.

CHAPTER 7

Conclusions

The synthesized and fully characterized salt, $[Co(NH_3)_6][Co(CO_3)_3]$, is formed as dark green needle-like crystals. The material is stable at room temperature and extremely insoluble in water, alcohol, acetone and acetonitrile. The X-ray structure of $[Co(NH_3)_6][Co(CO_3)_3]$ shows that all the carbonates are chelated. The interatomic distances and angles of $Co(CO_3)_3^{3-}$ are similar to those of other carbonato complexes of cobalt(III), as listed in Table 2.3.

The green crystals serve as a reliable source of the strongly oxidizing aqueous cobalt(III) ion. The crystalline salt reacts with an acid, HX, to give CO_2, $Co(NH_3)_6X_3$ (X = ClO_4^-, NO_3^- and $CF_3SO_3^-$) and $Co(OH_2)_6^{3+}$. The solid is easily separated from the solution by centrifugation. Solutions of cobalt(III) at a range of initial concentrations and acidities can be conveniently prepared by this method. The final acidity is easily controlled by starting with the appropriate excess amount of acid HX, and the cobalt(III) is controlled by the mass of $[Co(NH_3)_6][Co(CO_3)_3]$ used. From this work, the maximum yield of $Co(OH_2)_6^{3+}$ produced from $[Co(NH_3)_6][Co(CO_3)_3]$ was ~ 90 %. Based on general experience, the yield is best at higher acidity (> 1.0 M) and lower temperature (< 5 °C). The normal temperature was 0 °C in this work. The $Co(OH_2)_6^{3+}$ formed has extinction coefficients of 35 and 40 M^{-1} cm^{-1} at 605 and 400 nm, respectively.

The redox reaction between water and $Co(OH_2)_6^{3+}$ was monitored using spectrophotometry and the mechanism involves dimerization of $Co(OH_2)_6^{3+}$ followed by the decay of the dimer. This work proposed the steps shown in the mechanism in Scheme 7.1 that are consistent with the experimental data, where $Co(OH_2)^{3+}$ = $(Co(OH_2)_6^{3+} + Co(OH_2)_5(OH)^{2+})$ and H_2O is omitted to simplify the scheme.

Scheme 7.1

$$2Co(OH_2)^{3+} \xrightarrow{k_1} [(H_2O)Co(\mu-OH)Co]^{5+} + H^+$$

$$[(H_2O)Co(\mu-OH)Co]^{5+} \xrightarrow{k_2} [Co(\mu-OH)_2Co]^{4+} + H^+$$

$$[Co(\mu-OH)_2Co]^{4+} \xrightarrow{k_3} 2Co^{2+} + H_2O_2$$

$$2Co(OH_2)^{3+} + H_2O_2 \xrightarrow{k_4} 2Co^{2+} + O_2 + 2H^+ + 2H_2O$$

The reaction is biphasic, showing an initial increase and then decrease in absorbance at 325 and 605 nm. The rate of increase depends on $[Co(OH_2)_6^{3+}]^2$ and $[H^+]^{-2}$, while the decrease has an $[H^+]^{-1}$ dependence. The $[H^+]^{-2}$ and $[H^+]^{-1}$ dependence for the absorbance increase and decrease, respectively, may be accounted for by hydrolysis equilibria of $Co(OH_2)_6^{3+}$ and oligomeric species. The calculated values for k_1K_1 and k_2K_2 that fit the data are 3.5×10^{-3} s^{-1} and 3.2×10^{-3} M s^{-1}, respectively, where K_1 is the hydrolysis constant of $Co(OH_2)_6^{3+}$, k_1 is the rate for the absorbance increase, K_2 represent the hydrolysis constant for the oligomer and k_2 the rate constants for the absorbance decrease.

The reaction of $Co(OH_2)_6^{3+}$ with hydrogen peroxide was studied to provide data for the analysis of the redox reaction of $Co(OH_2)_6^{3+}$ with water. The latter reaction may produce initially hydrogen peroxide which is then oxidized by cobalt(III). The rate law shows a simple inverse dependence on $[H^+]$ that is consistent with a rapidly maintained equilibrium between $Co(OH_2)_6^{3+}$ and its hydrolyzed form $Co(H_2O)_5(OH)^{2+}$, followed by the rate controlling step, i.e. oxidation of H_2O_2 by $Co(H_2O)_5(OH)^{2+}$.

The rate controlling process could be simple outer-sphere electron transfer or ligand substitution of H_2O_2 on $Co(OH_2)_5(OH)^{2+}$, followed by inner-sphere electron transfer. If the latter is the case, then one would expect similar rate constants for simple substitution reactions and the redox process. There are several examples in the literature of reactions with an inverse $[H^+]$ dependence that have been assigned to substitution reactions on $Co(OH_2)_5(OH)^{2+}$. If one takes the literature values of $b = k_2K_a$, to make them independent of the uncertain value of K_a, then one finds values of 7.0 s^{-1} (7 °C), 16.0 s^{-1} (7 °C) and 44.0 s^{-1} (25 °C) for malic acid,[1] thiomalic acid[2] and chloride ion,[3] respectively. These values are quite similar, after due allowance for temperature differences, to our value of $b = 26.4 \pm 0.5$ s^{-1} (25 °C) for H_2O_2. This observation supports an inner-sphere mechanism for oxidation of H_2O_2 by $Co(OH_2)_5(OH)^{2+}$.

The hydrolysis constant K_a for $Co(OH_2)_6^{3+}$ was estimated kinetically in this work to be $\sim 9.5 \times 10^{-3}$ M ($\mu = 1.0$ M). This is in the published range of 2.2×10^{-1} M [3] to $\sim 9 \times 10^{-3}$ M [4] at 25 °C. Spectrophotometric measurements have in general yielded estimates close to the lower end of this range,[4-8] whereas estimates from kinetic studies have tended to give values of the order of 10^{-1} M.[1,9] Our K_a value compares well with the recently determined values of Martinez and co-workers[4] who studied the hydrolysis of $Co(OH_2)_6^{3+}$ spectrophotometrically. They determined the K_a values at 25 °C to be 0.012 ± 0.002, 0.009 ± 0.006, 0.015 ± 0.005 at respective ionic strengths of 1.0, 2.0, and 3.0 M $LiClO_4$.

The kinetics of the reaction of aqueous cobalt(III) with $Co(dmgBF_2)_2$ have been studied. The possible reaction mechanism involves a rapidly maintained equilibrium between $Co(OH_2)_6^{3+}$ and its hydrolyzed form $Co(H_2O)_5(OH)^{2+}$ and oxidation of $Co(dmgBF_2)_2(H_2O)_2$ by both of these species. The rate has an inverse dependence on $[H^+]$, indicating that $Co(H_2O)_5(OH)^{2+}$ is the only active oxidant. Since $Co(dmgBF_2)_2(H_2O)_2$ has a d^7 low-spin electronic configuration that is substitutionally labile, an inner-sphere mechanism is possible for the electron-transfer reaction. This could proceed through a bridged intermediate of the form $[(H_2O)_5Co\text{-}(OH)\text{-}Co(dmgBF_2)_2(H_2O)]^{2+}$. However, if an outer-sphere mechanism is assumed, then the self-exchange rate for $Co(dmgBF_2)_2(H_2O)_2^{+/0}$ can be estimated for the reaction with $Co(H_2O)_5(OH)^{2+}$ and this gives $k_{22} = 1.7 \times 10^{-4}$ M^{-1} s^{-1}. This is in reasonable agreement with estimates from other reactions, which range from 6.6×10^{-4} M^{-1} s^{-1} [10] to 8.7×10^{-3} M^{-1} s^{-1} (Chapter 6), especially when the approximations of K's and E^o for the $Co(H_2O)_5(OH)^{2+}$ system are considered. This result is consistent with an outer-sphere mechanism for the reaction of $Co(dmgBF_2)_2(H_2O)_2$ with $Co(H_2O)_5(OH)^{2+}$. However, there is an anomaly with this system in that the rate constant for $Co(H_2O)_6^{3+}$ is too small to determine ($< 2.0 \times 10^2$), whereas Marcus theory predicts a value of $\sim 10^7$ M^{-1} s^{-1}.

$Fe(bipy)_3^{3+}$ is inert with a d^6 low-spin configuration and a large amount of electron delocalization onto the highly conjugated ligand.[11] Both $Fe(bipy)_3^{2+}$ and $Co(dmgBF_2)_2(H_2O)_2^+$ formed in the reaction between $Co(dmgBF_2)_2(H_2O)_2$ and $Fe(bipy)_3^{3+}$ are inert with a d^6 low-spin configuration. The outer-sphere electron-transfer mechanism is expected for this reaction because $Fe(bipy)_3^{3+}$ has no atoms for bridging and the rate is much faster than that for chelate ring opening of the bipyridine ligand.[12]

The outer-sphere electron-transfer process for oxidation of $Fe(bipy)_3^{3+}$ by $Co(dmgBF_2)_2(H_2O)_2$ consists of three steps shown in Scheme 6.3 (Chapter 6); formation of the precursor complex, irreversible electron transfer, and dissociation of the successor complex to the reaction products. Of these steps, electron transfer is rate determining since precursor formation and successor dissociation are diffusion-controlled processes. Marcus theory and the known electron self-exchange rate constant for $Fe(bipy)_3^{3+/2+}$ have been used to calculate a self-exchange rate constant of 8.7×10^{-3} M^{-1} s^{-1} for $Co(dmgBF_2)_2(H_2O)_2^{+/0}$ at 25 °C and ionic strength of ~ 0.04 M.

The electron self-exchange rate constant (k_{22}) for $Co(dmgBF_2)_2(H_2O)_2^{+/0}$ calculated using Marcus theory for the reaction between $Co(dmgBF_2)_2$ with $Fe(bipy)_3^{3+}$ and $Co(H_2O)_5(OH)^{2+}$ are 8.7×10^{-3} M^{-1} s^{-1} and 1.7×10^{-4} M^{-1} s^{-1}, respectively. Ideally, these values should agree, and they do, within the accepted limitations of the theory.[13,14] It will be interesting to compare the calculated k_{22} to measured values. One method to measure k_{22} for such a system is to study the effect of paramagnetic $Co(dmgBF_2)_2(H_2O)_2$ on the NMR line-width or the relaxation rate R_2 of nuclei in the diamagnetic $Co(dmgBF_2)_2(H_2O)_2^{+}$.[15] The change in the line-width ($\Delta\nu_{½}$) can be calculated using equation 7.1,[15-17]

$$\Delta\nu_{1/2} = k_{22}[Co(II)] \qquad 7.1$$

provided the frequency difference between individual reactant species is greater than the rate of exchange.[16] However for our system, the change of line-width of the methyl protons of cobaloxime(III) due to the added cobaloxime(II) would be too small to measure if our calculated k_{22} values are true. For the accessible concentration range of ~ 5×10^{-4} M $Co(dmgBF_2)_2(H_2O)_2$, the k_{22} value of 8.7×10^{-3} M^{-1} s^{-1} would predict a linewidth change of only ~1×10^{-5} Hz.

Another way to measure k_{22} is to study the rate of isotope exchange between the species. If normal $(H_2O)_2Co(dmgBF_2)_2^+$ [18] or $(H_2O)_2Co(dmgH)_2^+$ [19] were mixed with the $-CD_3$ substituted $(H_2O)_2Co(dmgBF_2)_2$ or $(H_2O)_2Co(dmgH)_2$, respectively, in water, the attenuation of the $-CH_3$ peak with time due to the electron "self-exchange" between the two species could be monitored by NMR. The deuterated d_8-$dmgD_2$ could be prepared by isotopic exchange reaction of the $dmgH_2$ with DCl.[20,21]

References

(1) Hill, J; McAuley, A. *J. Chem. Soc. A,* **1968**, 1169.

(2) Hill, J; McAuley, A. *J. Chem. Soc. A,* **1968**, 2405.

(3) Conocchioli, T. J.; Nancollas, G. H.; Sutin, N. *Inorg. Chem.* **1966**, *5*, 1.

(4) Ferrer, M.; Llorca, J.; Martinez, M. *J. Chem. Soc. Dalton Trans.* **1992**, 229.

(5) Taube, H. *J. Gen. Physiol.* **1966**, *49*, 29.

(6) Baxendale, J. H.; Wells, C. F. *Trans. Faraday Soc.* **1957**, *53*, 800.

(7) Patel, R. C.; Endicott, J. F. *J. Amer. Chem. Soc.* **1968**, *90*, 6364.

(8) Fereday, F. J.; Logan, N.; Sutton, D. *Chem Commun.* **1968**, 271; *J. Chem. Soc. A,* **1969**, 2699.

(9) Conocchioli, T. J.; Nancollas, G. H.; Sutin, N. *J. Amer. Chem. Soc.* **1951**, *73*, 4028.

(10) Wang, K.; Jordan, R. B. *Can. J. Chem.* **1996**, *78*, 658.

(11) Merrithew, P. B.; Lo, C. C.; Modestino, A. J. *Inorg. Chem.* **1973**, *12*, 1927.

(12) Jordan, R. B. *Reaction Mechanisms of Inorganic and Organometallic Systems*; Oxford University Press; New York, New York, **1998**; pg. 96.

(13) Sutin, N. *Prog. Inorg. Chem.* **1983,** *30*, 441.

(14) Marcus, R. A.; Sutin, N. *Biochem. Biophys. Acta* **1985,** *811*, 265.

(15) Donelevy, T. M.; Gahan, L. R.; Hambley, T. W. *Inorg. Chem.* **1994,** *33*, 2668.

(16) Swift, T. J.; Connick, R. E. *J. Chem. Phys.* **1962,** *37*, 307.

(17) Günther, H. *NMR Spectroscopy*; John Wiley & Sons; Chichester, England, **1995**; pg 344.

(18) Wang, K. *PhD Thesis*, University of Alberta **1994**, pg. 114.

(19) Ablov, A. V.; Filippov, M. P.; Samus, N. M. *Dokl. Akad. Nauk. SSSR* **1960**, *133*, 575.

(20) Golding, B. T.; Kemp, T. J.; Sellers, P. J.; Nocchi, E. *J. Chem. Soc. Dalton Trans.* **1977**, 1266.

(21) Maillard, P.; Giannoti, C. *Can. J. Chem.* **1982**, *60*, 1402.

Appendix. Tables of Experimental Data

Appendix 2.1. Selected Interatomic Distances (Å)Within $[Co(CO_3)_3]^{3-}$.

Atom1	Atom2	Distances	Atom1	Atom2	Distances
Co1	O11	1.915(3)	Co2	O21	1.909(3)
Co1	O12	1.917(3)	Co2	O22	1.928(3)
Co1	O14	1.905(3)	Co2	O24	1.908(3)
Co1	O15	1.918(3)	Co2	O25	1.932(3)
Co1	O17	1.908(3)	Co2	O27	1.920(3)
Co1	O18	1.919(3)	Co2	O28	1.908(3)
O11	C11	1.309(5)	O21	C21	1.323(5)
O12	C11	1.319(5)	O22	C21	1.310(5)
O13	C11	1.233(5)	O23	C21	1.229(5)
O14	C12	1.312(5)	O24	C22	1.314(5)
O15	C12	1.312(5)	O25	C22	1.314(5)
O16	C12	1.237(5)	O26	C22	1.233(5)
O17	C13	1.312(5)	O27	C23	1.313(5)
O18	C13	1.310(5)	O28	C23	1.307(5)
O19	C13	1.242(5)	O29	C23	1.232(5)

Appendix 2.2. Selected Interatomic Angles (deg) Within $[Co(CO_3)_3]^{3-}$.

Atom1	Atom2	Atom3	Angle	Atom1	Atom2	Atom3	Angle
O11	Co1	O12	68.89(12)	O21	Co2	O22	69.01(12)
O11	Co1	O14	98.87(12)	O21	Co2	O24	99.47(13)
O11	Co1	O15	164.25(12)	O21	Co2	O25	91.90(12)
O11	Co1	O17	91.40(13)	O21	Co2	O27	164.30(13)
O11	Co1	O18	98.27(12)	O21	Co2	O28	98.30(13)
O12	Co1	O14	92.27(13)	O22	Co2	O24	164.77(13)
O12	Co1	O15	100.90(12)	O22	Co2	O25	100.73(12)
O12	Co1	O17	99.13(13)	O22	Co2	O27	100.74(13)
O12	Co1	O18	162.83(13)	O22	Co2	O28	91.34(13)
O14	Co1	O15	68.82(12)	O24	Co2	O25	68.86(12)
O14	Co1	O17	166.84(13)	O24	Co2	O27	92.50(13)
O14	Co1	O18	101.22(13)	O24	Co2	O28	100.56(14)
O15	Co1	O17	102.32(12)	O25	Co2	O27	101.93(12)
O15	Co1	O18	93.91(13)	O25	Co2	O28	166.07(13)
O17	Co1	O18	68.97(12)	O27	Co2	O28	68.65(13)

Appendix 5.1. Dependence of k_{1obs} on the Concentration of $Co(OH_2)_6^{3+}$ and Temperature in 8.25×10^{-5} M $Co(dmgBF_2)_2(H_2O)_2$ and 0.60 M $HClO_4$/0.40 M $LiClO_4$.

T (°C)	$10^4[Co(OH_2)_6^{3+}]$ (M)	k_{1obs} (s^{-1})
10	7.17	0.22
10	11.91	0.39
10	15.53	0.53
10	19.05	0.57
10	24.61	0.69
15	6.96	0.46
15	7.04	0.46
15	13.40	0.85
15	19.91	1.22
20	7.39	0.77
20	7.07	0.80
20	11.54	1.22
20	15.50	1.51
20	19.51	1.97
20	22.93	2.10
25	7.79	1.52
25	6.81	1.49

25	12.43	2.55
25	15.49	3.08
25	20.87	4.05
25	25.14	5.12

Appendix 5.2. Dependence of the Rate Constant on Reactant Concentrations and Temperature for the Reaction of $Co(OH_2)_6^{3+}$ with $Co(dmgBF_2)_2(H_2O)_2$ in μ = 1.0 M $LiClO_4/HClO_4$.

T (°C)	10^5[CoL] (M)	10^4[Co(III)] (M)	$10^2[HClO_4]$ (M)	k_{1obs} (s^{-1})	$10^{-2}k_{2obs}$ ($M^{-1}s^{-1}$)
10	6.00	6.56	2.1		61.6
10	6.00	7.25	2.6		46.4
10	6.00	7.15	3.0		45.4
10	6.00	6.97	4.0		44.1
10	6.00	7.43	8.0		18.5
10	6.00	7.47	14.0		11.0
10	8.25	6.02	20.0		10.9
10	8.25	7.98	40.0		4.09
10	8.25	7.17	60.0		2.99
10	8.25	11.91	60.0	0.39	3.24
10	8.25	15.53	60.0	0.53	3.43
10	8.25	19.05	60.0	0.57	3.00
10	8.25	24.61	60.0	0.69	2.79
10	8.25	7.56	80.0		2.14
15	5.50	6.34	2.1		113
15	5.50	6.47	2.6		95.3

15	5.50	6.36	3.0		94.7
15	9.00	6.45	3.5		78.0
15	5.50	6.69	4.0		64.0
15	9.00	7.48	4.5		62.3
15	9.00	7.71	6.5		49.5
15	8.78	5.09	6.9		41.1
15	5.50	7.30	8.0		34.2
15	9.00	8.11	8.5		37.5
15	8.78	4.94	11.5		23.1
15	8.78	4.94	11.5		27.0
15	5.50	7.66	14.0		19.7
15	8.25	5.97	20.0		18.5
15	9.00	8.27	20.0		16.3
15	8.25	7.41	40.0		8.27
15	8.25	6.76	60.0		6.51
15	8.25	7.04	60.0		6.34
15	8.25	13.40	60.0	0.64	4.78
15	8.25	16.14	60.0	0.85	5.25
15	8.25	19.91	60.0	1.22	6.13
15	8.25	24.86	60.0	1.28	5.14
15	8.25	7.09	80.0		4.77
20	8.25	7.39	20.0		26.9
20	8.25	7.40	40.0		14.3

20	8.25	7.07	60.0		10.7
20	8.25	7.39	60.0		9.84
20	8.25	11.54	60.0	1.22	10.6
20	8.25	15.50	60.0	1.51	9.75
20	8.25	19.51	60.0	1.97	10.1
20	8.25	22.95	60.0	2.30	10.0
20	8.25	7.50	80.0		7.96
25	6.60	4.56	20.0		42.8
25	9.00	8.24	20.0		43.5
25	8.78	9.20	20.0	3.921	42.6
25	6.60	4.60	40.0		22.3
25	6.60	4.29	60.0		15.9
25	6.60	4.46	80.0		12.0

Appendix 6.1. Least-squares Analysis of the Temperature and Concentration of NaCl Dependence of the Rate Constants for the Reaction of $Co(dmgBF_2)_2(H_2O)_2$ and $Fe(bipy)_3^{3+}$ in 3.0×10^{-3} M HNO_3 and 3.8×10^{-2} M ($NaCl/NaNO_3$).

T (^oC)	10^2[NaCl] (M)	$10^{-6}k_{obs}$ ($M^{-1}s^{-1}$)	$10^{-6}k_{cal}$ ($M^{-1}s^{-1}$)	%diff.
10.0	0.00	1.14	1.24	-8.622
10.0	0.50	1.75	1.76	-0.564
10.0	1.00	2.31	2.29	+1.239
10.0	1.50	2.79	2.81	-0.636
10.0	2.00	3.36	3.33	+0.799
14.9	0.00	1.36	1.35	+0.690
14.9	0.25	1.66	1.67	-0.542
14.9	0.50	2.16	1.98	+8.148
14.9	1.50	3.20	3.24	-1.528
14.9	2.00	3.96	3.87	+2.234
15.0	0.00	1.31	1.35	-2.963
15.0	0.00	1.37	1.35	+1.101
15.0	0.25	1.66	1.69	-0.449
15.0	0.25	1.64	1.56	-1.612
15.0	0.50	1.93	1.99	-2.851

15.0	0.50	1.94	1.99	-2.215
15.0	1.00	2.57	2.62	-1.912
15.0	1.00	2.60	2.62	-0.581
15.0	1.50	3.13	3.25	-4.040
15.0	1.50	3.29	3.25	+1.028
15.0	2.00	3.94	3.88	+1.462
15.0	2.00	3.90	3.88	+0.401
15.00	0.00	1.47	1.35	+8.096
15.0	0.00	1.39	1.35	+2.671
15.0	0.00	1.29	1.35	-4.799
15.0	0.00	1.36	1.35	+0.887
15.0	0.00	1.31	1.35	-3.278
15.0	0.00	1.43	1.352	+5.593
15.0	0.00	1.511	1.35	+1.053
15.0	0.00	1.44	1.35	+6.118
15.0	0.00	1.34	1.35	-0.831
20.0	0.00	1.40	1.47	-5.188
20.0	0.10	1.57	1.62	-3.179
20.0	0.50	2.18	2.23	-2.570
20.0	1.00	2.95	2.99	-1.367
20.0	1.50	3.89	3.76	+3.423
20.0	2.00	4.55	4.52	+0.762